

Spring 5-6-2012

# The Reorganization of Primary Auditory Cortex by Invasion of Ectopic Visual Inputs

Yuting Mao

*Biology department*

Follow this and additional works at: [https://scholarworks.gsu.edu/biology\\_diss](https://scholarworks.gsu.edu/biology_diss)

---

## Recommended Citation

Mao, Yuting, "The Reorganization of Primary Auditory Cortex by Invasion of Ectopic Visual Inputs." Dissertation, Georgia State University, 2012.

[https://scholarworks.gsu.edu/biology\\_diss/112](https://scholarworks.gsu.edu/biology_diss/112)

This Dissertation is brought to you for free and open access by the Department of Biology at ScholarWorks @ Georgia State University. It has been accepted for inclusion in Biology Dissertations by an authorized administrator of ScholarWorks @ Georgia State University. For more information, please contact [scholarworks@gsu.edu](mailto:scholarworks@gsu.edu).

# THE REORGANIZATION OF PRIMARY AUDITORY CORTEX BY INVASION OF ECTOPIC VISUAL INPUTS

by

YUTING MAO

Under the Direction of Sarah L. Pallas

## ABSTRACT

Brain injury is a serious clinical problem. The success of recovery from brain injury involves functional compensation in the affected brain area. We are interested in general mechanisms that underlie compensatory plasticity after brain damage, particularly when multiple brain areas or multiple modalities are included. In this thesis, I studied the function of auditory cortex after recovery from neonatal midbrain damage as a model system that resembles patients with brain damage or sensory dysfunction. I addressed maladaptive changes of auditory cortex after invasion by ectopic visual inputs. I found that auditory cortex contained auditory, visual,

and multisensory neurons after it recovered from neonatal midbrain damage (Mao et al. 2011). The distribution of these different neuronal responses did not show any clustering or segregation. As might be predicted from the fact that auditory neurons and visual neurons were intermingled throughout the entire auditory cortex, I found that residual auditory tuning and tonotopy in the rewired auditory cortex were compromised. Auditory tuning curves were broader and tonotopic maps were disrupted in the experimental animals. Because lateral inhibition is proposed to contribute to refinement of sensory maps and tuning of receptive fields, I tested whether loss of inhibition is responsible for the compromised auditory function in my experimental animals. I found an increase rather than a decrease of inhibition in the rewired auditory cortex, suggesting that broader tuning curves in the experimental animals are not caused by loss of lateral inhibition.

These results suggest that compensatory plasticity can be maladaptive and thus impair the recovery of the original sensory cortical function. The reorganization of brain areas after recovery from brain damage may require stronger inhibition in order to process multiple sensory modalities simultaneously. These findings provide insight into compensatory plasticity after sensory dysfunction and brain damage and new information about the role of inhibition in cross-modal plasticity. This study can guide further research on design of therapeutic strategies to encourage adaptive changes and discourage maladaptive changes after brain damage, sensory/motor dysfunction, and deafferentation.

**INDEX WORDS:** Cross-modal Plasticity, Inhibitory plasticity, Multisensory, GABA, Cortical development, Brain evolution, Stroke, Traumatic brain injury, Tinnitus

THE REORGANIZATION OF PRIMARY AUDITORY CORTEX BY INVASION OF  
ECTOPIC VISUAL INPUTS

by

YUTING MAO

A Dissertation Submitted in Partial Fulfillment of Requirements for the Degree of

Doctor of Philosophy

in the College of Arts and Sciences

Georgia State University

2012

Copyright by  
Yuting Mao  
2012

THE REORGANIZATION OF PRIMARY AUDITORY CORTEX BY INVASION OF  
ECTOPIC VISUAL INPUTS

By

YUTING MAO

Committee Chair: Prof. Sarah L. Pallas

Committee: Prof. Charles Derby

Prof. Donald Edwards

Prof. Robert Liu

Electronic Version Approved:

Office of Graduate Studies

College of Arts and Sciences

Georgia State University

May 2012

## **ACKNOWLEDGEMENTS**

I thank my advisor Dr. Sarah Pallas for her many years of instruction in scientific research, support in everyday life and work. I also appreciate the many years of guidance from my committee members: Profs. Charles Derby, Donald Edwards, and Robert Liu. I also thank members of the Pallas lab for technical assistance and their comments on manuscripts. I sincerely thank staff in animal facility for their strenuous work. Finally, I am also grateful for the friends and family who have supported me during these years.

## **TABLE OF CONTENTS**

<b>ACKNOWLEDGEMENTS</b>	iv
<b>LIST OF TABLES</b>	vi
<b>LIST OF FIGURES</b>	vii
<b>LIST OF ABBREVIATIONS</b>	ix
<b>CHAPTER 1 INTRODUCTION</b>	1
<b>CHAPTER 2 COMPETITION AND CONVERGENCE BETWEEN AUDITORY AND CROSS-MODAL VISUAL INPUTS TO PRIMARY AUDITORY CORTEX</b>	15
<b>CHAPTER 3 COMPROMISE OF AUDITORY TUNING AND TOPOGRAPHY AFTER CROSS-MODAL INVASION BY VISUAL INPUTS</b>	70
<b>CHAPTER 4 CROSS-MODAL PLASTICITY RESULTS IN INCREASED INHIBITION IN PRIMARY AUDITORY CORTICAL AREAS</b>	118
<b>CHAPTER 5 DISCUSSION</b>	148
<b>REFERENCES</b>	162



## LIST OF TABLES

<b>Table 2.1.</b>	The proportion of neuronal types and residual midbrain volumes in lesioned animals	47
<b>Table 3.1.</b>	The proportion of low-frequency neurons and residual midbrain volumes in lesioned animals	99

## LIST OF FIGURES

<b>Figure 2.1.</b>	Method for quantification of distribution of neuronal response types in auditory cortex.	49
<b>Figure 2.2.</b>	Assessment of midbrain damage. <i>A</i> : an example of a section through the inferior colliculus (IC).	50
<b>Figure 2.3.</b>	Neuronal response types. <i>A</i> and <i>B</i> : the relative proportions of neuronal response types in AC of all normal ( <i>A</i> ) and all lesioned ferrets ( <i>B</i> ).	51
<b>Figure 2.4.</b>	Relationship between midbrain lesion type and size and neuronal response type in AC of experimental animals.	53
<b>Figure 2.5.</b>	Statistical comparison of midbrain size between normal and lesioned animals.	55
<b>Figure 2.6.</b>	Neuronal response types in the 3 groups. <i>A</i> : the large-lesion group contained more visual neurons than the small-lesion group.	56
<b>Figure 2.7.</b>	Reconstruction of locations of recorded neurons in normal AC.	58
<b>Figure 2.8.</b>	Distribution of neuronal response types in normal AC. <i>A</i> : polar plot of pooled data from all 10 normal cases.	59
<b>Figure 2.9.</b>	Reconstruction of locations of recorded neurons in AC of the small-lesion group (8 examples from 10 animals are shown).	60

<b>Figure 2.10.</b>	Distribution of neuronal response types in AC across the population of small-lesion cases.	62
<b>Figure 2.11.</b>	Reconstruction of locations of recorded neurons in AC of large-lesion cases (5 examples from 5 animals are shown).	64
<b>Figure 2.12.</b>	Distribution of neuronal responses in AC of large-lesion cases.	65
<b>Figure 2.13.</b>	Latencies of responses to optic chiasm stimulation in normal AC and cross-modal AC.	67
<b>Figure 2.14.</b>	Schematic of possible inputs to normal AC, to XMAC of small-lesion animals, and to X-modal AC of large-lesion animals.	68
<b>Figure 3.1.</b>	Method for quantification of neuronal response type distribution in auditory cortex.	101
<b>Figure 3.2.</b>	Assessment of midbrain damage. ICc was lesioned bilaterally and sSC was unilaterally lesioned on the left side.	102
<b>Figure 3.3.</b>	Statistical comparison of residual volume of inferior colliculi in Xmodal animals and blind-lesioned animals.	103
<b>Figure 3.4.</b>	Examples of tuning curves of auditory and multisensory neurons.	104
<b>Figure 3.5.</b>	The response characteristics of neurons in Xmodal and control animals.	106

<b>Figure 3.6.</b>	Reconstruction of locations of frequency-tuned neurons in normal AC.	107
<b>Figure 3.7.</b>	Reconstruction of locations of frequency-tuned auditory neurons in AC of Xmodal animals.	108
<b>Figure 3.8.</b>	Reconstruction of locations of frequency-tuned multisensory neurons in AC of Xmodal animals.	110
<b>Figure 3.9.</b>	Reconstruction of locations of frequency-tuned neurons in AC of blind-lesioned animals.	111
<b>Figure 3.10.</b>	Reconstruction of locations of frequency-tuned neurons in AC of three blind animals.	112
<b>Figure 3.11.</b>	Distribution of frequency-tuned neurons in AC of ferrets using pooled data from each group.	113
<b>Figure 3.12.</b>	The location of frequency-tuned neurons in the 5 groups.	115
<b>Figure 3.12.</b>	The proportion of frequency-tuned neurons in the 5 groups.	116
<b>Figure 4.1.</b>	Effects of the GABA <sub>A</sub> R antagonist gabazine on evoked responses to sound.	138
<b>Figure 4.2.</b>	Two examples of gabazine's effect on sound frequency tuning.	139
<b>Figure 4.3.</b>	The effects of gabazine on thresholds and bandwidths of auditory tuning curves in the population of normal and XM neurons.	140

<b>Figure 4.4.</b>	The effects of gabazine on spontaneous activity and auditory responsiveness.	141
<b>Figure 4.5.</b>	One example of auditory neuron responses and to bisensory stimuli before and after blocking inhibition.	144
<b>Figure 4.6.</b>	One example of the response of multisensory neurons to auditory and optic chiasm stimuli before and after blockade of inhibition by gabazine.	145
<b>Figure 4.7.</b>	The comparison of mean spike numbers from responses to optic chiasm stimulation before and after gabazine application.	146
<b>Figure 4.8.</b>	The distribution of neuronal responses before and after application of gabazine. Each figure represents data from one animal.	147

## **LIST OF ABBREVIATIONS**

AC	Auditory cortex
A1	Primary auditory cortex
AAF	Anterior auditory field
BF	Best frequency
dLGN	Dorsal lateral geniculate nucleus
EPSP	Excitatory postsynaptic potential
FAES	Auditory field of the anterior ectosylvian sulcus
FRA	Frequency response area
GABA	$\gamma$ -aminobutyric acid
GAD	Glutamic acid decarboxylase
IC	Inferior colliculus
IM	Intramuscular injection
IP	Intraperitoneal injection
IPSP	Inhibitory postsynaptic potential
LGN	Lateral geniculate nucleus

LTP	Long term potentiation
LTD	Long term depression
MGN	Medial geniculate nucleus
MRI	Magnetic resonance imaging
PB	Phosphate buffer
PBS	Phosphate-buffered saline
PSTH	Poststimulus time histogram
RF	Receptive field
SC	Superior colliculus
SQ	Subcutaneous injection
TBI	Traumatic brain injury
TMS	Transcranial magnetic stimulation
XM	Cross-modal
XMAC	Cross-modal auditory cortex

## **CHAPTER 1: INTRODUCTION**

Brain dysfunction caused by brain injury, sensory deprivation, or motor disability can severely affect human life. Neuroplasticity is the ability of the brain to adapt to environmental changes or brain damage. This plasticity helps the brain to restore the loss of function and operates in sensory, motor, and higher cognitive brain areas. The success of recovery involves the rebuilding of function by sprouting or rewiring of neural connections, and the reorganization of excitatory and inhibitory circuitry. These changes may be limited to a single modality, but research is beginning to reveal that recovery from loss of inputs involves multiple modalities. Sensory deprivation or deafferentation can cause the spared sensory region to be taken over by other sensory modalities (Frasnelli et al. 2011; Kral and Sharma 2012). Traumatic brain injury (TBI) can also cause cross-modal (XM) projections, which affect the reaction time for cognitive tasks in TBI patients (Sarno et al. 2003). Sometimes cross-modal projection can be beneficial (Frassinetti et al. 2005), whereas at other times cross-modal plasticity can be harmful (Lee et al. 2001). Therefore, understanding the mechanisms behind cross-modal plasticity is important for understanding brain development and recovery of brain regions from damage.

In this project, I studied the reorganization of auditory cortex after invasion by visual inputs. I use ferrets with neonatal midbrain damage in which retinal projections are redirected to auditory thalamus (medial geniculate nucleus, MGN), then to auditory cortex. Because of the coexistence of auditory, visual and multisensory neurons in the reorganized auditory cortex (XMAC), this model system allows us to study the effect of cross-modal plasticity without elimination of inputs from any sensory modalities, in contrast to studies employing complete removal of sensory inputs. I investigated the functional changes in XMAC and the mechanisms



by which auditory function is compromised. Brain plasticity exists throughout life. In addition to providing important insights into recovery of sensory systems from sensory dysfunction and neonatal brain damage, results from this study may also help us to understand adult brain injury and sensory/motor deficits.

Because plasticity affects both excitation and inhibition, the following introduction discusses the changes in both excitatory and inhibitory circuits during recovery from sensory deafferentation and deprivation. I first discuss changes in excitation from macro to micro level within single modality, then recovery of brain across modalities. The third part of the introduction discusses changes in inhibition from physiology-level to receptor-level. Lastly, the introduction talks about the advantage of animal models and specific aims.

## **1. Changes in excitatory networks**

### **a) Changes in size of brain structures**

Sensory deprivation, deafferentation, and brain damage can result in shrunken subcortical target nuclei due to loss of their inputs. This can be illustrated using several examples. Olfactory deprivation by unilateral cauterization of the olfactory epithelium results in a smaller olfactory bulb on the deprived side (Benson et al. 1984). After destruction of vibrissal follicles, the nucleus interpolaris of the trigeminal nuclear complex is shrunken in mice (Hamori et al. 1986). A reduction in the volume of cochlear nuclei also occurs in the brainstem of ferrets with cochlear lesions (Moore and Kowalchuk 1988). In the visual system, neonatal monocular enucleation causes significant reductions in the volume of the dorsal lateral geniculate nucleus (dLGN), the visual cortex, and the number and average soma radius of geniculate neurons (Dehay et al. 1996; Trevelyan and Thompson 1995). Lesion of the occipital cortex can also cause reductions in the

volume of LGN and the lateral posterior nuclei of the thalamus (Restrepo et al. 2002). In contrast to the effects of loss of sensory input, sensory experience can increase the volume of related brain regions. Hippocampus is associated with spatial navigation. A study using Magnetic Resonance Imaging (MRI) on London taxi drivers found that their posterior hippocampi were significantly larger than those of normal subjects, indicating an experience-dependent increase in the size of the affected brain regions (Maguire et al. 2000).

#### **b) Changes in topographic representation**

In addition to shrinkage of subcortical nuclei, sensory deprivation, deafferentation, and brain damage can induce cortical reorganization. Much of sensory cortex is topographically organized (Kaas 1997). The topographic occupation of sensory inputs can be modified by experience and sensory deprivation. Loss of sensory inputs can cause cortical areas to respond to adjacent inputs that represent surrounding regions at receptor sheets or to contralateral inputs. These activity-dependent reductions in topographic area have been found in somatosensory cortex (Merzenich et al. 1983), visual cortex (Shatz and Stryker 1978), and auditory cortex (Robertson and Irvine 1989). In contrast to sensory deprivation and deafferentation, sensory experience can expand cortex that responds to certain stimuli. The cortical representation of musical scales in the auditory cortex of skilled musicians is much larger than that of normal subjects (Pantev et al. 2003). These expansions of auditory representations also occur in animal models with overexposure to selected tone frequencies since birth (Zhang et al. 2001).

#### **c) Sprouting in the central nervous system after loss of inputs**

After loss of inputs, the axons of nerve cells in the central nervous system normally degenerate. Because damaged nerves generally cannot regenerate in the central nervous system, sprouting of

remaining afferents to the deafferented brain area is a way to compensate for the loss of excitatory drive. Sprouting can come from the perilesional area, ipsilateral subcortical or cortical areas, and/or contralateral areas. Chronic peripheral nerve injuries can cause central somatosensory neurons to respond to afferents from undamaged peripheral axons (Kalaska and Pomeranz 1982), which reflects the sprouting or expansion of remaining afferents (Florence and Kaas 1995). In the visual system, after monocular enucleation, retinogeniculate inputs from the remaining eye sprout to LGN and the commissural connection is strengthened (Toldi et al. 1996). Corticothalamic inputs are also elevated after visual deafferentation (Somogyi et al. 1987). In addition, sprouting can occur within cortical areas. Binocular retinal lesions induce axon sprouting of long-range neurons that project laterally to non-deprived visual cortex (Darian-Smith and Gilbert 1994; Obata et al. 1999). An increase in intracortical connectivity was reported in the somatosensory cortex of macaque monkeys who had undergone trauma to a forelimb (Florence et al. 1998). Many times, sprouting is accompanied with change of topographic representation after sensory deprivation or deafferentation (Jones 2000).

#### **d) Changes in synaptic density**

At the cellular level, one effect of sensory deprivation and deafferentation is a decrease in synaptic density. Binocular deprivation decreases synaptic density of subcortical afferents in cat visual cortex (Turlejski and Kossut 1985). Whisker trimming from birth decreases symmetrical synapses and thalamocortical synapses (Sadaka et al. 2003) and dendritic spine density in layers 1 and 2/3 of barrel cortex (Briner et al. 2010). A decrease in dendritic spine density has also been found in visual cortex of visually-deprived animals (Montey and Quinlan 2011). In some cases, a decrease in axon and bouton density results from sensory deafferentation (Wimmer et al. 2010).

### **e) Modulation of synaptic strength (LTP, LTD)**

At the synaptic level, the adaption of the brain to a changing environment can be reflected by strengthening or weakening connections between synapses. Carla Shatz famously described this phenomenon as “cells that fire together, wire together” (Katz and Shatz 1996; Shatz 1990). Long term potentiation (LTP) represents an increase in synaptic strength following a brief but strong stimulation. Long term depression (LTD) represents a decrease in synaptic strength following a weak stimulation. Because synaptic strength relies on activity, loss of sensory inputs by sensory deprivation, deafferentation, or brain damage can significantly affect LTP and LTD.

#### **i) LTP**

Sensory deprivation can result in the reduction in size of target cortical areas and the expansion of neighboring cortical areas. Whisker deprivation alters short-term synaptic dynamics in barrel cortex (Finnerty et al. 1999; Fox 2002), increases the probability of inducing LTP, and decreases the probability of inducing LTD in barrel cortex (Hardingham et al. 2011). In visual cortex, visual deprivation facilitates LTP (Philpot et al. 2003) and depresses LTD (Kirkwood et al. 1996).

#### **ii) Neurotransmitter systems involved in plasticity**

N-methyl-D-aspartate (NMDA) type of glutamate receptors play an important role in LTP (Bear and Colman 1990; Bear et al. 1990). The ratio of two subunits, NR2A and NR2B, is subject to change during the critical period and this ratio affects synaptic plasticity. Insertion of NR2A in the membrane can shorten NMDA receptor currents, thereby decreasing excitation (Fagioli et al. 2003), whereas NR2B has the opposite effect. Visual deprivation by dark rearing in rats induces an upregulation of NMDA receptor function in visual cortex (Philpot et al. 2003), which

contains a higher proportion of NR2B and a longer duration of NMDA current than in light-reared rats (Philpot et al. 2001). In contrast, visual experience increases the ratio of NR2A/2B in visual cortex. As little as one hour of exposure reverses the effect of dark-rearing (Quinlan et al. 1999).

## **2. Cross-modal plasticity**

In addition to the post-injury compensation that occurs within brain areas responding to a single modality, compensation from cross-modal plasticity may help sensory-deprived and – deafferented animals and human subjects to overcome the loss of one sense.

### **a) Blindness**

Long-term visual deprivation leads to cross-modal plasticity.

#### **i) Human subjects**

Numerous studies have reported that auditory ability in blind people is better than sighted people. Blind humans exhibit supra-normal abilities in locating auditory targets (Voss et al. 2004) and respond to auditory tasks faster than normal subjects (Collignon and De Volder 2009). Magnetic resonance imaging (MRI) studies have shown that the visual cortex of blind patients is activated when sounds are presented (Kujala et al. 1995). Furthermore, when blind users wear a device that translates visual stimuli into auditory sensations, transcranial magnetic stimulation (TMS) in visual cortex impairs object recognition, further suggesting that visual cortex is recruited for decoding images by sound (Merabet et al. 2009).

Improved tactile ability also occurs in blind humans (Wittenberg et al. 2004). Primary visual cortex in blind patients can be activated by Braille reading, suggesting that visual cortex is recruited by somatosensory processing (Sadato 1996). Applying TMS in visual cortex disrupts

tactile perceptions in blind subjects but not in normal-sighted subjects (Cohen et al. 1997; Kupers et al. 2006). Some research argues that cross-modal projections can only be found in early-onset blindness (Cohen et al. 1999), whereas other research suggests that cross-modal plasticity can also occur in a mature brain (Kujala et al. 1997; Kujala et al. 2000).

## **ii) Animal studies**

Animal studies use both enucleated/eye-sutured animals and congenitally blind animals. As seen in studies of blind humans, both somatosensory and auditory functions are improved in blind animals. Behaviorally, visually-deprived cats can locate sound more precisely than normal cats (Rauschecker 1995b; Rauschecker and Knierpert 1994). Physiologically, visual cortical areas (Heil 1991; Kahn and Krubitzer 2002; Newton et al. 2002; Piché et al. 2007) and cortical regions along the anterior ectosylvian sulcus (Rauschecker 1996) are taken over by auditory and/or somatosensory systems after visual deprivation. Anatomically, visual cortex in blind animals receives both somatosensory and auditory inputs (Kahn and Krubitzer 2002; Karlen et al. 2006). Using c-Fos immunohistochemistry, it has been shown that auditory stimulation activates thalamic and cortical visual areas in congenitally anophthalmic mice (Piche et al. 2004). Where do these auditory inputs originate? Anatomical research shows that inferior colliculus can project directly to LGN or visual cortex in blind mole rats (Bronchti et al. 2002; Doron and Wollberg 1994), enucleated hamsters (Izraeli et al. 2002), and anophthalmic mice (Laemle et al. 2006). An increase in the proportion of auditory neurons is also found in multisensory areas such as the superior colliculus after enucleation (Rauschecker 1984). In addition to changes in visual cortex and LGN, visual deprivation also affects somatosensory cortex and auditory cortex. Electrophysiological recordings show an expansion of somatosensory cortical areas in enucleated

rats (Toldi et al. 1994), blind mole rats (Necker et al. 1992), and eyelid-sutured cats (Bronchti et al. 1992; Rauschecker et al. 1992). Compared to normal animals, neuronal density in auditory cortex of enucleated animals is increased (Ryugo 1975) and auditory spatial tuning is sharper (Rauschecker 1995b)

## **b) Deafness**

Long-term auditory deprivation leads to cross-modal plasticity.

### **i) Human subjects**

Although it has been widely accepted that blind patients have supranormal auditory and somatosensory perception, it remains unknown whether deaf people can see better than sighted people. Some research shows that auditory cortex in deaf patients can be activated by visual signals (Finney et al. 2001), whereas other research argues that not all aspects of vision are changed (see Bavelier et al. 2006 for review). Specifically, deaf patients show enhanced peripheral but not central (foveal) visual processing (Dye et al. 2007). Furthermore, visual activation of primary auditory cortex occurred only in deaf subjects with total hearing loss and not in subjects with residual hearing ability (Lambertz et al. 2005), suggesting a competition between sensory inputs from different modalities. The critical period for sensory plasticity is very important for recovery from sensory loss. Early deaf people are more likely to have cross-modal activity than late deaf people (Buckley and Tobey 2011).

### **ii) Animal studies**

Congenitally deaf cats have superior visual ability compared to normal cats (Lomber et al. 2011; Lomber et al. 2010). Electrophysiological recordings in auditory cortex of congenitally deaf mice revealed visual and somatosensory-responsive neurons and an expansion of the primary visual

cortical area (Hunt et al. 2006). Using positron emission tomography, researchers found that glucose metabolism in the primary visual cortex of deaf cats was significantly higher, and glucose metabolism in the primary auditory cortex was significantly lower than that in normal cats (Park et al. 2010). A recent study reported considerable somatosensory rewiring to auditory cortices in animals that were deafened as adults (Allman et al. 2009a). Other auditory cortical areas (auditory field of the anterior ectosylvian sulcus, FAES, and anterior auditory field, AAF) were also found to be visually-responsive in deaf cats (Meredith et al. 2011; Meredith and Lomber 2011).

### **c) Maladaptive plasticity**

Cross-modal interaction can be responsible for abnormal signals, sometimes referred to as phantom perceptions. Tinnitus can be triggered by cross modal sensory inputs (Cacace 2003). In patients who have acute unilateral deafferentation of the auditory system after removing a tumor in the posterior fossal region, tinnitus can be modulated by somatosensory cues such as skin movement (Herraiz et al. 2003). Intracortical facilitation has also been found in tinnitus patients (Langguth et al. 2005). This cross-modal interaction suggests that a maladaptive cortical reorganization underlies some phantom perceptions.

Cross-modal plasticity can have negative effects on auditory performance during rehabilitation of cochlear implant users (Champoux et al. 2009). Cochlear implants are auditory prostheses that are designed for restoring speech perception. In prelingually deaf children with cochlear implants, auditory cortex often cannot respond to auditory signals because it has been permanently taken over by cross-modal inputs (Lee et al. 2001). As a result of this maladaptive



cross-modal plasticity, deaf patients with cochlear implants may exhibit poorer than expected performance in auditory speech recognition tasks (Doucet et al. 2006).

#### **d) Cross-modal plasticity under normal conditions**

Cross-modal activity also occurs in people with normal sensory function. Long-term training in a sensory or motor task can induce cross-modal projections in sensory and motor systems.

Musicians demonstrate great plasticity in cortical organization. When the lips of trumpet players are stimulated at the same time as a trumpet tone, activation in the somatosensory cortex is increased more than it is during the sum of the separate lip and tone stimulation (Pantev et al. 2003). When musicians listen to a rehearsed music piece, their motor cortex shows an increase in excitability than when listening to a non-rehearsed piece (D'Ausilio et al. 2006). Interestingly, skilled Mah-Jong players can “see” visual images by touching Mah-Jong tiles, suggesting that their primary visual cortex is activated by somatosensory cues (Saito et al. 2006).

### **3. Changes in inhibition**

The classical literature on sensory physiology proposes that lateral inhibition from neighboring neurons sharpens excitatory responses to sensory stimuli. Blockade of inhibition enlarges visual receptive fields (Sillito 1975) and decreases orientation selectivity (Sillito 1979; Sillito et al. 1980; Tsumoto et al. 1979; Worgotter and Eysel 1991) in visual cortex. During development, refinement of synaptic connections involves suppression of some responses by increasing inhibition. Following brain damage, sensory deprivation, or deafferentation, in order to maintain the balance between excitation and inhibition, the strength of inhibition is decreased to compensate for the loss of inputs (Murphy 1985; Turrigiano 2011; Turrigiano 1999; Vale and Sanes 2002).

### **a) Physiological changes**

After somatosensory deafferentation, the spared sensory cortex begins to respond to stimuli carried by inputs to the surrounding brain tissue (Kaas et al. 1983; Merzenich et al. 1983b; Wall et al. 1983). After focal retinal lesions, receptive fields in visual cortex are expanded and axonal sprouting of laterally- projecting neurons is activated (Chino et al. 1992; Gilbert and Wiesel 1992). One mechanism underlying this expansion of representational area is removal of the lateral inhibition that normally suppresses the responses to other stimuli. Applying antagonists of GABA<sub>A</sub> receptors to the sensory cortex can alter spike number and receptive fields of neurons, revealing the strength of inhibition. The effect of GABA<sub>A</sub> receptor antagonists is decreased in sensory-deprived and deafferented animals as a result of loss of inhibition (Carrasco et al. 2011; Jung and Shin 2002).

### **b) Changes in expression of receptors, transmitters, and enzymes**

Changes in inhibition at the molecular level involve inhibitory neurotransmitter receptors, the transmitters themselves, and enzymes involved in producing them.  $\gamma$ -aminobutyric acid (GABA) is the main inhibitory neurotransmitter in mammalian central nervous systems. Glutamic acid decarboxylase (GAD) is the synthetic enzyme for producing GABA in neurons. GAD has two isoforms, GAD67 and GAD65, which are universally expressed in the brain. Considerable evidence exists that the expression of GABA, GABA<sub>A</sub> receptors, and GAD are decreased in target tissue after deafferentation. For example, peripheral nerve transection in monkeys induces cortical reorganization and a decrease in GABA expression in somatosensory cortex (Garraghty et al. 1991). Whisker trimming causes a loss of GABAergic neurons (Micheva and Beaulieu 1995b), GABA<sub>A</sub> receptors (Fuchs and Salazar 1998), and both density and proportion of

GABAergic synapses (Micheva and Beaulieu 1995a) in the whisker barrel field of primary somatosensory cortex. In the visual system, monocular deprivation in Old World monkeys (Hendry and Jones 1986; Hendry and Miller 1996) and rats (Ribak and Robertson 1986) reduces expression of GABA and GAD within ocular dominance columns associated with the deprived eye. A decrease in GAD mRNA levels has also been found in deafferented dLGN of cats (Arckens et al. 1998).

#### **4. Choice of Model System**

Many studies have shown that auditory inputs are introduced to LGN and carried to visual cortex in blind animals (Chabot et al. 2008; Chabot et al. 2007; Doron and Wollberg 1994; Piche et al. 2004). Retinal inputs invade MGN in deaf mice (Hunt et al. 2005). The disadvantage of studying deaf and blind animal models is that because the sensory organs are eliminated, it is impossible to study cross-modal plasticity unless a sensory prosthesis is installed. During recovery from sensory dysfunction, cross-modal inputs can interfere with processing of the original sensory modality. Users of artificial cochleae may have undergone invasion of visual inputs to auditory cortex prior to installation of the prosthesis, and it is then more difficult for them to regain auditory ability (Kral and Sharma 2012; Lee et al. 2001). Our model system can address this cross-modal plasticity in a manner that deaf/blind animal models cannot. Research on cross-modal central plasticity can provide important information for understanding the mechanism by which the original function is affected by cross-modal invasion and for design of rehabilitative strategies after recovery from sensory dysfunction and brain injury.

Ferrets are an advantageous model for studying plasticity. The species of pigmented ferret we use has been domesticated for centuries and has been tested as a good model for auditory and

visual research (Kelly et al. 1986; Linden et al, 1981. Moore et al. 1983; Stryker and Zahs 1983). Ferrets are born with a more immature brain than many other mammalian species, including monkeys and cats (Clancy et al. 2001; Gao and Pallas 1999; Herrmann et al. 1994), but in adulthood they have well developed sensory pathways similar to those of cats (Law et al. 1988; Zahs and Stryker 1988; Moore et al. 1983). Their thalamocortical projections do not reach cortex until two weeks after they are born (Herrmann et al. 1994; Linden et al. 1981). The auditory afferents reach the inferior colliculus but have not yet segregated into frequency bands at birth (Brunso-Bechtold and Henkel 2005; Henkel et al. 2007). The eyelids and the ear canals of ferrets open at 4 to 5 weeks after birth, providing an extended postnatal period for manipulating development of the visual and auditory system. This long postnatal period of immaturity provides an opportunity to create cross-modal rewiring. In our model system, neonatal dorsal midbrain lesions on the day of birth cause visual afferents to project anomalously to MGN. The recovered auditory cortex receives both residual auditory inputs and novel visual inputs. This animal model is thus useful for studying cross-modal plasticity.

## **5. Specific aims of dissertation**

**Specific Aim 1 (Chapter 2): Do the residual auditory inputs and the ectopic visual projections compete for limited auditory territory?** After introducing anomalous visual inputs, neurons in AC of cross-modal animals can respond to visual, auditory, or multisensory stimuli. This implies that a cortical area originally representing one modality can be induced to process information from two modalities. Previous anatomical research found that interhemispheric projections between AC on the lesioned side and AC on the unlesioned side were shifted laterally (Pallas et al. 1999), whereas intra-AC connections on the lesioned side were shifted

medially. **I hypothesize that the residual auditory and the ectopic visual inputs compete for auditory cortical territory and that neurons within cross-modal AC are segregated by modality.**

**Specific Aim 2 (Chapter 3): How is auditory function in auditory cortex affected by ectopic visual invasion?** I am also interested in how residual auditory function is affected by reorganization and incorporation of visual processing circuitry. Given that visual inputs occupy part of the originally auditory regions, and that visual neurons are intermingled with auditory neurons, it is possible that the auditory function in cross-modal auditory cortex is impaired by visual invasion. **Therefore, I hypothesize that competition from ectopic visual inputs compromises auditory function in cross-modal AC.**

**Specific Aim 3 (Chapter 4): What are the mechanisms underlying reorganization of cross-modal auditory cortex?** Inhibition plays an important role in establishing response properties in neocortex (Allison et al. 1996; Sillito 1975; Sillito and Versiani 1977). Numerous studies have shown that loss of inhibition is responsible for broadened tuning in sensory-deprived or – deafferented animals. It is possible that inhibition is decreased in the cross-modal AC after recovery from auditory deafferentation by midbrain damage. Alternatively, the coexistence of auditory and visual neurons in cross-modal AC may result in an increase in inhibition in order to prevent possible disruption by one modality of another. **Therefore, I hypothesize that invasion by visual inputs alters inhibition in cross-modal auditory cortex compared to normal AC.**

**CHAPTER 2 COMPETITION AND CONVERGENCE BETWEEN AUDITORY AND  
CROSS-MODAL VISUAL INPUTS TO PRIMARY AUDITORY CORTEX**

**by**

**Yu-Ting Mao, Tian-Miao Hua, and Sarah L Pallas**

J. Neurophysiology. 2011 105:1558-1573.

## **1. Abstract**

Sensory neocortex is capable of considerable plasticity after sensory deprivation or damage to input pathways, especially early in development. Although plasticity can often be restorative, sometimes novel, ectopic inputs invade the affected cortical area. Invading inputs from other sensory modalities may compromise the original function or even take over, imposing a new function and preventing recovery. Using ferrets whose retinal axons were rerouted into auditory thalamus at birth, we were able to examine the effect of varying the degree of ectopic, cross-modal input on reorganization of developing auditory cortex. In particular, we assayed whether the invading visual inputs and the existing auditory inputs competed for or shared postsynaptic targets, and whether the convergence of input modalities would induce multisensory processing. We demonstrate that although the cross-modal inputs create new visual neurons in auditory cortex, some auditory processing remains. The degree of loss of auditory input to MGN was directly related to the proportion of visual neurons in auditory cortex, suggesting that the visual and residual auditory inputs compete for cortical territory. Visual neurons were not segregated from auditory neurons, but shared target space even on individual target cells, substantially increasing the proportion of multisensory neurons. Thus spatial convergence of visual and auditory input modalities may be sufficient to expand multisensory representations. Together these findings argue that early, patterned visual activity does not drive segregation of visual and auditory afferents, and suggest that auditory function might be compromised by converging visual inputs. These results inform possible ways in which multisensory cortical areas may form during development and evolution. They also suggest that rehabilitative strategies designed to promote recovery of function after sensory deprivation or damage need to take into account that

sensory cortex may become substantially more multisensory after alteration of its input during development.

**Keywords:** cross-modal plasticity, sensory substitution, cortical development, traumatic brain injury, stroke

## **2. Introduction**

It is well-documented that loss of sensory drive, whether as a result of sensory deprivation or brain damage, can result in cortical plasticity, especially early in development. The changes in circuitry that occur as a result of this reactive plasticity may help to restore function or may instead prevent restoration of normal function. Although cortical plasticity can involve either intra-modal or cross-modal plasticity, interference with normal function seems more likely to occur as a result of ectopic, cross-modal invasion of the deafferented structure. For example, loss of visual input can lead to auditory activation of visual cortex (Yaka et al. 2000) and loss of auditory input can lead to cross-modal activation of the understimulated auditory cortex by somatosensory or visual inputs (Bavelier and Neville 2002; Fine et al. 2005; Finney et al. 2001; Hunt et al. 2006; Lomber et al. 2010; Neville 1990; Neville et al. 1983; Nishimura et al. 2000; Sharma et al. 2007; Sterr et al. 2003). Cross-modal plasticity is known to interfere with the effectiveness of subsequently implanted cochlear prostheses in humans (Lee et al. 2001; see Sharma et al. 2009, for review). In order to promote restorative plasticity after sensory inputs are compromised and to minimize interference from cross-modal inputs, it would be advantageous to understand how information from existing and ectopic inputs is coordinated, and in particular how cross-modal inputs affect the amount of territory devoted to the processing of the normal inputs.



Previous studies of sensory deafferentation or deprivation using animal models have examined cross-modal plasticity mainly from the perspective of a complete loss of normal input, such as bilateral enucleation or deafening by cochlear ablation. The disadvantage of using blind or deaf animals to study reactive plasticity in sensory cortex is that the original sensory modality can no longer be activated, preventing examination of how ectopic, cross-modal input affects recovery of the original function, whether through natural means or by implantation of a sensory prosthesis.

In this study, we instead employ an approach that brings both normal and cross-modal information to sensory cortex from birth. We tested the hypothesis that cross-modal inputs compete with normal inputs for cortical space. One possible outcome of competition is that the smaller or less active input modality could be suppressed or taken over by the other. Alternatively, segregation of neurons with different response modalities could occur, reducing cortical space available to each. A third possible outcome is that the cross-modal and the normal functions could coexist within the same cortical territory, expanding multisensory processing, or perhaps even converging onto single, multisensory neurons.

Using partial deafferentation of auditory thalamus in neonatal ferrets to examine how establishment of auditory cortical territory is affected by invasion of cross-modal, visual information, we find that, in addition to visual and auditory responses, multisensory responses are present at a rate much higher than that seen in normal auditory cortex. These three response types were not spatially segregated, suggesting that information carried by ectopic visual inputs is not sufficient to induce segregation. Our results demonstrate that primary auditory cortex can support both the original auditory and the novel visual function after recovery from damage to

afferent pathways, and that multisensory function can be induced simply by experimental convergence of two unisensory inputs. They provide insight into how multisensory cortex is created on developmental and evolutionary time scales. Additionally, our findings provide a more thorough understanding of the reorganization of an affected brain area after recovery from sensory damage or deprivation, and have important implications for rehabilitative strategies in patients with damage to sensory pathways.

Preliminary results from some of these experiments have been published previously in abstract form (Mao et al. 2007).

### **3. Materials and Methods**

Partial deafferentation of auditory cortex (AC) and invasion of ectopic visual inputs can be produced in ferret kits if retinal axons are induced to invade auditory thalamus (MGN) (Sur et al. 1988) as a result of neonatal midbrain lesions. The cross-modal auditory cortex (XMAC) in similarly-manipulated animals contains functional visual neurons (Roe et al. 1992; Sur et al. 1988; von Melchner et al. 2000). Auditory and multisensory responses were not reported in these previous studies, perhaps because the aim was a complete deafferentation of MGN.

#### **a) Animals**

Data were obtained from 25 pigmented ferrets (*Mustela putorius furo*) aged 4 months or more (ferrets reach full brain and body size at 16 weeks (Fox and Bell 1998)). Timed pregnant ferrets were obtained from Marshall Farms (North Rose, NY) two weeks prior to parturition. Nursing dams and kits were fed a high fat diet and kept on a 14h/10h light/dark cycle. Kits were weaned at 6-8 weeks of age. Normal ferrets were obtained either from Marshall Farms as adults or bred

in our colony. Non-lactating ferrets were fed Marshall Farms ferret diet and kept on a 12/12 light/dark cycle. Both male and female ferrets were included in the study. All protocols were approved by the Institutional Animal Care and Use Committee (IACUC) at Georgia State University and met or exceeded standards of care established by the USDA and the Society for Neuroscience.

#### **b) Neonatal surgery**

Surgical procedures were similar to those described previously (Pallas et al. 1999). Ferret kits were manipulated within 24 hr after birth. They were anesthetized by isoflurane (1-4%). All surgeries were performed under sterile conditions. After a kit was anesthetized, the skull over the midbrain was exposed and removed with a scalpel. The left superior colliculus and one or both inferior colliculi were then lesioned to varying extents with a heat cautery, and the brachium of the left inferior colliculus was severed with a scalpel blade. The incision was closed using either 6-0 prolene or surgical adhesive (VetBond, 3M, St. Paul, MN). After surgery, the kits were given subcutaneous fluids and a respiratory stimulant (doxapram, 2 mg/kg, SQ) and warmed under an incandescent lamp. Kits were observed carefully until they recovered from anesthesia, and were returned to their dam after they became ambulatory. Analgesics (buprenorphine 0.05–0.1 mg/kg bid) were given as needed to prevent postoperative pain.

#### **c) Preparation for Electrophysiology**

Electrophysiology experiments were done once ferrets reached adult size (>4 months of age). Before induction of anesthesia, atropine (0.4 mg/kg SQ,) and doxapram (2 mg/kg, SQ) were given to counteract bradycardia and to reduce mucosal secretions. Anesthesia was induced by ketamine (40 mg/kg, IM) and diazepam (2mg/kg, IM) or by ketamine (40 mg/kg, IM) and

medetomidine (0.08 mg/kg IM). Dexamethasone (1mg/kg, IM) was given every 24 hr to prevent brain swelling. Animals were intubated and the cephalic or femoral vein was cannulated. Anesthesia was maintained with an IV solution of medetomidine (0.022 mg/kg/hr) and ketamine (5 mg/kg/hr) in lactated Ringer's with 5% dextrose (Bizley and King 2008; Bizley et al. 2005). Atropine (0.06 mg/kg/hr, SQ) was given as necessary to counteract the bradycardia caused by medetomidine. Animals were artificially respired using a small animal ventilator (SAR 830/P ventilator, CWE Inc, Ardmore, PA). Vital signs including EKG, respiration rate, muscle tone, withdrawal reflexes, end-tidal CO<sub>2</sub>, and SpO<sub>2</sub> were monitored during the surgery and recordings to ensure maintenance of adequate anesthesia. Body temperature was maintained at 38° C with a heating pad. Pupils were dilated with atropine ophthalmic drops. Eyes were kept moist with commercial artificial tears solution and protected with custom plano contact lenses (Conforma Inc, Norfolk, VA). The head was stabilized in a stereotaxic device. After the scalp overlying auditory cortex was incised and the muscle was retracted from the skull, two burr holes (at coordinates A5.5 ±L1.5) were drilled for optic chiasm recording/stimulation electrodes. Two tungsten rods with Teflon insulation (0.008 bare, 0.011 coated, A-M Systems, Inc., Carlsborg, WA) connected to a preamplifier were lowered (8~10 mm) while recording responses to strobe light stimulation until a depth yielding strong visual responses was reached. These tungsten rods were then cemented to the skull and connected to a stimulus isolation unit (BAK Electronics, Inc, Mount Airy, MD). A 0.8~1.0 cm diameter craniotomy was drilled over the auditory cortex and the suprasylvian and pseudosylvian sulci were exposed.

*Recording sites:* The ferret AC is located on the middle ectosylvian gyrus, bounded above by the anterior and posterior arms of the suprasylvian sulcus (sss) and below by the pseudosylvian sulcus (pss) (Kelly et al. 1986). In this study, recording penetrations were targeted

to primary auditory cortex (A1) and anterior auditory field (AAF) (Bizley et al. 2005) and were unlikely to impinge on multisensory regions of the sulci surrounding AC for several reasons. First, we avoided the regions close to the sulci. In addition, our recording depths were generally very superficial given that we recorded the first unit in each electrode pass then moved on to the next location in the map. Further, the electrode angle combined with the shape of AC as an inverted parabola is such that increasing recording depth would move away from and not toward the banks of the sulci. These factors taken together argue that it is very unlikely that our recording sites were in the suprasylvian territory, although we cannot exclude the possibility. We cannot exclude the possibility that a few of our recording sites were located in the posterior ectosylvian gyrus, where higher-level auditory fields have been described (Bizley et al. 2005). The dura was removed and AC was covered by either sterile saline or 2% Agar (Fisher Scientific, Fair Lawn, NJ) in sterile saline to protect its surface from desiccation. The right side of the skull was cleaned of tissue and a metal bracket was cemented on the skull to hold it in position. The right ear bar was then released to allow access to the ear for auditory stimulation.

#### **d) Extracellular recording**

The cortical surface was photographed with a digital camera in order to record the location of each recording electrode penetration. A glass-coated tungsten microelectrode (1-2 M $\Omega$ , FHC, Bowdoin, ME) was used to investigate neuronal activity in AC in response to auditory and visual stimuli. Penetration locations were chosen to sample randomly from as many sites within AC as possible while avoiding sulci and blood vessels. The electrode was lowered in 5  $\mu$ m steps up to 2000  $\mu$ m under the pial surface using a hydraulic microdrive (Kopf Instruments, Tujunga, CA).

Once the first unit in each electrode pass was isolated and characterized, another recording location was selected. Most units were isolated within 800  $\mu\text{m}$  of the pial surface.

*Sensory stimuli:* For each penetration, bars of light from a pantoscope and white noise from a loudspeaker were used to search for responsive neurons. The loudspeaker was placed at a  $45^\circ$  angle between the right side and the front of the animal at a distance of approximately 10 cm. Auditory searching stimuli were white noise bursts (5 ms ramp, 40-100 ms duration) with a sound intensity of 60-80 dB SPL, as measured by a sound level meter (model 407764, Extech Instruments, Waltham, MA). After a responsive neuron was found, computer-generated auditory (noise or tones) and visual stimuli (moving or flashing bars of light) were used for testing responses. The speaker was replaced with a calibrated earphone. The earphone was placed in the pinna at the entrance to the ear canal and used to generate noise bursts or pure tone sounds in closed field. (ER-2 insert earphone, Etymotic Research, IL). The earphone was calibrated with a microphone (ER-7C probe microphone system, Etymotic Research, IL) via Sigal software (Tucker-Davis Technologies, Alachua, FL). The normalized file generated by Sigal was used to correct any non-linearities in the earphone output when sound was given. For assessing the responses of single units isolated in each penetration, auditory stimuli were generated by TDT System II hard- and software (Tucker-Davis Technologies, Alachua, FL) and visual stimuli were synthesized and delivered by a VSG card (Cambridge Research Systems Ltd, Kent, England). Light stimuli included moving bars or gratings at eight orientations moving in either direction, presented on a computer screen  $\sim 40$  cm distances from the eyes. Bipolar electrical stimulation of the optic chiasm was applied (single pulses at 0.5-1 mA, 60  $\mu\text{s}$  duration) in addition to light stimuli.

#### **e) Electrophysiological data analysis**

Neural responses were amplified (BAK Electronics, Inc, Mount Airy, MD), filtered (500 Hz to 5 kHz), and monitored on a digital oscilloscope (Hameg Instruments, Mainhausen, Germany). Responses to 10-15 stimulus presentations were gathered from each recording site and digitized at 25 kHz. The evoked responses were averaged and normalized to a sample of spontaneous activity recorded 50 ms before each trial. The recording continued for 1-2 days, after which the animal was deeply anesthetized with sodium pentobarbital (65 mg/kg) for humane euthanasia and harvesting of brain tissue for histological examination.

For each electrophysiological data point, Brainware software (Tucker-Davis Technologies Inc., Alachua, FL) was used off-line to isolate extracellularly recorded spikes derived from single neurons by their waveform. Artifact rejection was set in Brainware to extract biphasic action potential candidates with both peaks exceeding background noise level. Spikes with similar shape and duration were shown as clusters in the data-sorting window. Post-stimulus time histograms (PSTHs) of the selected single units were generated using the same software package. The mean and standard error of the number of spikes to each stimulus presentation were calculated after subtracting spontaneous activity. Response latencies were determined by the time between stimulus presentation and the time of the first bin in the PSTH that reached at least 20% above background firing rate. Multisensory units were defined either as neurons that responded both to visual and auditory stimuli or as neurons that only responded to one modality but could be significantly modulated by stimulation with the other modality (Stein et al. 1993). Statistically significant differences were determined by comparing the number of spikes per

sweep (obtained from the PSTHs) as a response to different stimulus modalities using Student's t-test ( $p < 0.05$ ). The proportion of response types was compared across groups.

For calculating the spatial distribution of response types, the area of each AC was normalized to a standard circle with a radius of 1. The locations of recorded units were reconstructed on this normalized AC. In order to analyze the distribution of different neuron types in AC, we divided AC into four quadrants numbered 1 to 4 as seen in **Figure 2.1**. The quadrants were not intended to correspond to particular auditory cortical areas, although quadrants 2 and 3 overlap more with the anterior auditory field (AAF) and quadrants 1 and 4 overlap more with primary auditory cortex (A1). Two lines were drawn along the anterior and posterior arms of the suprasylvian sulcus to form angle A. The third line was drawn just above the tip of the pseudosylvian sulcus and perpendicular to the dividing line of angle A. The center of the internally tangent circle (point 0) was defined as the intersection of the dividing lines of angle A and angle B.

Because the shape of the AC in each individual is unique, and the location of recording sites differed somewhat across animals, we examined whether pooling data from different animals into one polar plot would bias the data. We performed a heterogeneity Chi-square analysis to test the homogeneity of data from each group. Heterogeneity Chi-square is a statistical test based on the premise that if the samples are homogeneous, then the value of  $\chi^2_{\text{sum}}$  should be close to the value of  $\chi^2_{\text{pooled}}$ . Therefore, the heterogeneity Chi-square value is designated ( $\chi^2_{\text{het}} = \chi^2_{\text{sum}} - \chi^2_{\text{pooled}}$ ). The null hypothesis should be rejected if there is a large  $\chi^2_{\text{het}}$  (for details, see Sheskin 2004). If the value of the sum of Chi-squares from each sample is not significantly different from the value of the pooled Chi-squares ( $p > 0.05$ ),  $\chi^2_{\text{het}}$  will be small and



the data can be grouped. Applied to our data, the test showed that the electrode penetrations in the four quadrants of normal AC were homogenously distributed ( $p>0.05$ ). The same was true for small lesion and large lesion groups ( $p>0.05$ ). Therefore, data from all ACs in each group were pooled into one polar plot. A Chi-square analysis was then applied to determine whether recorded neurons were randomly distributed across quadrants independent of their response type. In cases where the distribution was not random ( $p<0.05$ ), an Analysis of Residuals (R value) was calculated to show which quadrant(s) contained the unexpected distribution.

To examine whether neurons with similar responses were clustered, we calculated the average distance between recording sites by translating X and Y values obtained from normalizing AC to polar coordinates on the standard circle using Microsoft Access database software. The distance between each pair of single units was calculated and exported to a spreadsheet. The average distances from each single unit to other auditory, visual or multisensory units were calculated. Then we compared the mean of average distance between pairs across groups.

Electrophysiological data were statistically analyzed using Sigmastat software (Systat Software Inc, Chicago, IL) and plotted with Sigmaplot (Systat Software Inc, Chicago, IL). A one way ANOVA for multiple groups was used. A Tukey post hoc test was used for groups that had uneven numbers, and a Fisher's LSD post hoc test was used for groups that had even numbers of members. A Mann-Whitney U test for non-normally distributed data was used for two group comparisons. Means are given with standard errors of the mean ( $\pm$  SEM) throughout.

#### **f) Assessment of lesion size**

##### **i) MRI Scanning:**

Magnetic Resonance Imaging (MRI) was performed in some lesioned ferrets to obtain an assessment of the midbrain lesions prior to electrophysiological recording. Atropine (0.4 mg/kg SQ) and doxapram (2 mg/kg SQ) were given 5 min prior to sedation. Then, medetomidine (1 mg/kg, IM) and diazepam (2 mg/kg, IM) were given to sedate the animal. Animals were put into an MRI cradle with a heating pad underneath to maintain body temperature. End-tidal CO<sub>2</sub>, SpO<sub>2</sub>, pulse rate, respiration rate, and body temperature were monitored during the entire process. MRI scanning of the midbrain was normally finished within 30 min. Animals were taken out of the cradle and given atipamezole (0.5 mg/kg, IM) to reverse the effects of the medetomidine. Animals were then continuously monitored over the next 1 to 2 hr before being returned to the colony to ensure that they were completely recovered from the drugs.

## **ii) Histology:**

After electrophysiology, animals were deeply anesthetized with sodium pentobarbital (65 mg/kg) for euthanization and perfusion with phosphate-buffered saline (PBS) followed by 2-4% paraformaldehyde in 0.1 M PB. Brains were extracted, postfixed in 4% paraformaldehyde in 0.1 M phosphate buffer (PB) for 24 hr, and stored in 30% sucrose in 0.1 M PB at 4° C. After the tissue was infiltrated by the sucrose solution, it was sectioned frozen at 50 µm in the coronal plane for reconstruction of lesions. A series of sections at 200 µm intervals was stained for Nissl substance using cresyl echt violet.

## **iii) Analysis:**

The size of the residual central nucleus of the inferior colliculus (ICc) and the superficial layers of the superior colliculus (sSC) in each animal's midbrain was measured from Nissl stained sections with a Zeiss microscope using Zeiss Axon Vision 3.1 software (Carl Zeiss

MicroImaging, Inc., Thornwood, NY). The borders of ICc and sSC (areas indicated by the dashed line in Figure 2A, B, and dark areas in Figure 2C) were very clear on our Nissl stained sections. The volume of sSC and ICc was calculated as the sum of each measured areas multiplied by 200  $\mu\text{m}$ . Proportions of residual midbrain area and volume in the lesioned animals were calculated by comparison with an average midbrain volume derived from five normal animals. Lesioned animals were sorted into small and large lesion groups as determined by these measurements (Figure 2.2).

#### **4. Results**

Twenty-five ferrets in total were used in this study. Ten were entered in the normal group and 15 received neonatal lesions leading to cross-modal plasticity. Below we characterize and compare the response properties of the 401 AC neurons recorded in the normal group and the 573 AC neurons recorded in the lesioned group.

##### **a) Normal AC contains primarily auditory responses plus rare multisensory responses**

Normal animals were used in the experiments as a negative control for the effects of the midbrain lesion. Although primary sensory cortices are traditionally defined as brain areas that respond only to a single sensory modality, recent research has challenged this view by reporting the existence of multisensory neurons and neurons responding to other modalities in primary sensory cortices. Bizley and colleagues have reported that primary auditory cortex in ferrets does contain some auditory/visual bisensory and some visual neurons (Bizley et al. 2007). In order to investigate whether and to what extent primary auditory cortices (A1 and AAF) in normal ferrets can respond to visual stimuli under our experimental conditions and methods of analysis, we characterized the response modality of 401 single neurons in AC of 10 normal animals using *in*

*vivo* extracellular recording. We defined auditory neurons and visual neurons as those that responded to only one modality. Multisensory neurons were defined as those that either responded to both modalities or responded to one modality but were significantly modulated by stimulation from the other modality (criterion of  $p < 0.05$ , t-test on number of spikes to single vs. bimodal stimuli, 10 trials or in some cases 15 trials, data obtained from PSTHs) (see Meredith and Stein 1986). We found that 11% of the 401 neurons recorded in AC of normal ferrets were multisensory. These multisensory neurons responded both to sound stimuli and to electrical stimulation of the optic chiasm ( $n=45$ , **Fig 2.3A**), but not to stimulation by light. No visual-only neurons were found in our sample of normal animals.

#### **b) XMAC contains visual, auditory, and multisensory response types**

We next tested whether auditory responses remain in AC of lesioned animals and whether the ectopic visual inputs to MGN were associated with an increased proportion of multisensory or visual-only units. We predicted that XMAC's residual inputs from auditory areas would preserve auditory responsiveness, despite earlier reports to the contrary (Roe et al. 1992; Sur et al. 1988). Callosal connections between XMAC and AC in the unlesioned hemisphere exist (Pallas et al. 1999), and the inferior colliculi are incompletely lesioned in many cases. These inputs could confer auditory responses on XMAC. In support of this prediction, our data showed a high proportion of auditory neurons in XMAC despite the presence of ectopic visual responses. Multisensory neurons were also found. In all of the lesioned animals considered together, the relative proportion of auditory-only neurons was 56%, the proportion of multisensory neurons was 32%, and the proportion of visual-only neurons (optic chiasm and/or light driven) was 12% (**Fig 2.3B**). Post-stimulus histograms are shown for each response type in **Fig 2.3C-F**. The

existence of auditory neurons in XMAC reveals that the neonatal midbrain lesions and ectopic visual inputs do not eliminate or suppress the auditory function of AC. The presence of a higher than normal proportion of multisensory neurons in XMAC suggests that auditory and visual inputs are more likely to converge in XMAC than in normal AC.

**c) Continuous and categorical differences in response type occurred by altering the extent of midbrain sparing**

The above finding that auditory and visual responses can be made to coexist in XMAC allowed us to address the relationship between the two response types in more detail, and in particular to examine how the induction of visually-responsive areas in auditory cortex would affect normal auditory processing. In patients with a sensory deficit or damage that deafferents a brain area, invasion of cross-modal inputs often occurs to varying extents, and at some point may become maladaptive. We wished to determine whether progressively increasing the extent of visual invasion of XMAC would result in competition (intermodal suppression) or cooperation (multimodal convergence) between modalities. Given previous reports that auditory responses are absent in XMAC (Roe et al., 1992), we wanted to test whether increasing levels of visual input activity would suppress or eliminate auditory responses. Such a finding could explain why we observed auditory responses in our data set whereas none were found in the Roe et al. (1992) study in which very large lesions were made.

In order to investigate the effect that increasing degrees of invasion of ectopic visual inputs would have on auditory responsiveness in AC, we measured the midbrain lesion size in each ferret using histological techniques, and compared this measure with the relative proportions of each response type in a systematic fashion. We quantified midbrain size of the

lesioned animals by comparing the volume of the left and right central nucleus of the inferior colliculus (ICc) and the left and right superficial superior colliculus (sSC) in each lesioned animal to that averaged across five normal animals used as a standard of comparison (cf. Figure 2.2, Table 2.1).

Next, it was necessary to demonstrate that increasing the lesion size would affect the relative proportions of auditory, visual, and multisensory neurons in XMAC. We found that midbrain lesion size was correlated with the proportion of auditory and visual response types in an interesting way. In general, overall lesion size was correlated with the proportion of visual units and inversely correlated with the proportion of auditory units (Fig 2.4A, D). There was a tight relationship between spared sSC size and visual responsiveness ( $r = -0.7$ ,  $p = 0.006$ ) and a correlation between spared ICc size and visual responsiveness ( $r = -0.48$ ,  $p = 0.085$ ; compare Figs 2.4B and C). These results suggest that establishment of visual neurons in XMAC relies more on damage to visual midbrain than to auditory midbrain. For auditory responsiveness, the correlations with total midbrain size, sSC size, and ICc size were similar to each other (Figs 2.4D-F). These data show that residual sSC volume predicts the relative proportions of visual and auditory neurons, whereas ICc volume is predictive only of the proportion of auditory neurons, demonstrating that the amount of retinal target area lost (SC lesion) is crucial for determination of neuron types in XMAC when both ICc and sSC are lesioned. It was also notable that even complete ablation of left IC did not eliminate auditory responses in XMAC (Table 2.1). We did not find any correlation between the proportion of multisensory units and the amount of spared auditory or visual midbrain.

The relationship between lesion size and proportion of auditory units (Fig **2.4D**) appeared roughly linear, with increasing lesion size correlating with a decreasing proportion of auditory responses. In terms of visual responsiveness, however, as may be predicted by examination of Figure **2.4A** and **2.4B**, there was evidence of an exponentially decreasing relationship (Fig **2.4A**,  $r=0.8$ ,  $p=0.0007$ ; Fig **2.4B**,  $r=0.88$ ,  $p<0.0001$ , exponential fit) or perhaps a categorical response to lesion size rather than a progressive, linear response.

XMAC contained light-responsive neurons (that is, neurons that responded to light as well as to optic chiasm stimulation) only in animals in which most of the left midbrain was ablated (less than 10% residual left midbrain). In animals with more than 10% residual left midbrain there were no light-responsive neurons. We used this categorical distinction to divide the cases into a large lesion or small lesion group, respectively, and conducted further analyses according to these categories. We performed statistical analysis to examine whether small vs. large lesion groups have significantly different residual midbrain sizes. We found that the spared left midbrain size of animals in both the large ( $5.4 \pm 1.76\%$ ,  $n=5$ ) and small lesion groups ( $43.7 \pm 5.34\%$ ,  $n=10$ ) was significantly smaller than that of the normal group (ANOVA,  $p<0.001$ , **Fig 2. 5**). The spared midbrain size in the large lesion group was also significantly reduced compared to that in the small lesion group (Tukey post hoc test,  $p<0.001$ ), allowing us to consider these groups along with the unlesioned group as distinct categories for statistical analyses.

#### **i) Responsiveness to light requires minimal sparing of visual midbrain**

In order to determine the relationship between lesion group membership and distribution of response types, we calculated the relative proportions of auditory, visual, and multisensory responders in each group. This analysis allows us to compare the proportion of neuronal

responses among groups, including the proportion of multisensory neurons that has not been shown in the correlation analysis.

Animals in the small lesion group had few visual neurons in XMAC ( $1.8\% \pm 0.96\%$ ,  $n=8$  of 414 neurons from 10 animals) and those neurons responded to electrical stimulation of the optic chiasm (OX) but not to light. The low proportion likely results from the minimal redirection of retinal axons to MGN in small-lesion cases (Angelucci et al. 1998). In contrast,  $33.8 \pm 7.92\%$  of recorded neurons in the large lesion group were visual neurons ( $n=61$  of 159 neurons from 5 animals, **Fig 2.6A**). Of the 61 visual neurons, 48 of them (78.7%) responded to light in addition to optic chiasm stimulation. This is a significant increase (Mann-Whitney U-test,  $p=0.003$ ) and represents a categorical difference between the large and small lesion groups. These results indicate that considerable visual information was reaching AC in the large lesion animals.

## **ii) Auditory neurons become visual rather than converting to multisensory neurons**

Although auditory neurons were found in all groups, the proportion of auditory neurons to total recorded neurons in both groups of lesioned animals varied with lesion size (large lesion group:  $43.8 \pm 6.47\%$ ,  $n=65$  of 159; small lesion group:  $60.0 \pm 3.22\%$ ,  $n=256$  of 414, normal group:  $88.6 \pm 1.65\%$ ,  $n=356$  of 401, ANOVA,  $p<0.001$ , **Fig 2.6B**). Furthermore, the proportion of auditory neurons in large lesion groups was less than that in the small lesion group ( $p=0.003$ , Tukey post-hoc). These results suggest that increasing lesion size resulted in an increase in visual neurons largely at the expense of auditory neurons, rather than a conversion of auditory neurons into multisensory neurons.



### **iii) Multisensory neurons were found in all groups**

We found that neurons in AC of all three groups responded to both auditory and optic chiasm stimulation (multisensory neurons in the large-lesion group: mean  $22.4 \pm 5.60\%$ ,  $n=33$  of 159; in the small-lesion group: mean  $38.3 \pm 3.51\%$ ,  $n=150$  of 414, in the normal group: mean  $11.5 \pm 1.65\%$ ,  $n=45$  of 401, ANOVA,  $p < 0.001$ , **Fig 2.6C**), but interestingly that the proportion of multisensory neurons in the small-lesion group was significantly higher than the proportion of multisensory neurons in the normal group (Tukey post hoc test,  $p < 0.001$ ) and in the large lesion group (Tukey post hoc test,  $p < 0.05$ ). Although the large-lesion group contained more multisensory neurons than did the normal group, statistical analysis indicated that there was no significant difference (large vs. normal,  $p = 0.11$ ). This probably results from the large proportion of purely visual neurons in the large lesion group, and suggests that the response of XMAC to minimal invasion of visual activity (making multisensory neurons) is different from its response to substantial visual influence (making purely visual neurons). This result has interesting implications for rehabilitation strategies for patients with sensory loss or brain damage that cause cross-modal redirection of afferent inputs. Selective stimulation of the original modality would be expected to produce very different results depending on the amount of redirection.

### **d) Auditory and multisensory neurons have distinct spatial distributions in normal animals**

To determine whether neuronal responses to different modalities are preferentially located in one or multiple regions of AC, we calculated the distribution of recorded neurons in the normal AC across the four quadrants (cf. Fig 2.2). **Figure 2.7** shows examples of the penetration locations and neuronal response types in recordings of normal AC from 8 of the 10 normal animals. We found that auditory neurons were distributed randomly across the entire AC, but most

multisensory neurons were located laterally. Using statistical analysis, we found that auditory neurons were evenly distributed (Chi-square,  $p > 0.05$ ). However, the distribution of multisensory neurons was skewed to one of the four quadrants (Chi-square,  $p < 0.001$ , analysis of residuals,  $R = 6.93 > R_{0.001} = 3.29$ ) (**Figure 2.8**). The polar plot (Fig **2.8A**) shows that the population of multisensory neurons was preferentially located in the lateroposterior (quadrant 4; see Fig **2.2**), in normal animals. The observed incidence of multisensory neurons in quadrant 4 was significantly higher than the expected value of 25% (Fig **2.8B**). These data show that auditory responses in normal animals are distributed evenly across the AC, whereas multisensory neurons are preferentially located lateroposteriorly.

**e) The spatial distribution of auditory, visual, and multisensory neurons in lesioned animals was different from normal**

**i) Spatial distribution of neuronal response types in small-lesion cases**

We next investigated whether neurons with auditory and visual responses in AC of small lesion animals would be segregated as seen for multisensory neurons in normal auditory cortex. Such clustering would likely facilitate efficient processing of visual information separately from auditory information after the midbrain injury. Eight examples of raw data are presented in **Figure 2.9** to indicate recording locations and neuronal response types in each small lesion animal. Pooled data from all 10 small lesion animals showed that auditory neurons in small lesion AC were randomly distributed across the four quadrants (Chi-square,  $p > 0.05$ , **Fig 2.10**). Multisensory neurons could also be found in any of the quadrants in XMAC of small-lesion animals, but were more likely to be found in Q4. The number of multisensory neurons in the anteromedial quadrant Q1 was below the expected value for a random distribution (Chi-square,

$p < 0.01$ , analysis of residuals,  $R = 2.79 > R_{0.01} = 2.58$ , Fig. **2.10B**), and the number in the lateroposterior quadrant Q4 was above the expected value (Chi-square,  $p < 0.001$ , analysis of residuals,  $R = 3.61 > R_{0.001} = 3.29$ , Fig. **2.10B**). In addition to auditory and multisensory neurons, we recorded some purely visual neurons (8 out of 414 neurons) that were located exclusively in lateral AC (dark triangles in Fig. **2.10**). These results suggest that ectopic visual inputs can invade the entire AC, even though they are concentrated in the lateroposterior quadrant. This is interesting given the result that quadrant Q4 already contains multisensory neurons in normal animals (Fig. **2.8**). Although the multisensory neurons were preferentially located in the lateroposterior quadrant of both normal and small lesion animals, the extent of clustering in small lesion animals was reduced compared to that in normal animals. These findings imply that the random distribution of ectopic visual inputs to XMAC may weaken the tendency of visually-responsive neurons in normal AC to cluster.

In addition to the analysis of distribution of neuronal responses in the four quadrants, we measured the distance between each single unit and its neighbors in order to further test the segregation hypothesis. We found that the average distance between pairs of sound-responsive neurons was significantly shorter than the average distance between auditory and multisensory neurons (ANOVA,  $p < 0.05$ , A-A vs. A-M, Fisher LSD method, Fig **2.10C**). This finding suggests that auditory neurons are more likely to cluster with each other than with multisensory neurons. This result may be attributable to the smaller number of multisensory responses compared to auditory responses in XMAC of small lesion animals. We were prevented from including visual responses in the analysis because some animals had only one visual neuron in the entire AC.

## ii) Spatial distribution of neuronal response types in large lesion cases

Because some clustering of neuronal response types was seen in AC of small lesion cases, we wondered if the more extensive visual inputs resulting from larger lesions would either promote or reduce clustering of neuronal response types in XMAC. Note that it is difficult to generate animals with large midbrain lesions, thus there is a smaller number ( $n=5$ ) of large lesion cases compared to small lesion cases (**Fig 2.11**). We found that auditory, visual, and multisensory neurons were evenly distributed across the four quadrants of AC in large lesion cases (Chi-square,  $p>0.05$ , **Fig 2.12**). This was different from normal and small lesion cases, in which the multisensory and visual neurons were preferentially located in the lateroposterior quadrant Q4. Although there was variation in the sample, there was no significant degree of segregation of neuronal response types in XMAC of the large lesion group. These results suggest that the ectopic visual inputs introduced by the large neonatal midbrain lesions projected evenly across the entire AC rather than being more strictly segregated as we expected.

As with the small lesion group, we measured the distance between pairs of auditory, visual, and multisensory neurons in the large lesion group to test the hypothesis that neurons with similar response properties would be clustered together. We compared the average distance between pairs of auditory neurons to the average distance between auditory-visual pairs and auditory- multisensory pairs of neurons. We did not find any significant tendency to cluster (ANOVA,  $p>0.05$ , A-A vs. A-M or A-V, Fisher LSD method, **Fig 2.12C**), nor did we find any significant clustering when we compared average distance between pairs of visual neurons to the average distance between visual-auditory and visual- multisensory pairs (ANOVA,  $p>0.05$ , V-V vs. V-A or V-M, Fisher LSD method, **Fig 2.12C**). We did find that the average distance

between pairs of multisensory neurons was significantly shorter than the average distance between multisensory -visual pairs (ANOVA,  $p < 0.05$ , M-M vs. M-V, Fisher LSD method, Fig 2. 12C), but found no significant difference between M-M and A-M pairs. These results suggest that multisensory neurons are closer to each other than to visual neurons. Overall, these results are in agreement with our polar plot data and further suggest that auditory and visual inputs to AC of large lesion animals do not segregate.

**f) The latency of visually-responsive neurons to optic chiasm stimulation differed between normal and lesioned animals**

Previous research demonstrated that ectopic visual inputs to XMAC originate from the retino-MGN-AC projection (Pallas et al. 1990; Sur et al. 1988), whereas visual inputs to normal AC come from corticocortical projections (Bizley et al. 2007). We found clustering of multisensory neurons lateroposteriorly in normal AC, whereas in AC of large lesion animals, multisensory neurons were randomly distributed. To investigate whether visual inputs to multisensory and visual neurons in lesioned animals came from expanded corticocortical projections or from retino-MGN-AC afferents, we compared the latency of responses to optic chiasm stimulation. The latency to optic chiasm stimulation of the multisensory neurons recorded in normal animals ( $n=40$ ) was  $13.4 \pm 1.75$  ms whereas the latency to optic chiasm stimulation of multisensory and visual neurons from lesioned animals was  $8.76 \pm 1.03$  ms ( $n=86$ ) in the small lesion group and  $5.72 \pm 0.65$  ms ( $n=65$ ) the large lesion group, which was significantly shorter (ANOVA, small vs. normal  $p=0.015$ , large vs. normal,  $p < 0.001$ , Fig 2.13). No significant difference was found between small and large lesion groups. The comparison between latency of response to optic chiasm in normal visual cortex and Xmodal auditory cortex was reported in a previous study in

which the authors showed that visual neurons in Xmodal AC have longer latencies than visual neurons in visual cortex (Roe et al. 1992). Taken together, these results provide further evidence to support the contention that normal AC receives its visual inputs indirectly, perhaps from other cortical areas, but not directly from thalamus, whereas XMAC receives visual inputs more directly, probably from the retina to MGN to AC pathway.

## **5. Discussion**

Early lesions to sensory structures in one sensory modality can result in profound reorganization across multiple sensory pathways, due to the many interconnections between structures (Karlen et al. 2006; Kingsbury et al. 2000; Kingsbury et al. 2002; Pallas et al. 1990; Pallas and Sur 1993). The fact that such reorganization can result in cross-modal connections has important clinical implications for recovery from perinatal brain damage because the different modalities could either cooperate or compete with each other. We found that auditory neurons and multisensory neurons coexist with visual neurons in XMAC after recovery from neonatal midbrain damage. The existence of multisensory neurons indicates that the two modalities can converge and cooperate to activate individual target neurons, rather than competitive suppression of one input by the other. The proportions of auditory and visual neurons were directly related to the amount of residual midbrain tissue. Rather than being segregated from visual neurons, auditory neurons were evenly distributed across XMAC of lesioned animals, and an increase in the number and a broadening of the distribution of multisensory neurons was observed. These findings are reminiscent of phenomena such as acquired auditory-tactile synesthesia, which was reported in a patient following recovery from a thalamic infarct. In this patient, sound induced BOLD responses in somatosensory cortices (Beauchamp and Ro 2008; Ro et al. 2007). Collectively,

these results suggest that both cooperation and competition between the two input modalities are involved in the reorganization of sensory areas after damage to sensory inputs.

**a) Auditory function is retained in core auditory cortical regions despite visual inputs**

Previous studies using neonatal midbrain lesions in ferret kits focused on visual responses in XMAC (Roe et al. 1990; Roe et al. 1992; Sur et al. 1988; von Melchner et al. 2000). Those studies, which used very large midbrain lesions, reported that there was no residual auditory function in cross-modal AC. We used lesions of varying size, and find that considerable auditory function is retained despite the visual input, especially in animals with smaller lesions. This fortuitous finding allowed us to examine the effect of different degrees of cross-modal input on development and plasticity of auditory cortex in response to deafferentation.

Our finding that a large proportion of the neurons in XMAC retain auditory responsiveness supports the hypothesis that residual auditory afferents can compensate even for complete loss of the ipsilesional inferior colliculus, but raise the question of where the auditory information derives from. The most likely sources of auditory input to XMAC are the ipsilateral MGN (as a conduit of input from spared contralateral ICc (Angelucci et al. 1998; Moore et al. 1998) and the contralateral auditory cortex (via the corpus callosum (Pallas et al. 1999)) (**Fig 2. 14**). Whether the auditory neurons in XMAC function as they would in normal animals is an important question and is the subject of a current study. Preliminary results suggest that function is somewhat compromised (Mao and Pallas 2010).

## **b) Competition between visual and auditory inputs may determine response type**

Our results show that with decreasing size of IC and SC, the percentage of recorded neurons responding to sound went down, and the percentage of visual neurons went up. These results are consistent with competition as an explanatory mechanism (Crair et al. 1997; Hubel and Wiesel 1962; Stryker 1982; Stryker and Harris 1986). During recovery, when the normal sensory drive may be maximally compromised, activity-dependent processes may allow invading, cross-modal inputs to out-compete preserved inputs from the normal pathway. These findings suggest that optimizing rehabilitation of patients suffering from sensory dysfunction or brain damage will require not only increasing the activity of the original inputs but also decreasing activity in the ectopic inputs. For example, rearrangement of somatosensory circuits in early blind humans can degrade somatosensory representations (see Sathian and Stilla 2010 for review; Sterr et al. 2003) and cross-modal changes in deaf patients can interfere with the success of cochlear implants (Lee et al. 2001).

Our findings may also be of relevance to studies on recovery from partial deafness following cochlear damage. Fallon et al (2009), using neonatally deafened cats, found that large portions of A1 were non-responsive to sound activation of cochlear implants. These non-responsive regions may actually be visually responsive, perhaps interfering with the efficacy of cochlear implants due to loss of territory for sound processing. Similar loss of auditory cortical territory for sound processing may result from damage to IC due to disease or injury (Bognar et al. 1994; Hoistad and Hain 2003; Kimiskidis et al. 2004; Lee et al. 2009; Masuda et al. 2000; Meyer et al. 1996; Musiek et al. 2004). Understanding how to manipulate competition between



sensory modalities converging on a cortical territory would be helpful in designing clinical therapies.

### **c) Unisensory auditory or visual neurons are intermingled within cross-modal AC**

In contrast to research on cortical plasticity within one modality, this study addressed how ectopic, cross-modal inputs that invade a deafferented cortex affect normal function. We examined the possibility that both modalities could function independently through the segregation of their representations in XMAC. Neurons with similar response properties tend to be clustered together in unisensory sensory cortex (Hubel and Wiesel 1962; 1963; see Mountcastle 1997 for review) and in multisensory cortex (Dahl et al. 2009). Activity-dependent sorting of inputs can drive spatial segregation of different response types (Miller et al. 1989; Reh and Constantine-Paton 1985). As in other mammals, primary auditory cortex in ferrets maps sound frequency in one-dimension (Kelly et al. 1986; Phillips et al. 1988), whereas primary visual cortex maps visual space in two-dimensions (Law et al. 1988). If this remains the case in XMAC, it seems unlikely that visual and auditory neurons would be simultaneously active. It has been suggested that evolutionary pressure causes neurons with similar response properties to group together in order to reduce axon length and connection distance (Chklovskii and Koulakov 2004; Chklovskii et al. 2002; Kaas 2006; Ringo 1991). Such a tendency would also reduce the difficulty of wiring developing circuits appropriately. We reasoned that this economic pressure along with activity-dependent sorting could induce clustering of neurons with similar responses on an acute basis after brain damage and reorganization. For this reason, and because we found previously that callosal, auditory connections between the non-lesioned hemisphere and the ipsilesional AC were shifted laterally in AC (Pallas et al. 1999), we expected that neurons with

auditory responses in cross-modal AC would be segregated from those with visual responses. Instead, visual and auditory responses were intermingled throughout the entire AC. It is interesting that the competitive interaction between auditory and visual inputs in terms of proportion of response types did not also affect their spatial distribution within AC. It is possible that microclusters of similarly-responding neurons escaped our detection, or that processes that cause segregation are not operational in cross-modal auditory cortex. At any rate, these results imply that differences in the modality of information carried by the auditory and visual inputs from MGN during postnatal development are not sufficient to induce segregation or splitting of the cortical target areas.

#### **d) Multisensory neurons in Normal AC**

In addition to auditory neurons, we found multisensory neurons both in normal AC and XMAC. Previous studies in ferrets and other species have also reported the existence of multisensory responses in primary auditory cortex, and several investigators have thus begun to question the degree of modality-specificity in the primary sensory cortices (e.g. Bizley and King 2009; Ghazanfar and Schroeder 2006). Research on primates (de la Mothe et al. 2006; Lakatos et al. 2007; Smiley et al. 2007) and on rodents and carnivores (Bizley et al. 2007; Campi et al. 2010; Cappe and Barone 2005; Wallace et al. 2004) has shown that multisensory responses exist in traditionally-defined primary sensory cortices (cortices with direct thalamic input, which would include A1 and AAF, defined here as AC). In normal ferrets, King and colleagues reported that 15% of recorded units in A1 and AAF had non-auditory inputs, and these were located primarily along the outer edges of AC (Bizley and King 2008; Bizley et al. 2007). We encountered a similar proportion of multisensory to total neurons in normal ferret AC. The multisensory

neurons we recorded in the present study were primarily located at the margins of normal AC, but particularly in lateroposterior AC, near the border between A1 and the posterior pseudosylvian and posterior suprasylvian fields. They responded to direct stimulation of the optic chiasm but not to light, suggesting that they receive only weak visual input. Bizley et al. (2007) used a more sensitive method of response analysis that included spike timing information, which may explain why they found greater sensitivity to light. Although we cannot completely rule out the possibility that some visual units that we recorded were located in non-primary AC, similarly-placed recordings using pure tone stimuli indicate to the contrary.

#### **e) Multisensory neurons in XMAC**

In XMAC the proportion of multisensory neurons was much higher than in normal AC, but it was lower in large lesion animals than in the small lesion group. This was contrary to expectation, because the large-lesion group had more visual input to AC than the small-lesion group, leading to more potential interaction between auditory and visual afferents. One possible explanation is that sensory cortical neurons are more likely to be multisensory when they have weaker cross-modal inputs, perhaps because stronger inputs would outcompete and displace the original modality. Another possibility is that multimodal responsiveness represents an intermediate state between an auditory-dominated normal AC and a visual-dominated XMAC in cases with large lesions.

It is possible that multisensory responses are first created in MGN before reaching XMAC, although previous investigation of retino-MGN projections reported that they were clustered and segregated in small subregions of the ventral MGN, arguing against convergence at the thalamic level (Angelucci et al. 1997; Angelucci et al. 1998; Roe et al. 1993). We propose

that the most likely explanation for our data, then, is that new convergences between auditory and visual inputs are made at the level of AC in the lesioned animals.

Although normal AC and XMAC both contain multisensory neurons, our latency data suggest that the origin of visual inputs to these neurons is different in the two cases. The response latency of multisensory neurons to optic chiasm stimulation in XMAC was much shorter than that in normal AC, suggesting that AC in normal animals receives its visual inputs indirectly from other cortical areas, but that XMAC receives them more directly. Tracer injections made by Bizley and colleagues (2007) in AC of normal ferrets revealed projections from visual cortical regions to AC that may contribute to the multisensory responses seen there. In XMAC however, additional visual inputs come from the retina via the medial geniculate nucleus (MGN) (Sur et al. 1988), and these would be expected to exhibit the shorter latencies that we have seen. The connectional differences between multisensory neurons in normal AC and multisensory neurons in AC of lesioned animals are likely to account for the latency difference, and may result in different response properties as well.

The expanded proportion of multisensory neurons in XMAC is intriguing. Previous perceptual studies on lesioned ferrets with cross-modal visual input to AC argued that they could “see” rather than “hear” visual cues in the rewired auditory cortex (von Melchner et al. 2000). Recent clinical studies showing that thalamic lesions can produce synesthesia (Beauchamp and Ro 2008; Ro et al. 2007) imply that subjects may not be able to identify sensory modalities accurately after cross modal plasticity, however.

In conclusion, the data from this study provide information about the recovery of sensory function after damage to afferent pathways, and suggest a mechanism whereby visual takeover of auditory cortex during cross-modal plasticity might interfere with auditory function through competition for cortical territory. Appropriate and inappropriate inputs can coexist in the affected cortex without strict segregation, and this may not only interfere with efficient processing, but also create barriers to rehabilitation of the compromised modality. Understanding the processes leading to the coexistence of neurons with different functional roles in the affected cortical areas would be important for designing effective rehabilitation strategies for patients during recovery.

## **6. Acknowledgements:**

We thank Dr. Xiaoping Hu's group at Emory University for conducting the MRI scans, Dr. Yu-sheng Hsu's lab at GSU for advice on statistics, Taylor Brooks for help with data analysis, and both Dr. Jeff Ko at Purdue University and Dr. Andrew King's group at University of Oxford for advice on ferret anesthesia. Drs. Charles Derby, Donald Edwards and Robert Liu provided helpful advice on experimental design, and members of the Pallas lab gave helpful comments on the manuscript as well as technical assistance. We are indebted to the Department of Animal Resources at GSU, and particularly Cindy Marshall, for their dedication to animal welfare and expert animal care. This work was funded by grants to SLP from NSF (IBN-0451018), NIH (NIH EY/MH12696) and the GSU Research Foundation, by a GSU Brains and Behavior scholarship to YTM, and by the STC Program of the National Science Foundation (IBN-9876754).

**Table 2.1.** The proportion of neuronal types and residual midbrain volumes in lesioned animals.

The midbrain volumes were normalized to average midbrain volumes of normal animals. IC represents inferior colliculus, SC represents superior colliculus. L- Represents left. R- Represents right.

	Auditory (%)	Multisensory (%)	Visual (%)	L-IC (%)	R-IC (%)	L-SC (%)	R-SC (%)
Small lesion							
07-40	52.73	47.27	0	42.78	66.48	17.93	31.12
07-52	68.75	29.69	1.56	62.55	57.5	50.62	74.87
07-176	69.09	29.09	1.82	43.07	21.14	54.71	72.86
08-09	67.39	23.91	8.7	35.5	39.78	63.51	67.39
08-240	37.5	62.5	0	0	12.66	38.19	70.12
08-253	60	40	0	1.06	15.47	51.12	20.72
09-15	51.43	42.86	5.71	11	73.36	64.36	42.43
09-172	60	40	0	51.38	26.95	23.79	59.83
09-203	68.42	31.58	0	47.86	66.59	62.90	77.31
Large lesion							
07-61	35	10	55	0	55.36	3.89	69.59
07-107	26.33	28.95	44.74	21.38	63.78	0	35.48
08-201	45.45	40.91	13.64	0	34.69	5.44	93.59
09-21	47.62	14.29	38.14	0	37.70	6.26	82.54
09-191	64.71	17.65	17.65	5.62	23.59	11.48	55.65

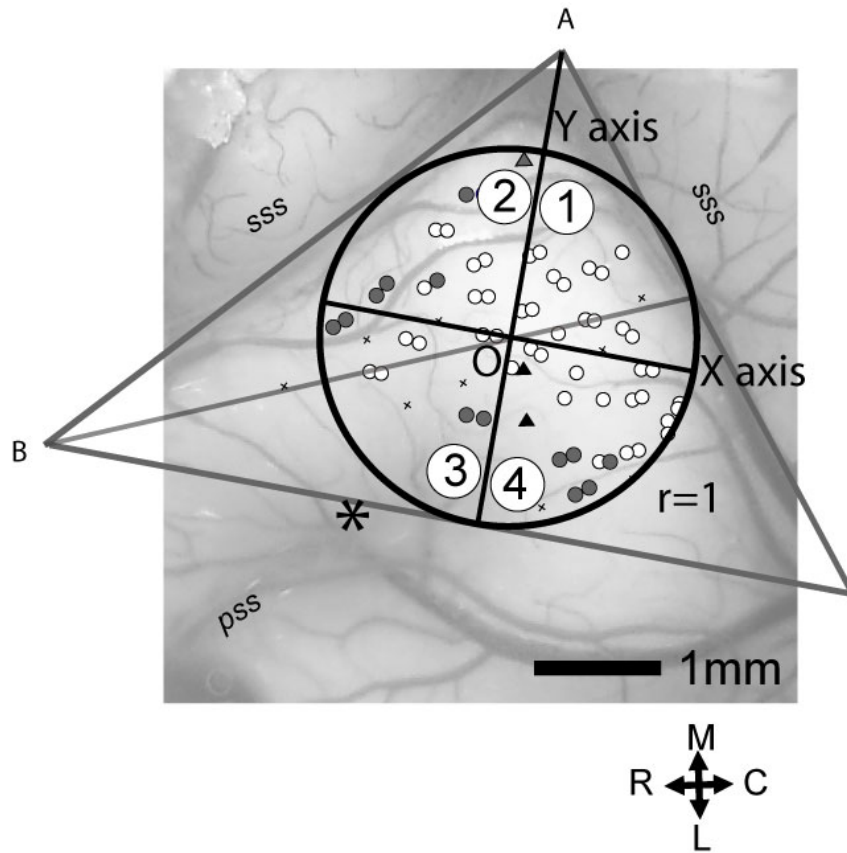


**Figure 2.1.** Method for quantifying the distribution of neuronal response types in auditory cortex. Based on the location of AC on the middle ectosylvian gyrus, we drew an equilateral triangle along the anterior and posterior suprasylvian sulcus and across the tip of the pseudosylvian sulcus (*pss*) (\* indicates the tip of *pss*). An internally tangent circle was drawn and divided into four quadrants numbered from one to four as shown. Neurons in these four quadrants were counted and identified by response type (see methods for detail).



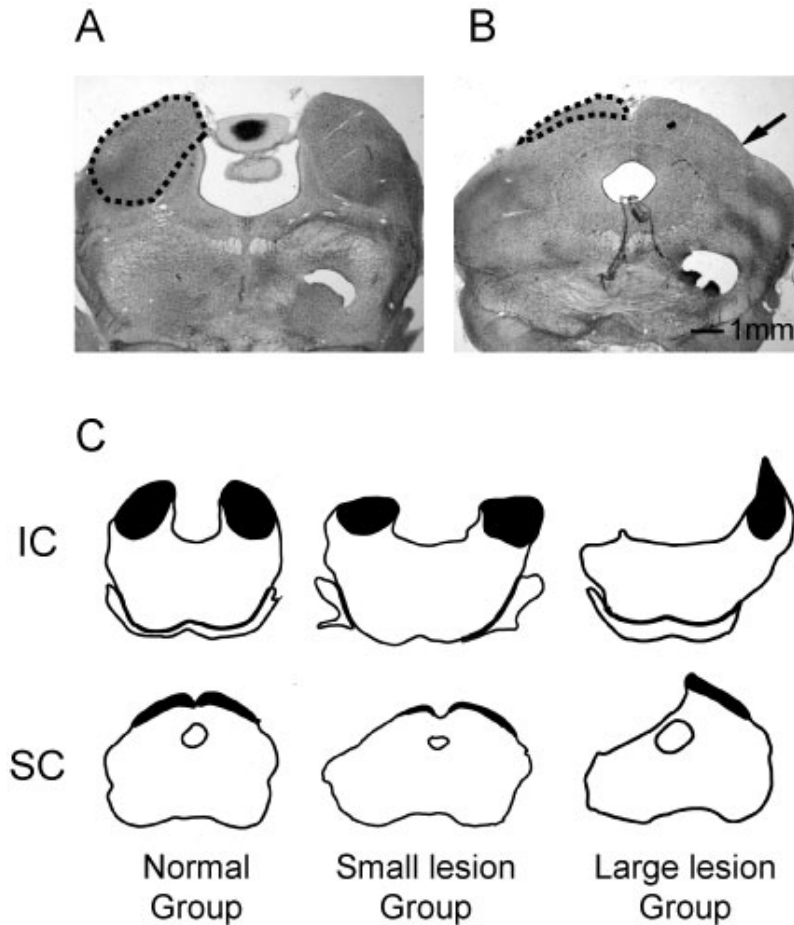


**Figure 2.2.** Assessment of midbrain damage. **A.** An example of a section through the IC. The central nucleus of the inferior colliculus (ICc) was more darkly stained than the surrounding areas (dashed line). **B.** An example of a section through the SC. The superficial layers of SC are marked by a boundary (arrow) that can be recognized under the microscope. **C.** Sketches showing examples of midbrains from one normal and two lesioned animals. Darkened areas show the residual, post-lesion inferior colliculi (IC, top) and superficial layers of the superior colliculi (SC, bottom). The animal with the smaller lesion (center) has some residual SC and IC bilaterally, whereas the animal with the larger lesion (right) is missing left SC and IC entirely.

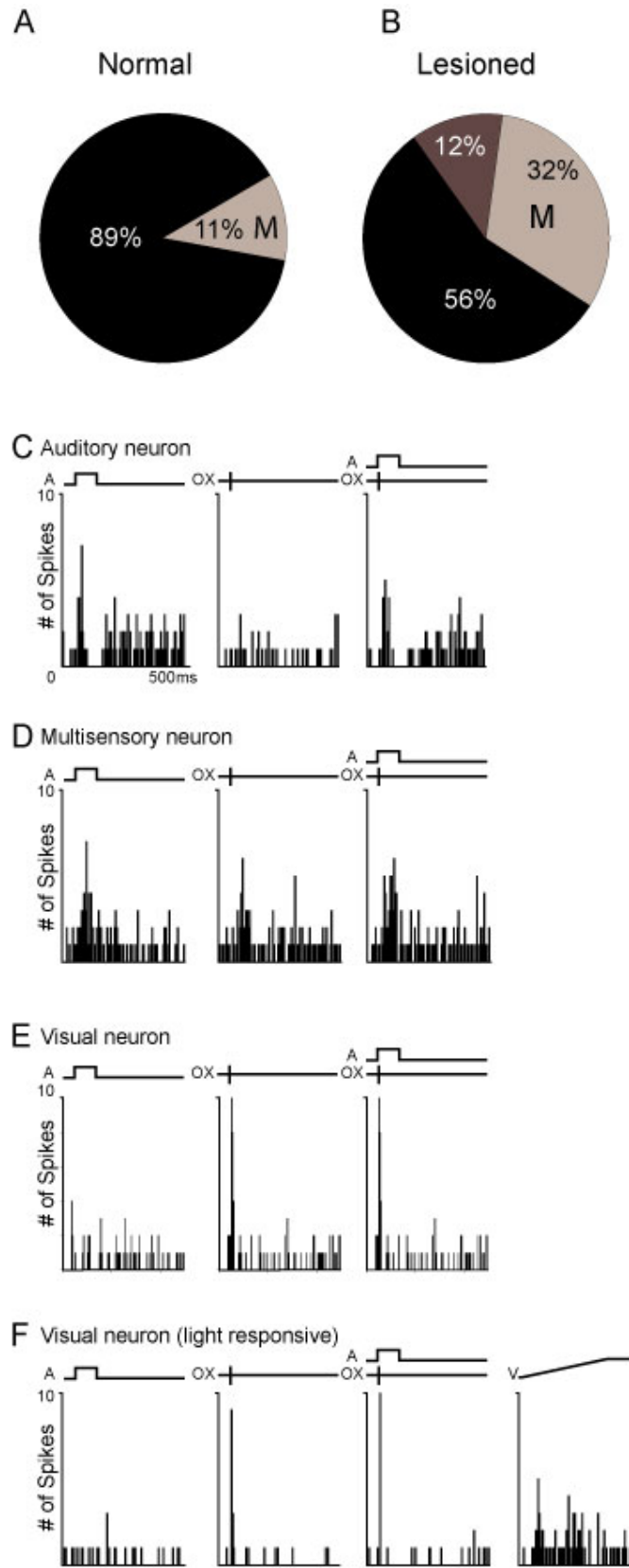


**Figure 2.3.** Neuronal response types. A-D. Representative post-stimulus response histograms for the different neuronal response types in cross-modal AC. The letter A in the top traces indicates the time course of the auditory stimulus, OX indicates the time of optic chiasm stimulation, and V indicates the timing of the light stimulation. A. Auditory neurons respond to sound but not optic chiasm stimulation. B. Multisensory neurons respond to both sound and optic chiasm stimulation. C. This visual neuron responded to optic chiasm stimulation but not sound. D. This visual neuron was also responsive to light. E-F. The relative proportions of neuronal response types in AC of E. all normal and F. all lesioned ferrets. A: Auditory neurons. M: Multisensory neurons. V: Visual neurons.

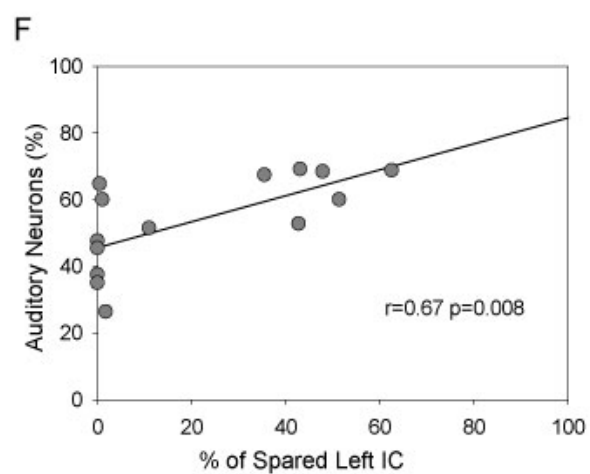
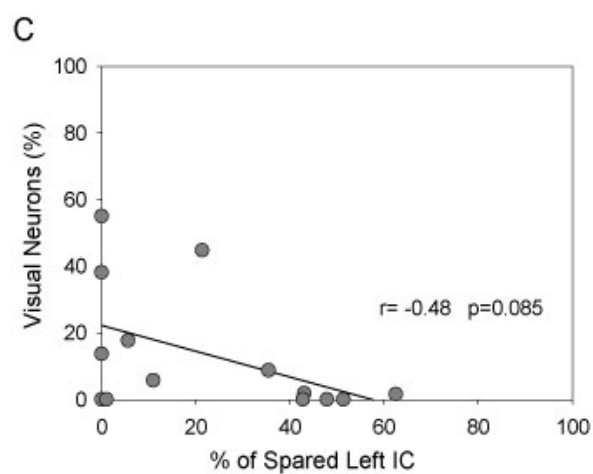
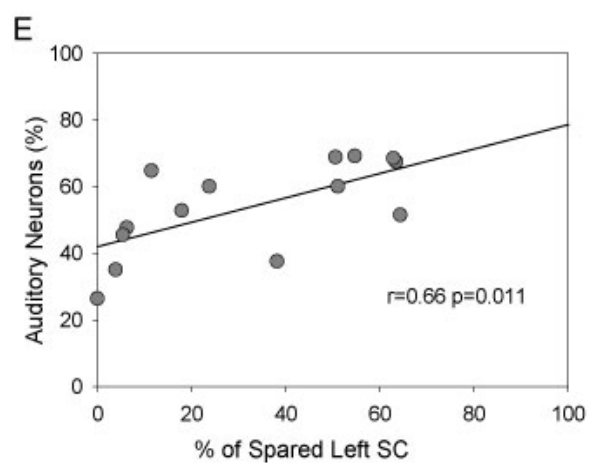
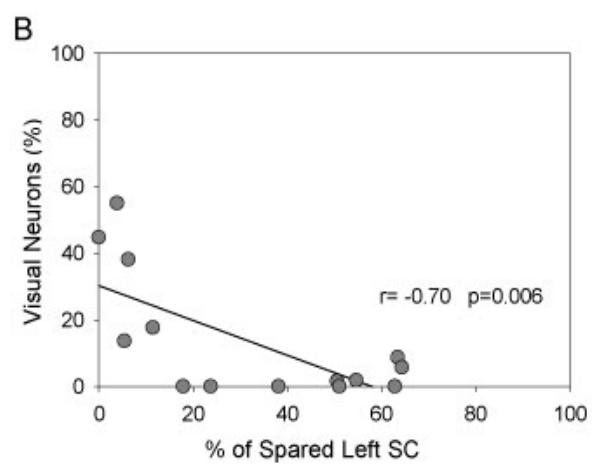
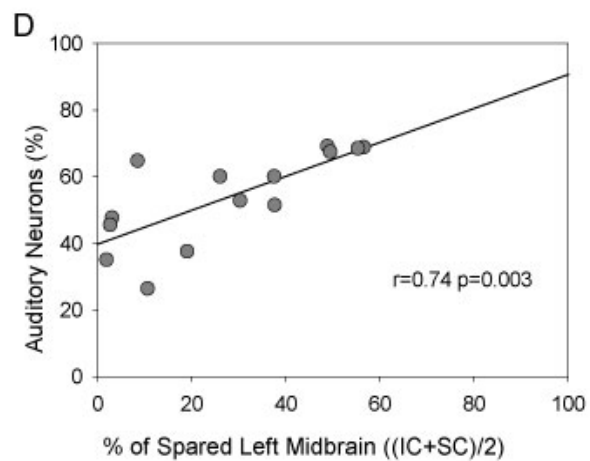
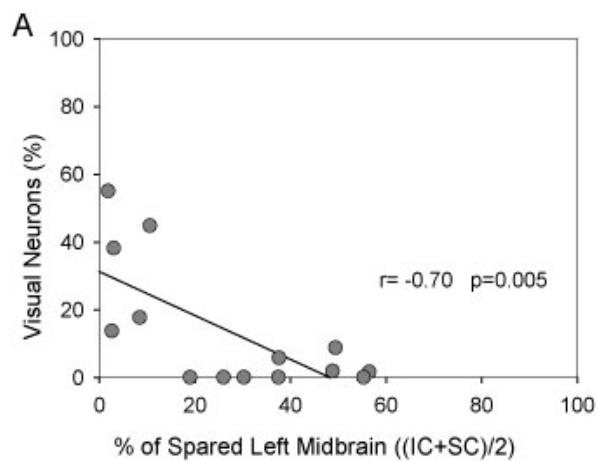


**Figure 2.4.** Relationship between midbrain lesion type and size and neuronal response type in AC of experimental animals. **A.** The proportion of visual neurons was negatively correlated with midbrain size. **B.** The proportion of visual neurons was negatively correlated with left SC size. **C.** The proportion of visual neurons was not correlated with left IC size. **D.** The proportion of auditory neurons was positively correlated with midbrain size. **E.** The proportion of auditory neurons was positively correlated with left SC size. **F.** The proportion of auditory neuron was positively correlated with left IC size. Each symbol corresponds to one animal (n=14).

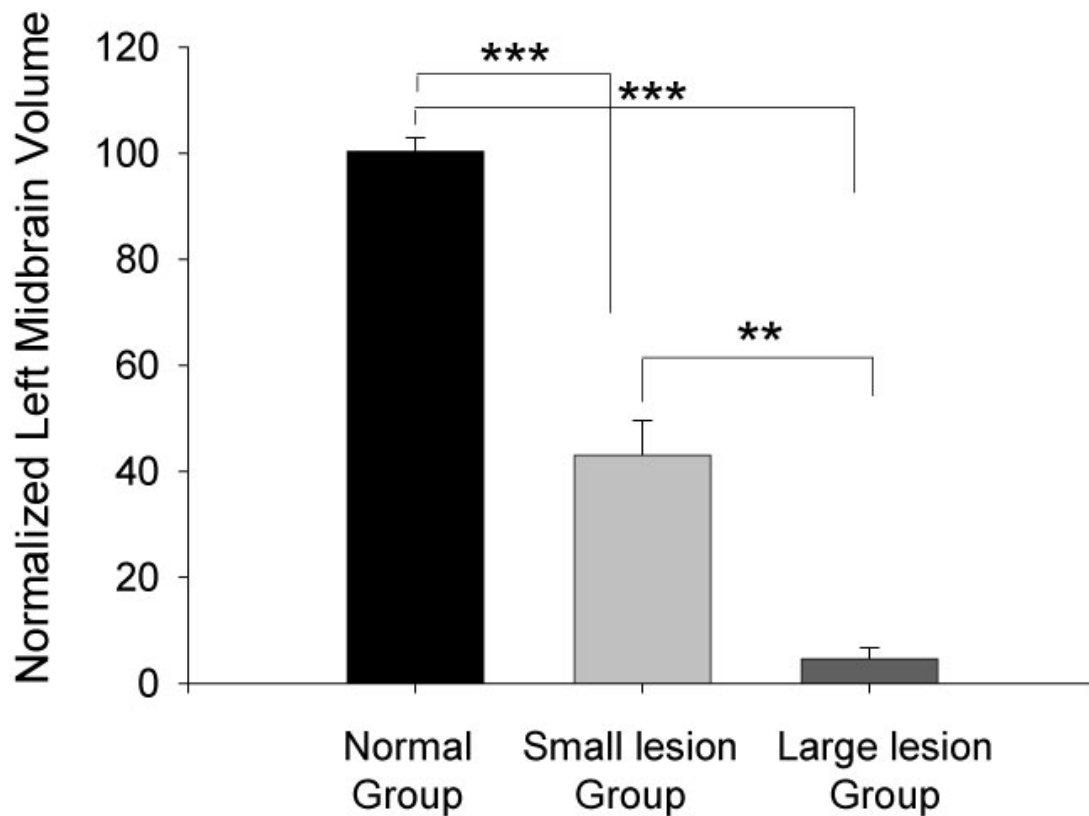


**Figure 2.5.** Statistical comparison of midbrain size between normal and lesioned animals.

Cases were divided into groups of small and large lesions according to whether they contained AC neurons that responded to light. The ipsilesional (left) midbrain sizes of lesioned animals in both the small and large lesion groups were significantly smaller than those of normal animals. (\*\*\*) represents  $p < 0.001$ , \*\* represents  $p < 0.01$  (ANOVA)).

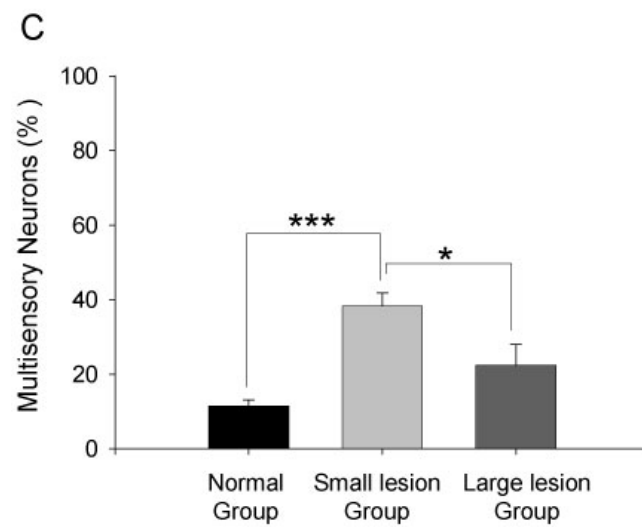
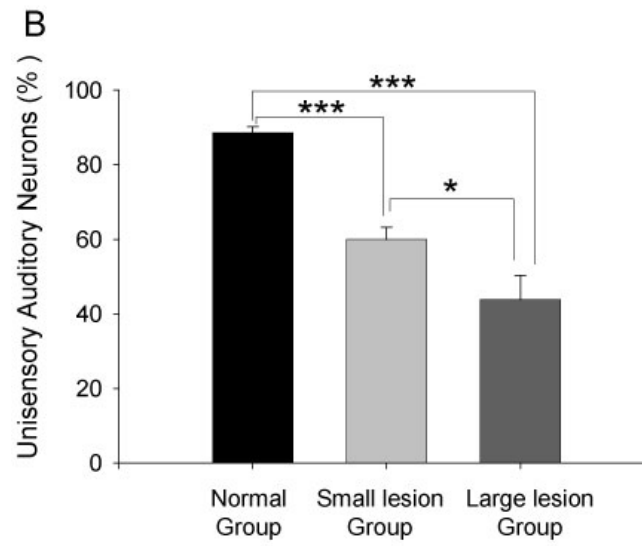
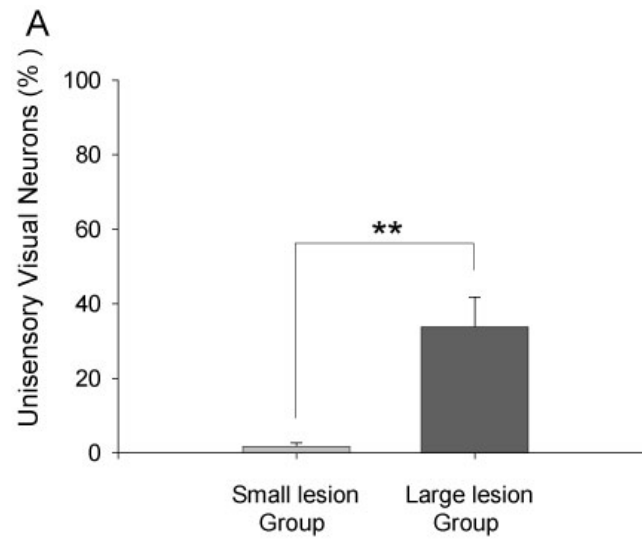


**Figure 2.6.** Neuronal response types in the three groups. **A.** The large-lesion group contained more visual neurons than the small-lesion group. **B.** The proportion of auditory neurons decreased with lesion size. **C.** The proportion of multisensory neurons in the small-lesion group was significantly higher than that in the normal and large-lesion groups. (\*\*\*) represents  $p < 0.001$ , \*\* represents  $p < 0.01$ , \* represents  $p < 0.05$ ).



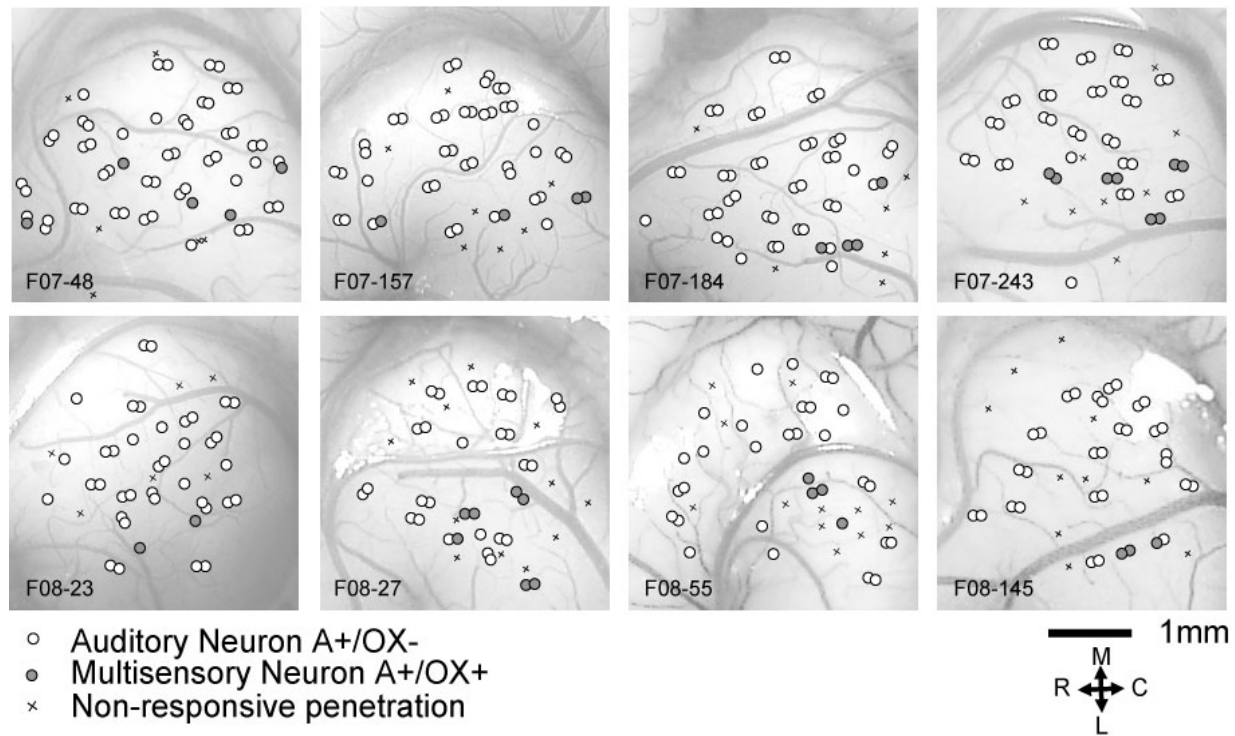
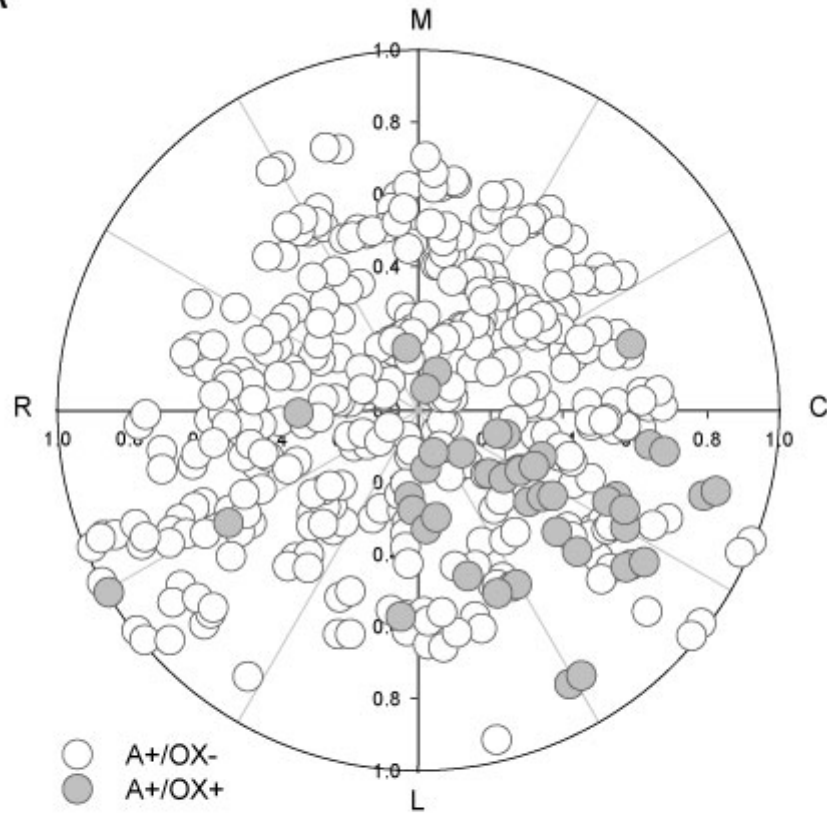
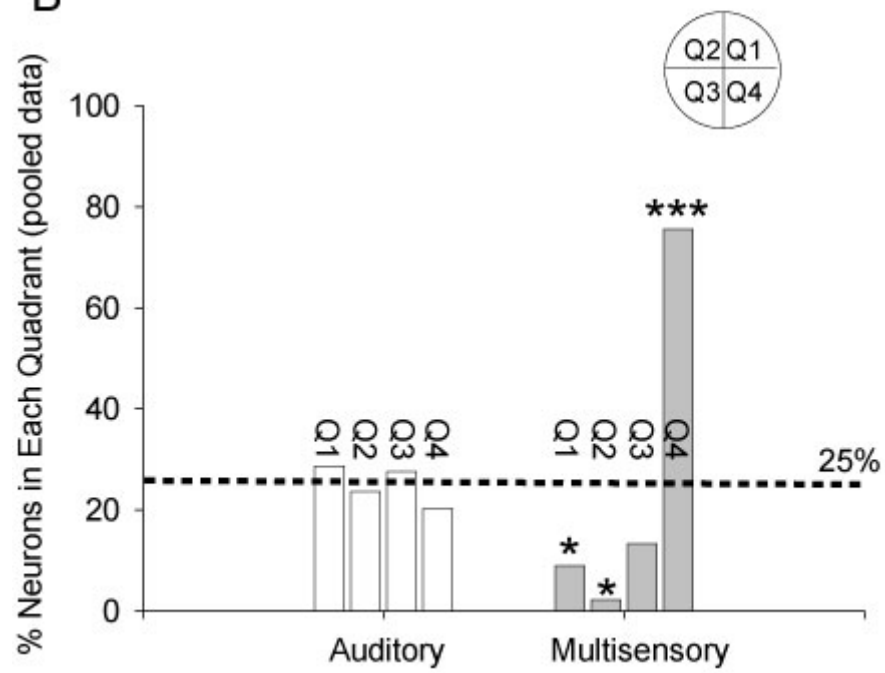


**Figure 2.7.** Reconstruction of locations of recorded neurons in normal AC. Each figure exhibits data from one animal (8 of the 10 cases are shown). Each circle represents one unit with response types as shown in the legend. A indicates auditory stimulation, OX indicates optic chiasm stimulation. The + symbol represents neurons that were responsive to the stimulus, whereas – represents neurons that were not responsive to that modality. A+/OX- indicates responsiveness to auditory stimulation but not to optic chiasm stimulation, A+/OX+ indicates responsiveness to both auditory and optic chiasm stimulation. x indicates a non-responsive site. Scale bar: 1 mm. Arrows at lower right show orientation. M, medial, L, lateral, R, rostral, C, caudal.

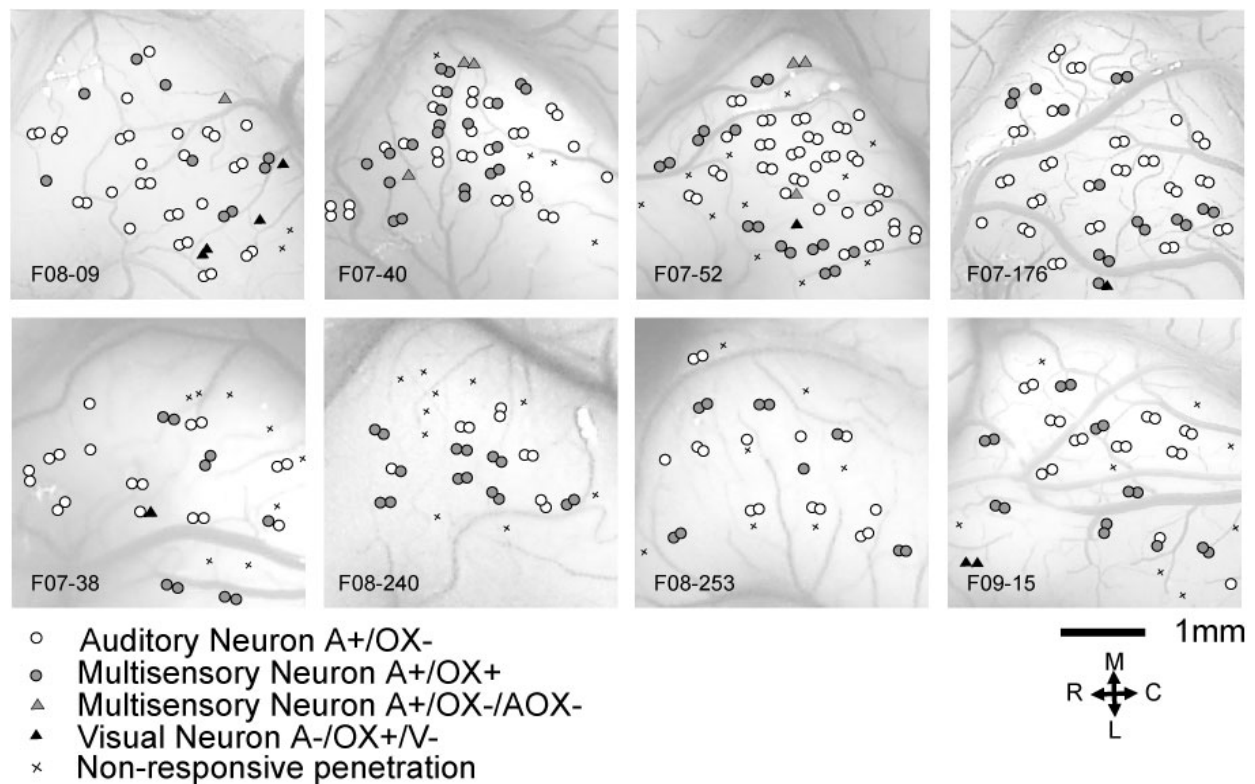
A



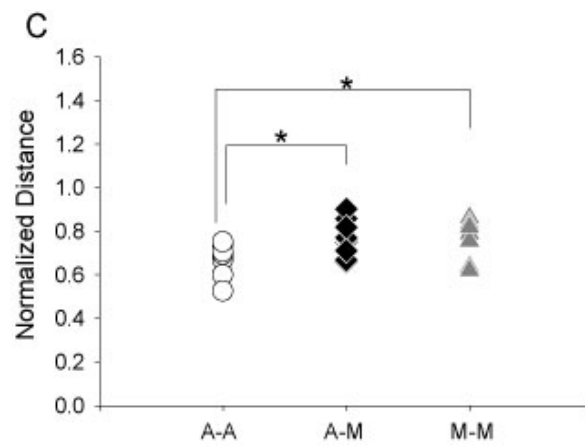
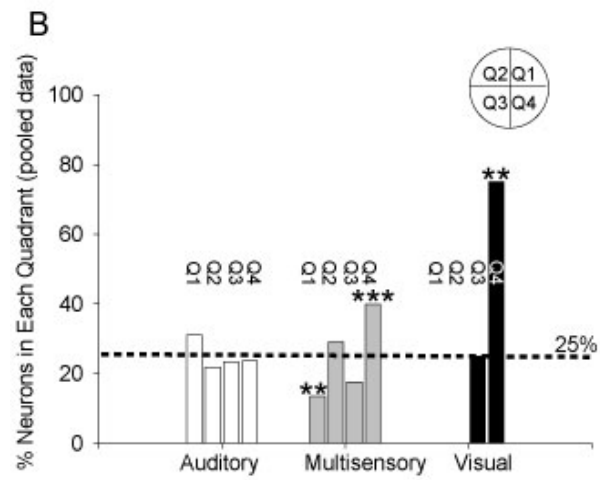
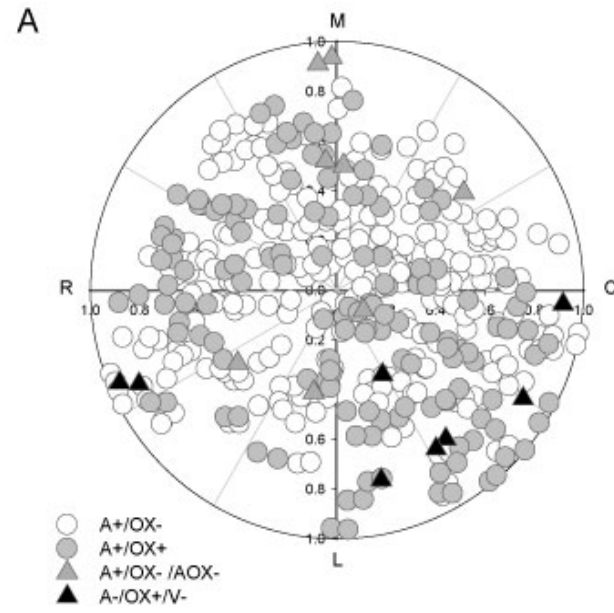
B



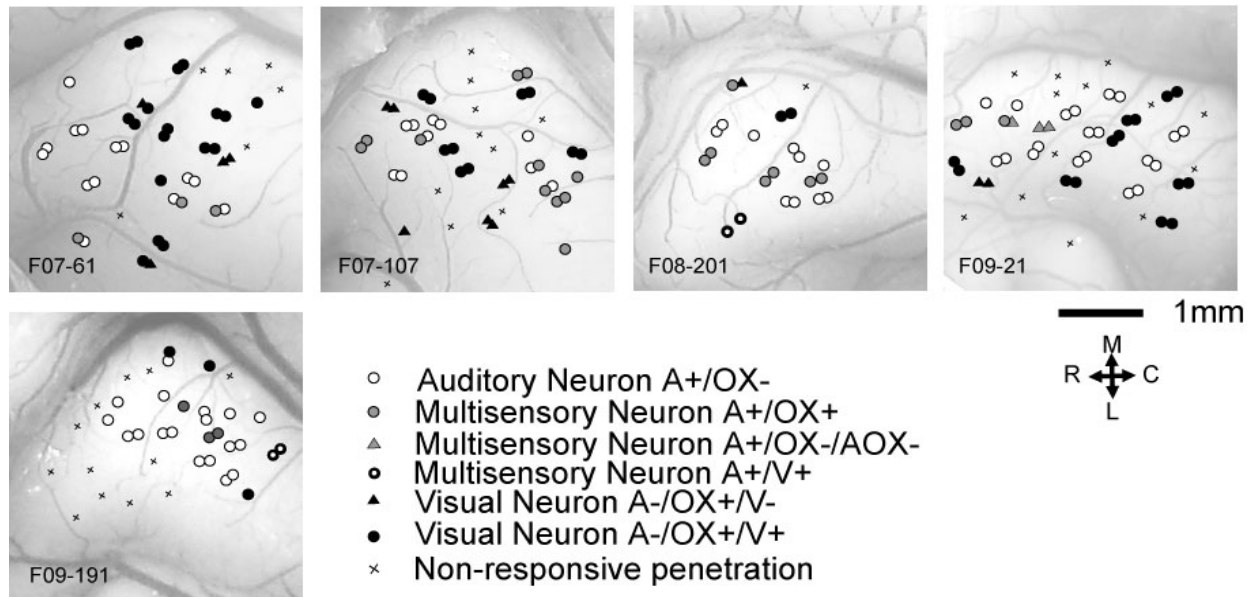
**Figure 2.8.** Distribution of neuronal response types in Normal AC. **A.** Pooled data from all 10 normal cases. Each open circle represents one auditory unit. Each gray circle represents one multisensory unit. Acronyms and abbreviations as in Figure 7. **B.** The proportion of neurons in each of the four quadrants (pooled data). Auditory stimulus-responsive neurons were uniformly distributed across quadrants but visually responsive neurons were clustered in Q4, in the lateroposterior portion of AC (Chi-square, \* indicates  $p < 0.05$ , \*\*\* indicates  $p < 0.001$ ). The dashed line at 25% indicates the value to be expected if response types were evenly distributed.



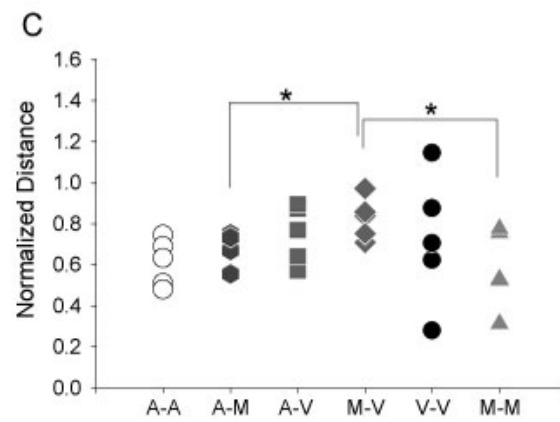
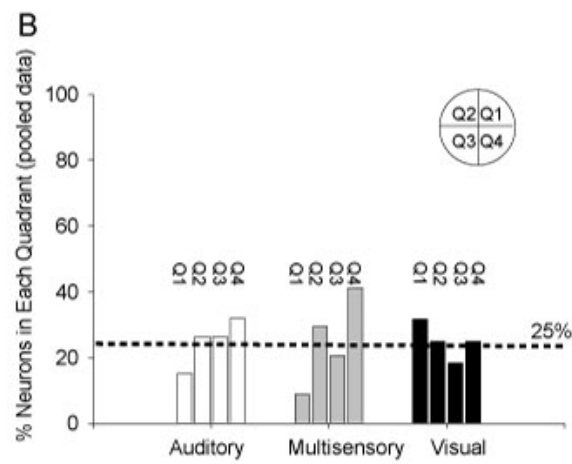
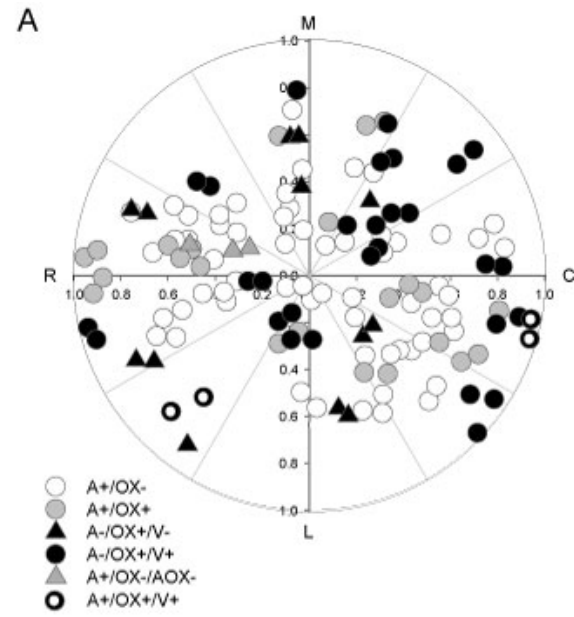
**Figure 2.9.** Reconstruction of locations of recorded neurons in AC of the small-lesion group (8 examples from 10 animals are shown). Acronyms and abbreviations as in Figure 7. V+ indicates responsiveness to light stimulation. AOX indicates auditory and OX stimuli were given simultaneously. A+/OX-/AOX- indicates multisensory neurons that did not respond to OX stimulation alone but whose auditory response could be modulated by it in a suppressive way. Multisensory neurons increased in frequency in this group but none could be driven by light. Neurons in the small lesion group defined as visual (A-/OX+/V-) did not respond to sound and responded to electrical stimulation of the optic chiasm but not to light.



**Figure 2.10.** Distribution of neuronal response types in AC across the population of small lesion cases. Acronyms and abbreviations as defined previously. **A.** Pooled data from all 10 animals. Open circles represent auditory neurons. Gray circles or triangles represent multisensory neurons. Dark triangles represent visual neurons. **B.** The proportion of neurons in each quadrant (pooled data). The distribution of auditory neurons was even across quadrants (Chi-square,  $p>0.05$ ), but the numbers of multisensory neurons in Q1 and Q4 were significantly different from expected values (Chi-square, \*\* indicates  $p<0.01$ , \*\*\* indicates  $p<0.001$ ), with the numbers significantly higher in Q4 and lower in Q1. Visual neurons were located only in Q3 and Q4. The proportion of visual neurons in Q4 was significantly higher than expected ( $p<0.01$ ). The dashed line at 25% indicates the value expected if response types were evenly distributed. **C.** The average distance between single units of each response type in AC. A-A is the average distance between all pairs of auditory neurons. A-M is the average distance between all auditory and multisensory pairs of neurons. M-M is the average distance between all pairs of multisensory neurons. Each symbol represents the mean of average distances for each comparison type from one animal. The average distance between auditory neurons was less than that between multisensory neurons or between auditory and multisensory neurons (ANOVA, \* indicates  $p<0.05$ ).

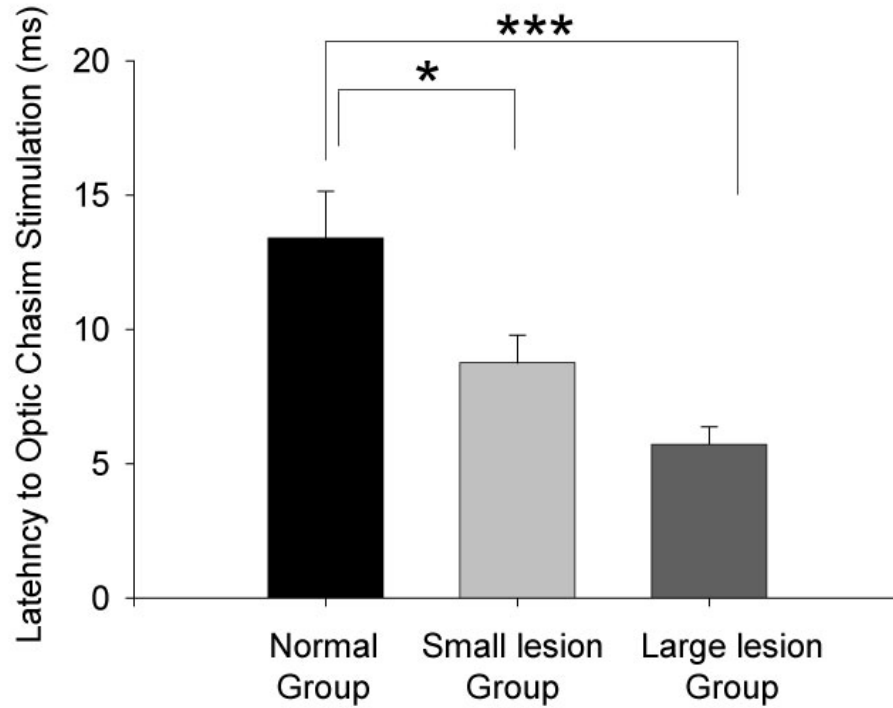


**Figure 2.11.** Reconstruction of locations of recorded neurons in AC of large lesion cases (5 examples from 5 animals are shown). Neurons responsive to light (A-/OX+/V+) were seen in this group (dark circles). Four multisensory neurons (A+/V+) that responded to both sound and light stimuli were recorded in 2 of the animals (F08-201, F09-191) (dark circles with white dot in center indicate A+/V+ neurons; other conventions as in Figs. 2.7 and 2.9).

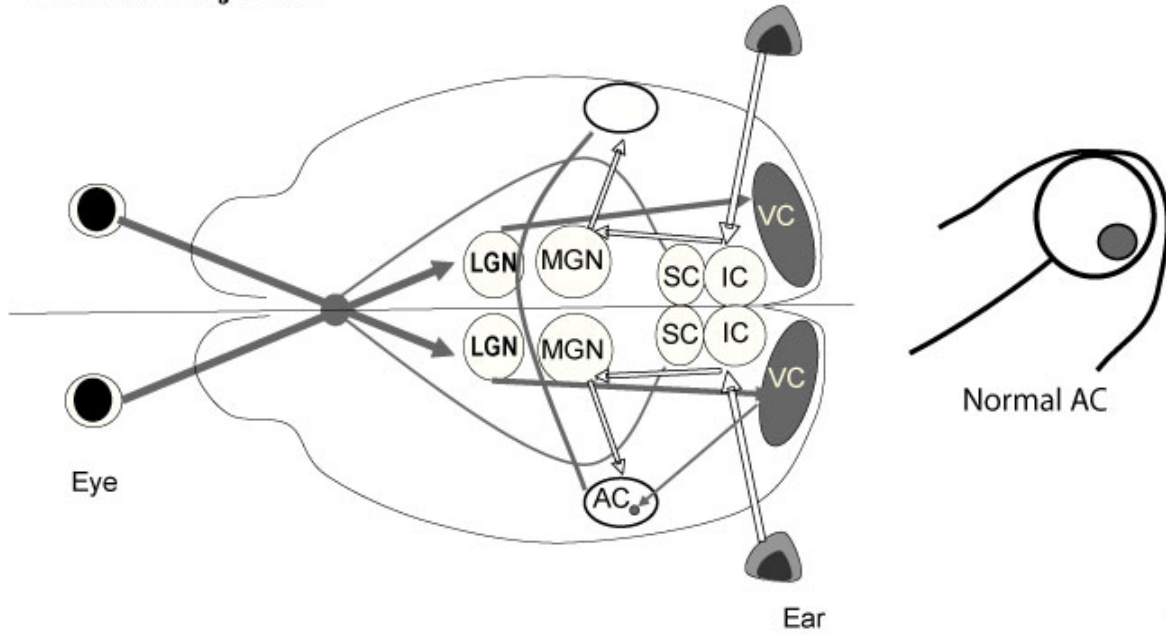
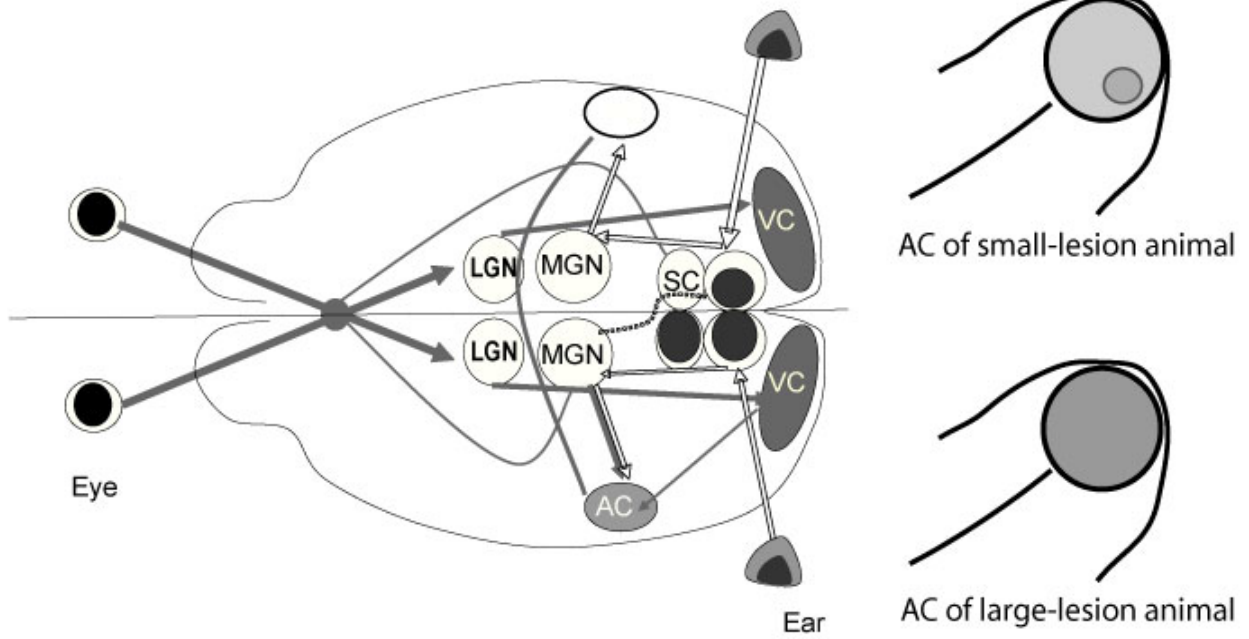




**Figure 2.12.** Distribution of neuronal responses in AC of large lesion cases. **A.** Pooled data from 5 animals. Acronyms and abbreviations as defined previously. **B.** The proportion of neurons in each quadrant in relation to total recorded auditory, multisensory or visual neurons in AC. Auditory, multisensory and visual neurons are randomly distributed across quadrants (Chi-square,  $p>0.05$ ). The dashed line at 25% indicates the value to be expected if response types were evenly distributed. **C.** The average distance between pairs of single units of each response type in AC. V indicates light responsiveness. Each symbol represents the mean of average distances for each comparison type from one animal. The average distance between multisensory and visual neurons was significantly greater than that between pairs of multisensory neurons and between pairs of multisensory and auditory neurons (ANOVA, \* indicates  $p<0.05$ ).



**Figure 2.13.** Latencies of responses to optic chiasm stimulation in normal AC and cross-modal AC. The response latency in AC of the small-lesion group ( $8.76 \pm 1.03$  ms) and in AC of the large-lesion group ( $5.72 \pm 0.65$  ms) was significantly shorter than that in normal AC ( $13.4 \pm 1.75$  ms). No significant difference was found between small and large-lesion groups. \* indicates  $p < 0.05$  and \*\*\* indicates  $p < 0.001$  (ANOVA).

**A****Normal Projection****B****Xmodal Projection (Possible source of auditory projection)**

**Figure 2.14.** Schematic of possible inputs to normal AC, to XMAC of small-lesion animals, and to XMAC of large-lesion animals. The gray scale to the right provides the key to the gray levels used in lines and structures in the drawings. The letter A represents auditory and V represents visual, with intermediate gray levels corresponding to degrees of multisensory responsiveness.

**A.** Normal connectivity pattern. **B.** The small, dark circle in this left side lateral view of Normal AC represents a cluster of multisensory neurons in the auditory field (large light gray circle). **C.** Dashed line indicates the rewiring of retinal axons to the left MGN. The left AC then receives reduced auditory input and ectopic visual input from MGN. White ovals in left and right IC and left SC indicate neonatal, partial lesion of these midbrain structures. The spared right IC may provide auditory input to the left MGN after the lesion. The narrow lines from left ear to spared IC indicate preserved auditory projections. **D.** The AC of small-lesion animals has increased visual responsiveness and decreased auditory processing. The darker, small circle in AC represents clustered multisensory neurons. The extent of clustering is smaller in XMAC than in normal AC. **E.** The XMAC of large lesion animals has the highest proportion of visual neurons in the three groups of animals. No clustering of multisensory neurons was seen in AC of large-lesion animals.

# **CHAPTER 3 COMPROMISE OF AUDITORY TUNING AND TOPOGRAPHY AFTER CROSS-MODAL INVASION BY VISUAL INPUTS**

**by**

**Yu-Ting Mao and Sarah L Pallas**

Submitted.

## **1. Abstract**

Brain damage resulting in loss of sensory stimulation can induce reorganization of sensory and motor maps in cerebral cortex. Previous research on recovery from brain damage has focused primarily on adaptive plasticity within the affected modality. Less attention has been paid to maladaptive plasticity that may arise due to ectopic innervation from other modalities. Using animals in which neonatal midbrain damage results in diversion of retinal projections to the auditory thalamus, we investigated how auditory cortical function is impacted by the resulting ectopic visual activation. We found that although auditory neurons in cross-modal auditory cortex (XMAC) retained sound frequency tuning, their thresholds were increased, their tuning was broader, and tonotopic order in their frequency maps was disturbed. Multisensory neurons in XMAC, unlike those in normal AC, also exhibited frequency tuning, but they had longer latencies than normal auditory neurons, suggesting they arise from multi-synaptic, non-geniculocortical sources. In a control group of animals with neonatal deafferentation of auditory thalamus but without redirection of retinal axons, tonotopic order and sharp tuning curves were seen, indicating that auditory function had largely recovered. This result suggests that the compromised auditory tuning and tonotopy in XMAC results from invasion by ectopic visual inputs but not from deafferentation. These findings suggest that the cross-modal plasticity that commonly occurs after loss of sensory input can significantly interfere with recovery from brain damage, and suggest that mitigation of maladaptive effects is critical to maximizing the potential for recovery.

**Keywords:** cross-modal plasticity, sensory substitution, cortical development, traumatic brain injury, stroke

## **2. Introduction**

Alterations of sensory inputs can result in plastic changes to sensory pathways. Research on within-modality plasticity following sensory manipulations has provided important information about how sensory systems compensate for a loss of input (see Buonomano and Merzenich 1998, for review). Recovery can involve multiple brain areas and sensory modalities, however (see Kral and Sharma 2012, for review). Visual areas can become responsive to sound stimulation in blind animals (Izraeli et al. 2002; Piche et al. 2004; Rauschecker 1995a), and recordings from deaf animals show visual responses in auditory regions (Kral 2007; Lomber et al. 2010). Thus, although cross-modal plasticity is a common outcome of sensory loss, it has received considerably less study than unimodal plasticity.

The success of clinical interventions after damage to sensory pathways can be negatively affected by cross-modal plasticity. Research on deaf patients (e.g. Sharma et al. 2007; Sharma et al. 2009) shows that auditory cortices have often received cross-modal projections by the time that cochlear prostheses can be implanted, interfering with the success of the implants (Lee et al. 2001). These findings point out the importance of studying cross-modal interactions for purposes of optimizing rehabilitation. Animal models employing deafness have yielded crucial information (Kral 2007; Lomber et al. 2010) but do not allow study of competitive interactions between auditory and cross-modal visual inputs to auditory cortex. Our approach of partial midbrain damage reroutes retinal axons to auditory thalamus, placing visual and auditory inputs in a controlled state of competition (Mao et al. 2011; Pallas et al. 1999; Sur et al. 1988), while still allowing sensory activation of both modalities, thus enabling study of the effects of different degrees of cross-modal plasticity on residual auditory function.

We reported previously that auditory cortex (AC) of ferrets after unilateral neonatal midbrain damage contains neurons that respond to a single modality (auditory and visual neurons) and to both modalities. Because these different response types are randomly distributed within XMAC rather than in a segregated fashion, communication between unimodal neurons might be disrupted by adjacent cross-modal neighbors. We tested whether competition from ectopic visual inputs compromises auditory tuning and topography in XMAC using *in vivo* single unit recordings in anesthetized ferrets.

We found that auditory tuning and tonotopic mapping in auditory cortex are impaired after cross-modal plasticity. Because the same neonatal midbrain lesions coupled with enucleation of both eyes did not produce the effects, we argue that the compromised function results specifically from the ectopic visual inputs. Interestingly, early enucleation by itself increased auditory sensitivity. These results provide support for the hypothesis that competition between auditory and visual inputs after cross-modal plasticity underlies the compromised auditory function in patients with partial hearing loss, and they also provide a potential explanation for the improved auditory function often observed in blind humans (Bavelier and Neville 2002).

Preliminary results from some of these experiments have been published previously in abstract form (Mao and Pallas 2010).

### **3. Materials and Methods**

#### **a) Animals**



In total, 26 adult pigmented ferrets (*Mustela putorius furo*) were included in this study. Timed pregnant ferrets were either obtained from Marshall Farms (North Rose, NY) two weeks prior to parturition or bred in the GSU facility, and were kept on a 14h/10h light/dark cycle. Kits were weaned at 6-8 weeks of age. Non-lactating adults were fed Marshall Farms ferret diet and kept on a 12/12 light/dark cycle. Animals were divided into normal (n=8), cross-modal (n=9), blind (n=3) and blind-lesioned groups (n=6). Both cross-modal and blind-lesioned groups were subjected to neonatal surgeries. All animals were treated in accordance with protocols approved by the Institutional Animal Care and Use Committee (IACUC) at Georgia State University and met or exceeded standards of care established by the USDA and the Society for Neuroscience.

#### **b) Neonatal surgery**

Surgical procedures to induce cross-modal plasticity were similar to those described previously (Mao et al. 2011; Pallas et al. 1999). All invasive procedures were performed under sterile conditions. Within 12 hours after birth, ferret kits were anesthetized by isoflurane (1-4% prn). The skull overlying the midbrain was exposed and removed through an incision in the skin. The superficial, retinorecipient layers of the superior colliculus (sSC) primarily on the left side and the central nucleus of the inferior colliculi (ICc) on both sides were then cauterized to varying extents, and the brachium of the left inferior colliculus was severed. The incision was closed using surgical adhesive (VetBond, 3M, St. Paul, MN). For generating blind animals, both eyes were enucleated within the first postnatal week (the eyes open at ~P30 in ferrets). The surgical site was cleaned and draped. The lids were opened along the future eyelid margin (visible at this age) by a scalpel or a microscissor. The orbits were separated from the surrounding conjunctiva and were completely removed, taking care to eliminate all pigmented epithelium that could

conceivably regenerate photoreceptors. Typically there was no bleeding during this procedure. The eyelids were reclosed with tissue glue. To generate blind-lesioned animals, the two procedures were combined. After surgery, the kits were given subcutaneous fluids and a respiratory stimulant (doxapram, 2 mg/kg, SQ) and warmed on a heating pad. Kits were returned to their dam after they recovered from anesthesia. Analgesics (buprenorphine 0.01 mg/kg bid) were given if warranted to eliminate postoperative pain. Note that enucleation results in degeneration of the optic nerve, preventing any subsequent activation of the peripheral visual pathway by light or by optic nerve stimulation.

### **c) Preparation for Adult Electrophysiology**

Animals were prepared for electrophysiology experiments as described previously (Mao et al, 2011). The ear canals of each ferret were examined before surgery with an otoscope and cleaned if necessary. Atropine (0.4 mg/kg SQ,) and doxapram (2 mg/kg, SQ) were given as a pre-anesthetic to counteract bradycardia and to reduce mucosal secretions. Animals were anesthetized with ketamine (40mg/kg, IM) and diazepam (2mg/kg, IM) during the craniotomy procedure. Dexamethasone (1mg/kg, IM) was given every 24 hours to prevent cerebral edema. For the recording session, the cephalic or femoral vein was cannulated and an IV solution containing a combination of medetomidine (0.022 mg/kg/hr) and ketamine (5 mg/kg/hr) in lactated Ringer's with 5% dextrose (Bizley and King 2008; Bizley et al. 2005) was continuously infused at a rate sufficient to maintain a state of unconsciousness (2-5 ml/h). Atropine (0.4 mg/kg, SQ) was given as necessary to counteract the bradycardia caused by medetomidine. The animal was intubated and artificially ventilated using a small animal ventilator (SAR 830/P ventilator, CWE Inc, Ardmore, PA). Body temperature was maintained at 38° C with a heating pad. EKG,

respiration rate, muscle tone, withdrawal reflexes, and end-tidal CO<sub>2</sub> were monitored and recorded every 30 min at the beginning of surgery and every hour after surgery. Eyes were kept moist with commercial artificial tears solution and protected with custom plano contact lenses (Conforma Inc, Norfolk, VA). The animal was placed in a stereotaxic device and an incision was made on the top of the head with a scalpel. The temporal muscles were retracted from the skull and two burr holes (at coordinates A5.5 ±L1.5) were drilled for optic chiasm recording/stimulation electrodes. To protect the brain from overheating during the drilling, saline was frequently dripped on the surface. Two tungsten rods with Teflon insulation (0.008 inch bare, 0.011 inch coated, A-M systems, Inc., Carlsborg, WA) were advanced in the two holes to a depth (8~10 mm) that yielded strong visual responses. These tungsten rods were then connected to a stimulus isolation unit (BAK Electronics, Mount Airy, MD). A 0.8~1.0 cm diameter craniotomy was made over the left auditory cortex. After removing the skull, the ferret auditory cortex (AC, defined as primary auditory cortex (A1) and the anterior auditory field (AAF)) was exposed (Fig. 2) (Kelly et al. 1986). The dura was removed carefully and the AC was covered with sterile saline. The skull on the right side was cleaned and a metal bracket was cemented on the surface to stabilize the head. The right ear bar was then released to allow access to the ear for auditory stimulation.

#### **d) Acoustic stimuli and optic chiasm stimuli**

Acoustic stimuli were generated using TDT system II or TDT system III hard- and software (Tucker-Davis Technologies, Alachua, FL). A calibrated earphone (ER-2 insert earphone, Etymotic Research, IL) was placed in the pinna at the entrance to the right ear canal. All auditory stimuli were presented contralateral to the recording site. White noise bursts (5 ms ramp, 40-100

ms duration, 80 dB SPL) were used to search for sound-responsive units. Pure tones of different frequencies were presented in random order after a responsive neuron was found. Calibrated, pure tones ranging in 2 kHz steps from 2 kHz to 18 kHz or ranging in half octave steps from 500 Hz to 16 kHz with an intensity of 30 to 80 dB SPL (50 ms duration, 5 ms ramp) were given to define tuning curves. Electrical stimulation of the optic chiasm was used to activate visual fibers. Because visual inputs to MGN in XM animal are weak and comprised of W retinal ganglion cells (Pallas and Sur 1994; Roe et al. 1993; Sur et al. 1988), it was rarely possible to activate visual and multisensory neurons by light. Bipolar electrical stimulation of the optic chiasm was applied (single pulses at 0.5-1 mA, 60  $\mu$ s duration) to test whether the units were bimodal.

#### **e) Extracellular recording**

Recordings were made with glass-coated tungsten microelectrodes (1-2 M $\Omega$ , FHC, Bowdoin, ME). The cortical surface was photographed in order to record the penetration locations. Penetration sites were chosen to sample randomly while avoiding sulci and blood vessels. The electrode was advanced in 5  $\mu$ m steps down to 2000  $\mu$ m under the pial surface by a hydraulic microdrive (Kopf Instruments, Tujunga, CA). For each penetration, the first stable unit encountered was isolated and characterized. No more than two recording sites were made in each penetration, though generally two units could be separately isolated at each site using the spike isolation software. Most units were isolated within 800  $\mu$ m of the pial surface. Sampling densities and locations were comparable across groups. In this research, recording penetrations were limited to primary auditory cortex (AI) and anterior auditory field (AAF) (Bizley et al. 2005). There is a low frequency reversal at the ventral edge of primary auditory areas (Bizley et al, 2005, 2008) and recording was stopped when the reversal was encountered (see Fig 2).

Neural responses were bandpass filtered (500 Hz to 5 kHz), amplified (10,000 times, BAK Electronics, Inc, Mount Airy, MD), and monitored on a digital oscilloscope (Hameg Instruments, Mainhausen, Germany). Responses to 5-10 stimulus presentations were gathered from each recording site and digitized at 25 kHz using TDT systems. Spontaneous activity was recorded for 50 ms before each trial in order to normalize the evoked response levels. Digitized data were acquired by Brainware software (Tucker-Davis Technologies Inc., Alachua, FL). The recording continued for 1-2 days, after which the animal was deeply anesthetized for perfusion and the brain was extracted for histological examination.

#### **f) Electrophysiological data analysis**

Brainware software (Tucker-Davis Technologies Inc., Alachua, FL) was used for off-line spike sorting. Biphasic action potentials were extracted by artifact rejection set in Brainware. Single units were isolated according to their waveform, amplitude, and width. Post-stimulus time histograms (PSTHs) of the selected single units were generated using the same software package. Response latencies were determined by the time between stimulus presentation and the time of the first bin in the PSTH that reached at least 20% above background firing rate. For isolated single units, a frequency response area (FRA) was reconstructed by summing the responses to each pure tone across 5-10 trials. The response threshold was defined as 20% above the mean spontaneous firing rate (Bizley et al. 2005; Sutter and Schreiner 1991). The boundaries of the frequency tuning curve were defined by the stimuli yielding excitatory responses above this threshold (Moore et al. 1983; Sutter and Schreiner 1991). The best frequency (BF) of each unit was defined as the frequency at which the lowest threshold responses were elicited. Some neurons responded similarly to two contiguous frequencies, in which case their BF was defined

as the mean of these two frequencies. If neurons responded at a low threshold to two contiguous frequencies, BF was defined as the frequency that induced the larger response. Neurons were defined as tuned if they had single peaked or double peaked tuning curves. Neurons that responded to at least 3 contiguous frequencies at the same threshold level were defined as untuned neurons. Bandwidth was determined by the width of the tuning curve at 10 dB above this minimum threshold. Multisensory units were defined either as neurons that responded both to visual and auditory stimuli or as neurons that only responded to one modality but could be significantly modulated by stimulation with the other modality (Stein and Meredith 1993). Statistical significance was determined by comparing the number of spikes per sweep (counted from PSTHs) as a response to the different stimulus modalities using Student's t-test ( $p < 0.05$ ). For calculating the spatial distribution of frequency-tuned neurons, the area of each AC was normalized to a standard circle with a radius of 1 (**Fig 3.1**) (see Mao et al. 2011). The locations of recorded units were reconstructed on this normalized AC. .

Electrophysiological data were statistically analyzed using Sigmastat software (Systat Software Inc, Chicago, IL) and PASW statistic 18 (SPSS Inc, Chicago, IL) and plotted using Sigmaplot (Systat Software Inc, Chicago, IL). A one way ANOVA was used for multiple comparisons of normally distributed data. A one way ANOVA on ranks (Kruskal-Wallis test) was used for multiple comparisons of non-normally distributed data. A Student's t- test was used for normally distributed data. For two group comparison of ranks on non-normally distributed data, a Mann-Whitney U test was used. Means are given with standard errors of the mean ( $\pm$  SEM) throughout.

#### **g) Assessment of lesion size**

After electrophysiological recordings were completed, animals were deeply anesthetized with sodium pentobarbital (65 mg/kg, IP) and perfused with phosphate-buffered saline (PBS) followed by 4% paraformaldehyde in 0.1M PB. Brains were extracted and postfixed in 4% paraformaldehyde in 0.1M phosphate buffer (PB) for 24 hr at 4° C. The brains were transferred to 30% sucrose in 0.1M PB at 4° C after postfixation. After the tissue was infiltrated by the sucrose solution, it was sectioned frozen at 50µm in the coronal plane for reconstruction of lesions. A series of sections at 200 µm intervals was mounted on gelatin-subbed slides and stained for Nissl substance with cresyl echt violet. The volumes of the residual auditory midbrain (central nucleus of the inferior colliculus (ICc)) and the residual visual midbrain (superficial layers of the superior colliculus (sSC)) were measured from Nissl-stained sections with a Zeiss microscope using Zeiss Axio Vision 3.1 software (Carl Zeiss MicroImaging, Inc., Thornwood, NY). The borders of ICc and sSC were very clear on our Nissl stained sections (Mao et al. 2011). The volumes of sSC and ICc were calculated as the sum of the size of each measured area multiplied by the length of the interval between assayed sections of 200 µm (**Fig 3.2**). Proportions of residual midbrain volume in the lesioned animals were calculated by comparison with an average midbrain volume derived from five normal animals (as in Mao et al., 2011).

#### **4. Results**

The goal of this study was to investigate the mechanism through which the cross-modal plasticity that results from neonatal, partial deafferentation of auditory thalamus impairs eventual recovery of auditory function. It is well-accepted that auditory cortex is subject to unimodal, experience-dependent modification (Insanally et al. 2009; Popescu and Polley 2010; Zhang et al. 2002;

2001), but how it might be negatively or positively affected by cross-modal modification is less clear. The cross-modal group had neonatal damage to auditory and visual midbrain, redirecting retinal inputs to auditory thalamus (MGN) and thus providing visual activation of auditory cortex (Sur et al., 1988). In a previous study we showed that after recovery from surgery, XMAC can respond to both auditory and visual stimuli (Mao et al. 2011). We were interested in whether that residual auditory function is compromised by invasion of the ectopic visual inputs. Because damage to both auditory and visual midbrain is necessary to induce cross-modal plasticity, it was important to establish whether auditory cortical function was impaired by anomalous visual inputs, loss of auditory inputs, or both. In order to distinguish between these two possibilities, we designed a blind-lesioned group that had the same neonatal midbrain lesions as XM animals but no visual inputs, as a control for the effects of the visual activation of XMAC. Because this group introduces enucleation as another experimental variable, in order to rule out the effect of enucleation on recovery of auditory function, we added a group of blind-only animals. The study thus contained four groups: normal, cross modal, blind-lesioned, and blind animals.

Twenty-six ferrets in total were used. Eight were in the normal group, 9 were in the cross modal group, 6 were in the blind-lesioned group, and 3 were in the blind group. XM ferrets were lesioned on the day of birth (P1). Blind ferrets were enucleated on P1-7. Enucleation on P7 increased the survival rate of kits and would be expected to have the same effect as enucleation on P1 because the thalamocortical projection does not reach cortex until P14. Blind-lesioned ferrets were enucleated and lesioned on the same day (P1) to avoid multiple survival surgeries. Statistical analyses included both parametric and non-parametric methods depending on the normality of the sample distribution, but in all cases we present error bars as standard error of the mean (SEM).



**a) The residual midbrain volume of Xmodal animals was not significantly different from the residual midbrain volume of blind-lesioned animals**

The blind-lesioned animals were introduced as a control for the alternative hypothesis that the changes in XMAC are caused by auditory deafferentation rather than visual activation. Because variable lesion sizes between groups could potentially affect the interpretation of results, we examined whether the lesions in these two groups were similar in size. We compared the volumes of residual midbrain components from these two groups against midbrain volumes from a reference set of normal animals (Mao et al. 2011). We found that the volumes of residual left midbrain (sSC plus ICc) were not significantly different between the Xmodal ( $24 \pm 5.9\%$ ,  $n=9$ ) and the blind-lesioned groups ( $22 \pm 3.6\%$ ,  $n=6$ ,  $p=0.78$ , t-test). In particular, the average volume of residual IC in Xmodal animals was not significantly different from that of the blind-lesioned animals (Xmodal  $27 \pm 6.0\%$ ,  $n=9$ , Blind-lesioned  $32 \pm 3.5\%$ ,  $n=6$ ,  $p=0.58$ , t-test) (**Fig 3.3, Table 3.1**). Because the majority of projections to left auditory cortex come from ipsilateral inferior colliculus via the left MGN, we also compared the residual volume of left IC between the Xmodal and the blind-lesioned groups. We did not find a significant difference between these two groups (Xmodal  $17 \pm 7.2\%$ ,  $n=9$ , Blind-lesioned  $25 \pm 5.4\%$ ,  $n=6$ ,  $p=0.41$ , t-test) (**Fig 3, Table 1**). These results show that the extent of neonatal midbrain damage was similar in lesioned animals with or without enucleation. Therefore it is unlikely that different response characteristics in auditory cortex can be attributed to differences in neonatal lesion size in the Xmodal compared to the blind-lesioned animals.

## **b) Auditory and multisensory neurons in AC of Xmodal animals were tuned to pure tones**

The majority of sound-responsive neurons in the primary auditory areas of normal adult ferrets have a single best frequency (BF) between 1 kHz and 18 kHz (Kelly et al. 1986; Phillips et al. 1988). To test the hypothesis that auditory function in XMAC is impaired by invasion of visual inputs, we first asked whether neurons in XMAC exhibit normal tuning to pure tones. Neurons that had a single peak in their sound frequency tuning curves were considered to be tuned to a single Best Frequency (BF) (see Methods for detail). Neurons that responded to frequencies above 12 kHz ( $\geq 12$  kHz) were defined as high-frequency neurons, neurons that responded to frequencies between 6 to 12 kHz ( $\geq 6$  kHz,  $<12$  kHz) were defined as mid-frequency neurons, and neurons that responded to frequencies below 6 kHz ( $<6$  kHz) were defined as low-frequency neurons. We found that nearly all of the recorded neurons from normal, blind, blind-lesioned, and XM ferrets were tuned to pure tones in these ranges (**Figure 3.4**). This was true of auditory-only neurons in XMAC (Aud-XM neurons) and of multisensory neurons in XMAC (Multi-XM neurons). Thus neurons in XMAC and AC of blind-lesioned animals retain selectivity for sound frequency despite the significant early damage to the auditory midbrain (IC).

In addition to the single peak neurons, we encountered a small proportion of multi-peaked auditory neurons in the lesioned animals only (XM group: 3.4%,  $n=8$  from 235 neurons; Blind-lesioned group: 12%,  $n=18$  from 152 neurons) (Fig **3.4F**). These multi-peaked neurons had two BFs, either at 4 kHz and 12 kHz or at 8 kHz and 16 kHz, etc, with 1 to 2 octaves between peaks, distinct from typical multi-peaked neurons that have been described in normal auditory cortex (Sutter and Schreiner 1991). The proportion of auditory neurons that were not tuned to pure tones was 2% for the Normal group ( $n=4$  from 192 neurons), 1% for the XM group ( $n=2$  from

235 neurons), 1.3% for the Blind-lesioned group (n=2 from 152 neurons), and 3.3% for the Blind group (n=3 from 89 neurons) (Fig **3.4E**).

### **c) Visual inputs affect the threshold of auditory and multisensory cortical neurons to sound**

We also examined whether the ectopic visual inputs reduced the responsiveness of XMAC neurons to sound. We did not find any significant differences between groups in the proportion of non-responsive recording sites (Figure **3.5A**). For the responsive sites, because our intention was to compare the differences in auditory response thresholds between groups rather than determine absolute threshold values, we normalized all auditory threshold measurements to the average threshold of the set of normal auditory neurons, which was  $51 \pm 0.7$  dB (n=154). We found significant differences in thresholds of sound-responsive neurons between the normal, blind, blind-lesioned, and XM groups (ANOVA,  $p < 0.001$ , **Fig 3.5B**). First, the normalized thresholds of auditory neurons in blind-lesioned animals were significantly higher than those of normal auditory neurons (Normal:  $1.01 \pm 0.015$ , n=154, Blind-lesioned:  $1.08 \pm 0.016$ , n=108,  $p < 0.001$ , Fisher LSD). These results suggest that the sensitivity to sound in the AC was impaired by IC lesion, as would be expected. Second, we found that the thresholds in XMAC were significantly higher than those in the AC of blind-lesioned animals (Aud-XM neurons:  $1.15 \pm 0.021$ , n=121, Multi-XM neurons:  $1.17 \pm 0.03$ , n=22, Aud-XM vs Blind-lesioned, Multi-XM vs Blind-lesioned,  $p < 0.05$ , Fisher LSD). These findings suggest that the ectopic visual invasion of XMAC further decreases auditory sensitivity, in addition to the impairment brought by IC lesion. Third, we did not find any significant difference in normalized thresholds between the multisensory neurons and the auditory neurons in XMAC (Aud-XM vs Multi-XM, Fisher LSD,  $p = 0.6$ ). Finally, the normalized thresholds of auditory neurons in blind animals were

significantly lower than those of normal auditory neurons (Blind:  $0.89 \pm 0.023$ ,  $n=84$ ,  $p < 0.001$ , Fisher LSD). These data imply that neonatal visual deafferentation increases the sensitivity of auditory neurons to sound, a finding that has been reported by others in several model systems (see Discussion).

**d) Auditory neurons in AC of Xmodal animals had broader tuning to sound frequency than auditory neurons in normal AC**

The width of the tuning curves of sound- responsive neurons has been used as an important metric for the sensitivity of auditory responses (see Aitkin et al. 1984 for review). We expected that auditory deafferentation would result in broader tuning of auditory responses in the AC. In support of this prediction, we found that the bandwidths of sound-responsive neurons were significantly different between normal, blind, blind-lesioned, and Xmodal animal groups (Aud-XM and Multi-XM groups) (Kruskal-Wallis test,  $p < 0.05$ ) (**Fig. 3.5C**). On the one hand, we found that the bandwidths of auditory and multisensory neurons in XMAC were significantly broader than those of auditory and multisensory neurons in normal animals (Normal:  $0.87 \pm 0.04$ ,  $n=154$ , Aud-XM:  $1.09 \pm 0.06$ ,  $n=121$ , Normal vs. Aud-XM,  $p=0.008$ , Mann-Whitney U; Multi-XM:  $1.18 \pm 0.13$ ,  $n=22$ , Normal vs. Multi-XM,  $p < 0.05$ , Mann-Whitney U). These data suggest that visual invasion of XMAC decreases the sharpness of auditory tuning. On the other hand, we did not find any significant differences in sharpness of tuning between the normal group and the two control groups (blind and blind-lesioned groups) (Blind:  $0.87 \pm 0.07$ ,  $n=84$ , Blind-lesioned:  $0.76 \pm 0.05$ ,  $n=108$ , Normal vs. Blind and Normal vs. Blind-lesioned,  $p > 0.05$ , Mann-Whitney U test). These data demonstrate that although auditory cortical neurons in the XM animals have broader tuning, the sharpness of tuning is not affected in the blind-lesioned animals, suggesting

that possible circuitry underlying tuning such as thalamocortical convergence or lateral inhibition in adult AC is not altered by neonatal IC damage. Thus cross-modal visual input decreases the specificity of auditory responses in XMAC, suggesting that cross-modal plasticity could interfere with auditory perception.

**e) Multisensory neurons in AC of Xmodal animals had a longer latency response to sound stimuli than unisensory auditory neurons in either normal AC or Xmodal AC**

In previous research, we measured response latencies to visual stimuli and found that multisensory neurons in XMAC had longer than normal latencies (Mao et al. 2011). Here we calculated the latencies of auditory responses to gain insight into whether the multisensory neurons obtain their auditory inputs directly from thalamus or from cortical sources. We found that the latencies of sound-responsive neurons were significantly different between groups (Kruskal-Wallis test,  $p < 0.05$ ) (**Fig. 3.5D**). Latencies of auditory responses in the multisensory neurons of XMAC were nearly three times longer than those of normal auditory responses (Normal:  $13 \pm 0.6$  ms,  $n=136$ , Multi-XM:  $36 \pm 10$  ms,  $n=22$   $p=0.001$ , Mann-Whitney U), whereas latencies of auditory neurons in XMAC were not significantly different from those of normal auditory neurons (Normal:  $13 \pm 0.6$  ms,  $n=136$ , Aud-XM:  $18 \pm 2.0$  ms,  $n=121$   $p=0.66$ , Mann-Whitney U). These results suggest that auditory neurons in XMAC receive direct thalamocortical projections whereas multisensory neurons are more likely to obtain their auditory inputs from other cortical sources. As expected, we did not find significant differences in latency between the normal and the two control groups (Blind-lesioned:  $19 \pm 1.8$  ms,  $n=126$ ,  $p=0.366$ , Mann-Whitney U, Blind:  $19.6 \pm 2.4$  ms,  $n=84$ ,  $p=0.24$ , Mann-Whitney U). For comparison we also measured the auditory latencies of the small proportion of multisensory neurons seen in normal AC. The

auditory latencies of the multisensory neurons in normal AC were not significantly different from those of normal auditory neurons (Multi-normal:  $19 \pm 9.4$ ,  $n=10$ , Mann-Whitney U,  $p=0.18$ ), supporting the idea that multisensory neurons in normal AC may receive direct projections from thalamus and function in auditory processing as do typical auditory-only neurons.

#### **f) The tonotopic arrangement of auditory and multisensory neurons was altered by cross-modal plasticity**

Tonotopic arrangement is an essential characteristic of neurons in primary auditory areas. We found auditory and visual neurons to be intermingled in XMAC in our previous study (Mao et al., 2011), leading us to hypothesize that invasion of ectopic, cross-modal visual inputs to auditory thalamus disrupts tonotopic order. In order to examine whether IC lesion affects the distribution and proportion of neurons tuned to each part of the sound frequency scale, we divided the scale into 3 bins (low-frequency  $<6$  kHz, mid-frequency 6-12 kHz, high-frequency  $>12$  kHz) and plotted the topographic locations of units responding in these ranges.

#### **i) The tonotopic map of auditory neurons in normal AC**

We first mapped the spatial distribution of low-, mid-, and high-frequency neurons across the primary auditory areas in normal animals, using *in vivo* extracellular recording, for comparison to the other groups. **Figure 3.6** shows examples of the electrode penetration locations and neuronal response types from recordings in normal AC. In each case, the circles represent a single responsive unit. Generally we could isolate two neurons from each penetration using offline spike sorting. As reported in previous research (Kelly et al. 1986; Phillips et al. 1988), we found that the tonotopic map of auditory neurons in normal ferrets showed a high-to-low frequency trend approximately along the mediolateral axis of AC.

## **ii) Tonotopic arrangement of auditory neurons in XMAC**

To determine whether cross-modal visual inputs can disrupt topography of auditory neurons, we plotted the tonotopic maps in the AC of XM cases. We found that high-, mid-, and low-frequency auditory neurons in XMAC were scattered, rather than being arrayed along the medio-lateral axis as observed in normal animals (**Fig 3.7**). These results suggest that auditory tonotopy was severely disrupted by the visual invasion into AC of Xmodal animals.

## **iii) Tonotopic arrangement of multisensory neurons in XMAC**

In addition to assaying the tonotopic arrangement of auditory neurons, we also reconstructed the tonotopic map of multisensory neurons in XMAC (**Fig 3.8**). The sample size of multisensory neurons was smaller than that of auditory neurons in XMAC because they are rarely encountered. In some cases (**Fig 3.8B, C**), we recorded only high- and mid-frequency neurons. In others (**Fig 3.8A, F**), we almost recorded only middle-and low-frequency neurons. Quantified distributions of frequency-tuned neurons in pooled data from this group are compared to those of the normal group below.

## **iv) Tonotopic arrangement of auditory neurons in AC of blind-lesioned animals**

To test the hypothesis that the ectopic visual inputs and not the deafferentation of MGN are responsible for disrupting the tonotopic map in the XMAC, we recorded neurons from AC of the blind-lesioned group. These cases had deafferentation of MGN but no retinal input and thus no visual activation of AC. In support of our hypothesis, we found that the tonotopy of AC in the blind-lesioned animals was quite normal. Neurons responding from high to low best frequencies were aligned along the medio-lateral axis as in normal AC (**Fig 3.9**). These data argue that

neonatal IC damage (MGN deafferentation) did not disrupt tonotopy of auditory neurons in AC of the blind-lesioned animals.

#### **v) Tonotopic arrangement of auditory neurons in AC of blind animals**

To rule out the alternative hypothesis that the recovery of tonotopy in the blind-lesioned animals results from removal of the eyes, we also mapped the distributions of auditory neurons in AC of the blind animals. **Figure 3.10** shows the penetration locations and the neuronal response types from three cases. We found that the tonotopic maps in AC of blind animals were arranged with high-to-low best frequencies along the mediolateral axis, as in normal tonotopic maps.

#### **g) Quantitative comparison of tonotopic maps between groups**

In order to analyze tonotopy between groups statistically, we pooled data within each group (**Fig 3.11**), using methods similar to those used in a previous study (Mao et al. 2011). The recorded primary auditory areas were normalized with respect to their area and were fit to a circle that standardized their orientation with respect to the posterior suprasylvian sulcus and the pseudosylvian sulcus (cf. **Fig 3.2**). Although the tonotopic map in ferrets is oriented roughly along the mediolateral axis, it is important to consider that the exact orientation of tonotopic maps varies between ferrets (Kelly et al. 1986; Phillips et al. 1988), as can be seen in Figure 6. Therefore, the combined plots are useful for comparing between groups but in themselves will blur the map detail somewhat. Our pooled data from normal AC are consistent with the results from previous ferret research, with high frequencies represented medially and low frequencies laterally (**Fig 3.11A**). The insets in **Figure 3.11A** and in the other panels show the center of spatial distribution of the units tuned to low-, mid-, and high-frequency stimuli, with error bars



showing the standard error of the mean of these distributions. In Normal AC there is a mediolateral progression in the spatial distribution centers in each frequency tuning category.

We also plotted the distribution of the group of multisensory neurons recorded in normal AC (Fig **3.11B**). As we shown in a previous study (Mao et al. 2011), multisensory neurons in normal AC were preferentially located laterally. Consistent with this location in the tonotopic map, most were tuned to low- and mid-frequencies.

In contrast to the tonotopic arrangement seen in normal AC, auditory neurons in XMAC were distributed diffusely across the entire AC (Figure **3.11C**). As a result, the distribution centers of the different frequency tuning classes were overlapped (inset, Fig **3.11C**), further reflecting the lack of tonotopy. Interestingly, the distribution centers of the frequency classes of multisensory neurons in XMAC retained some tonotopic order along the mediolateral axis, with the distribution center of the high-frequency neurons separated from the distribution centers of low- and mid-frequency neurons (see below for quantification). On the other hand, the mid- and low-frequency multisensory neurons were more diffusely distributed in XMAC (Fig **3.11D**). The long latencies of Multi-XM neurons (cf. Fig **3.5C**) suggest that they receive indirect corticocortical inputs rather than direct thalamocortical inputs. Taken together, these results suggest that visual invasion may affect the thalamocortical pathway more severely. However, we cannot rule out the possibility that the no-overlapped location of high-frequency neurons results from sampling error due to the low proportion of high-frequency neurons in this group (8 out of 61, Fig **3.11D**).

The tonotopic organization of auditory neurons in AC of blind-lesioned animals and in the blind animals was very similar to the tonotopy in the normal group (Figs **3.11E, F**). The

tuning progressed from high to low along the mediolateral axis, as reflected by the distribution centers seen in the insets.

Overall, these results suggest that the ectopic visual inputs led to a disrupted topography of frequency-tuned neurons in XMAC. In combination with the higher thresholds and broader tuning, it is clear that auditory function of XMAC is compromised. The tonotopic organization of AC in each group will be analyzed and discussed below.

#### **h) The spatial distribution of high- and low-frequency neurons were altered in X-modal animals**

Because the tonotopic map in normal ferret AC is oriented along the mediolateral axis, we quantified the mediolateral location of frequency-tuned neurons across groups (**Fig 3.12**; smaller numbers represent more lateral locations). We found that high-frequency auditory neurons in XMAC were located significantly more laterally than those in normal AC ( $p < 0.001$ , ANOVA, **Fig 3.12A, D**), whereas low-frequency auditory neurons in XMAC were located significantly more medially than those in normal AC ( $p < 0.05$ ,  $t$ -test, **Fig 3.12C, D**). No significant difference was found with respect to the location of mid-frequency neurons across the five groups ( $p > 0.05$ ,  $t$ -test, **Fig 3.12B, D**). These data suggest that high- and low-frequency neurons are more overlapped in XMAC than in normal AC, as suggested by the insets in **Fig 3.11C**. We did not observe any significant difference between normal and blind-lesioned groups or normal and blind groups ( $p > 0.05$ ,  $t$ -test, **Fig 3.12A-C**), suggesting that in the blind-lesioned animals the auditory pathway can largely compensate for early damage to IC and contribute normally to auditory tonotopy in AC. Because the enucleation did not affect tonotopy in ferret AC, the data

imply that the disruption of tonotopy in the Xmodal group was caused by the ectopic visual invasion.

**i) The frequency distribution of tuned neurons was not altered by cross-modal plasticity**

We showed in a previous study that an increasing degree of damage to IC is associated with a decrease in the proportion of auditory neurons and an increase in the proportion of visual and multisensory neurons in XMAC (Mao et al. 2011). In ferrets and cat IC is arranged from low to high frequency along its dorso-ventral axis (Merzenich and Reid 1974; Moore et al. 1983). Because we use a dorsal approach to lesion the IC of Xmodal and blind-lesioned ferrets, the dorsal aspect of IC is preferentially damaged. Therefore, we asked in the current study whether all frequencies were represented in XMAC. We hypothesized that low-frequency neurons would be lost in the lesioned ferrets. Alternatively, neonatal, partial damage to IC could trigger a compression of IC's tonotopic map, similar to what occurs with neonatal, partial lesions of SC (Finlay et al. 1979; Pallas and Finlay 1989). In that case we would expect all frequencies to be represented. We did not find any significant difference in the proportions of mid- and high-frequency neurons between groups ( $p > 0.05$ , ANOVA, **Fig 3.13**). The proportion of low-frequency neurons in the Aud-XM group was significantly lower than that in the normal group ( $p = 0.005$ , t-test, **Fig 3.13C**), suggesting a failure of the IC tonotopic map to compress. This interpretation does not consider the fact that many of the sound-responsive neurons in XMAC are bisensory, however. When we included all low-frequency-tuned neurons (Aud-XM plus Multi-XM) in the analysis, we found that the proportion of low-frequency neurons was not significantly different from that in the normal group ( $p > 0.05$ , t-test, **Fig 3.13C**). Taken together, these results suggest that dorsal midbrain lesions do not eliminate low-frequency-tuned neurons

from the pathway between IC and AC. The apparent compression of the tonotopic map in IC is an interesting finding that we hope to follow up in future studies.

## **5. Discussion**

In a previous study (Mao et al. 2011) we demonstrated that, contrary to previous reports, auditory cortex retains its ability to respond to sound stimuli after invasion of cross-modal visual inputs. In the present study we tested the hypothesis that such cross-modal plasticity negatively affects residual auditory cortical function. We found that considerable auditory function remains in XMAC after recovery, in that most neurons respond to sound and have a preferred frequency. The sensitivity to sound, the sharpness of tuning, and the organization of the tonotopic map in XMAC are impaired, however. These results imply that sound discrimination ability is still compromised after several months of recovery. The results from the blind-lesioned control group show that it is the anomalous visual input to auditory cortex and not simply deafferentation of the auditory pathway that is responsible for the impairments of auditory function, suggesting that loss of input to auditory thalamus can be compensated during recovery. In the blind group, the auditory map was normal but the sensitivity of auditory neurons to sound was increased, suggesting that visual impairment can boost auditory processing ability, as seen in blind humans (Roder et al. 1999).

### **a) Auditory tuning and tonotopy are impaired by invasion of ectopic visual inputs**

Cross modal plasticity has been widely studied in auditory, visual, and somatosensory systems. For example, auditory cortex of early-deaf cats is recruited for somatosensory and visual functions (Lomber et al. 2010; Meredith and Lomber 2011). Auditory prostheses can rescue auditory function to some extent in deaf patients and animal models (Klinke et al. 2001; Kral

2007; Middlebrooks et al. 2005). The success of cochlear implants can be compromised if auditory cortex exhibits cross-modal activation before implantation is performed, however (Lee et al. 2001). The basis for this effect is unknown. Here, using a model system in which the degree of cross-modal contamination of auditory cortex can be varied experimentally, we addressed whether visual input can negatively impact residual function in the auditory pathway. We found that tonotopy was disrupted by cross-modal inputs. We also found that response thresholds and sharpness of auditory tuning were degraded in the XMAC group compared to the control groups. These results demonstrate that after recovery from neonatal midbrain damage, ectopic visual inputs to the auditory pathway impair auditory function in several ways, providing a possible explanation for the deficits remaining after cochlear prostheses are provided to early-deaf patients. They may also provide insight into the phenomenon of tinnitus that can occur after hearing loss. As in patients who can perceive their amputated limb after surgery, tinnitus patients may hear phantom tones or noise in a quiet environment (Jastreboff 1990). Tinnitus may be triggered or modulated by cross-modal somatosensory, somatomotor or visuomotor inputs (Cacace 2003). We show that many new multisensory neurons are created in XMAC, and that they can respond to optic nerve stimulation while simultaneously being tuned to particular sound frequencies. These novel multisensory neurons provide a possible way to explain how visual activity may express itself as auditory stimulation, creating perceptual confusion and thus phantom sounds. These results suggest avenues for further study of tinnitus patients with peripheral auditory damage, and may also help to guide a general understanding of how maladaptive plasticity can occur after brain damage, interfering with rehabilitation.

## **b) Auditory tuning and tonotopy of multisensory neurons**

In addition to the classically multisensory brain areas such as the superior colliculus and anterior ectosylvian sulcus (AES) (Meredith and Stein 1983; Wallace et al. 1992), primary sensory cortices exhibit multisensory responses, although to a lesser extent (Ghazanfar and Schroeder 2006; Schroeder et al. 2003; Wallace et al. 2004). Experiments on normal ferrets show that multisensory neurons in primary auditory cortex have frequency tuning similar to that seen in auditory-only neurons (Bizley et al. 2007). Consistent with these results, we found that bisensory neurons in XMAC exhibited normal auditory characteristics. They were not only tuned to pure tones, but were arranged in tonotopic fashion. This frequency selectivity and tonotopic arrangement of multisensory neurons in XMAC suggests that their dominant functions are auditory, even though they receive visual input. We also found that multisensory neurons in XMAC had longer response latencies to sound stimuli than multisensory neurons in normal AC. It is possible that auditory neurons receiving direct thalamocortical auditory input are less likely to receive cross-modal visual inputs than are auditory neurons receiving longer latency auditory inputs. The competition between afferents may push visual afferents to innervate neurons that receive corticocortical auditory connections, giving those neurons longer auditory latencies.

## **c) Multi-peaked auditory neurons appear in XM and blind-lesioned animals**

Most auditory neurons recorded in normal primary auditory cortex of ferrets are single-peaked with very narrow tuning curves (Kelly et al. 1986; Phillips et al. 1988). We observed some neurons in AC of XM animals and the blind-lesioned animals, but not in normal AC, that had more than one best frequency, creating multiple peaks in their tuning curves. Unlike multi-peak neurons reported by others in normal AC (Sutter and Schreiner 1991), the two peaks were

widespread in frequency, making it unlikely that unmasking of surround inhibition (Rajan 2001; 1998) could provide an explanation. Alternatively, residual auditory inputs from subcortical auditory nuclei may sprout and project to adjacent areas in MGN or auditory cortex. Whatever the explanation, the creation of multi-peaked tuning curves in XMAC implies that auditory neurons in XMAC have lost considerable frequency specificity as a result of the loss of some auditory input and gain of visual input. Our finding that tuning curves in XMAC were broader than those in normal AC supports this idea.

#### **d) Auditory tuning and tonotopy are largely normal in blind-lesioned animals**

Research on peripheral deafferentation in the somatosensory system (Kaas 1991; Merzenich et al. 1983), auditory system (Irvine 2000), and visual system (Lund and Lund 1976) shows that sensory responsiveness can largely recover in the denervated areas. For example, in animals with partial cochlear lesions, an area of expanded representation corresponding to the lesion-edge frequencies is found in inferior colliculus (Harrison et al. 1998; Harrison et al. 1993; Irvine et al. 2003), medial geniculate body (Kamke et al. 2003), and auditory cortex (Irvine et al. 2001; Kakigi et al. 2000; Rajan et al. 1993). In this study, we ablated the dorsal aspect of the inferior colliculi of neonatal ferrets (see Figure 1), which may have resulted in loss of sensory drive from low to mid-frequency channels (Merzenich and Reid 1974; Moore et al. 1983; Serviere et al. 1984). We found that auditory tuning and tonotopy in the blind-lesioned animals were not significantly different from those in normal AC. These results suggest that the auditory tonotopic map is compressed rather than incomplete after recovery from IC damage, as occurs in visual midbrain superior colliculi after neonatal damage (Finlay et al. 1979), and thus that the inferior colliculus has the potential to rearrange its connections when it is damaged. This may

have been facilitated by the late onset of hearing (about P30 in ferrets) (Moore and Hine 1992) and the fact that the auditory afferents reach the inferior colliculus but have not yet segregated into frequency bands at birth when lesions are made (Brunso-Bechtold and Henkel 2005; Henkel et al. 2007).

Overall, our results show that auditory function in the IC-lesioned, blind animals is largely recovered, independent of any contribution from the visual pathway. These results suggest that compensatory plasticity can substantially rebuild auditory function after deafferentation.

#### **e) Auditory tuning is improved in blind ferrets**

Many behavioral studies in humans and in animal models have demonstrated that perceptual ability in the spared sensory modality is improved after blindness or deafness (King and Parsons 1999; Rauschecker and Korte 1993), perhaps as a result of cross-modal plasticity. Auditory cortex in deaf humans is recruited during visual processing (Finney et al. 2001), and the cortical area activated by sound is expanded in blind humans (Elbert et al. 2002). Auditory response thresholds are also reduced in the auditory cortex of the early blind, suggesting that their auditory processing is more efficient (Stevens and Weaver 2009). Auditory spatial tuning of neurons in the anterior ectosylvian cortical region of early-blind cats is sharpened (Korte and Rauschecker 1993). Here we show that auditory tuning characteristics in primary auditory cortex of blind animals are improved compared to normal, perhaps leading to improved perceptual ability as seen in blind and deaf patients. Thus, cross-modal ferrets may be a useful animal model for study of sensory substitution after deafness.



In conclusion, these findings provide further evidence that although auditory cortex can recover from neonatal deafferentation in some respects, its function is impaired by ectopic cross-modal visual inputs, suggesting that minimization of cross-modal activity may improve recovery. Understanding the mechanism that underlies the compromise of auditory function will be important for facilitating recovery from brain damage, sensory/motor deafferentation, and sensory dysfunction, and is the subject of a current study (Mao and Pallas 2011).

## **6. Acknowledgements**

The authors wish to thank Profs. Khaleel A. Razak, Robert Liu, Donald Edwards, and Charles Derby for their comments in the preparation of the manuscript. We also thank Dr. Jennifer Bizley, Ph.D. and Dr. Jeff Ko, DVM for advice on ferret anesthesia. We are indebted to the Department of Animal Resources at GSU, and particularly Cindy Marshall, for expert animal care. This research was supported by grants to SLP from NSF (IBN-0451018), NIH (NIH 744 EY/MH12696) and the GSU Research Foundation, by a GSU Brains and Behavior scholarship to YTM, and by the STC Program of the National Science Foundation (IBN-746 9876754).

**Table 3.1.** The proportion of low-frequency neurons and residual midbrain volumes in lesioned animals. The midbrain volumes were normalized to average midbrain volumes of normal animals. IC represents inferior colliculus, SC represents superior colliculus. L- Represents left. R- Represents right.

	Low-frequency neuron (%)	L-IC (%)	R-IC (%)	Ave IC (%)	L-SC (%)	Ave left midbrain (%)
Xmodal						
08-240	12.5	0	12.66	6.33	38.19	19.10
09-21	0	0	37.70	18.85	6.26	3.13
08-201	0	0	34.69	17.34	5.44	2.72
08-253	0	1.06	15.47	8.26	51.12	26.09
09-191	3.86	5.62	23.59	14.61	11.48	8.55
09-15	0	11.00	73.36	42.18	64.36	37.68
11-01	12.5	35.96	46.29	41.12	19.84	27.90
09-203	9.76	47.86	66.59	57.23	62.90	55.38
09-172	33.33	51.38	26.95	39.17	23.79	37.58
Average		24 ± 5.9		27± 6.0		17± 7.2
Blind-Lesioned						
10-119	12.5	10.41	64.53	37.47	13.69	12.05
11-36	8.70	15.90	30.07	22.99	11.87	13.89
10-104	16.67	20.28	47.83	34.05	19.00	19.64
10-98	45	29.20	11.10	20.15	39.98	34.59
10-110	47.37	29.20	37.74	33.47	16.30	22.75
10-116	8.7	47.54	37.01	42.27	10.50	29.02
Average		22 ± 3.6		32± 3.5		25± 5.4

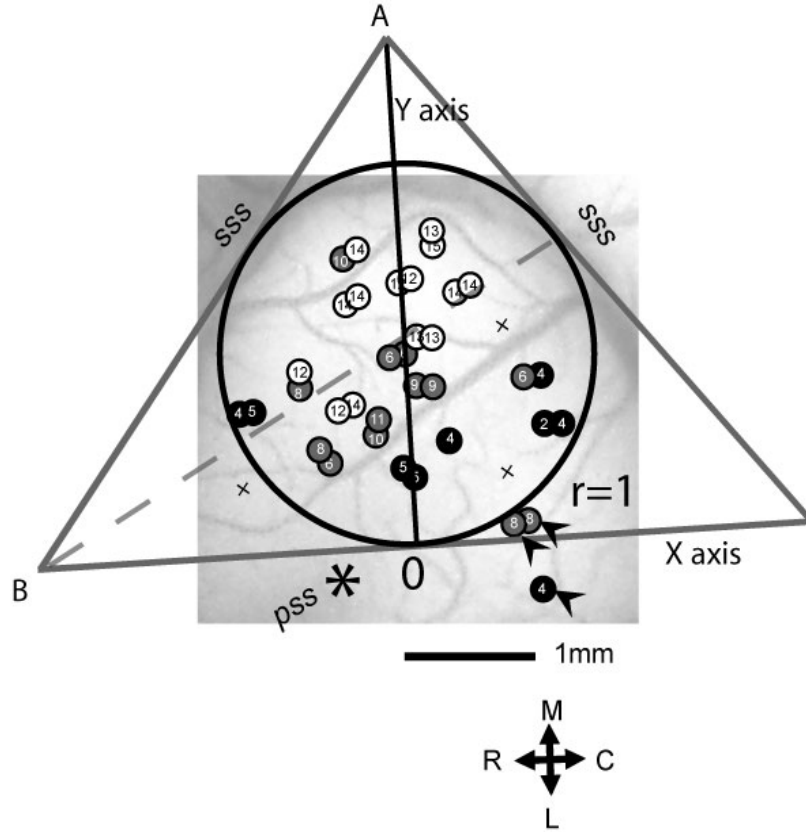


**Figure 3.1.** Method for quantification of neuronal response type distribution in auditory cortex.

Based on the location of ferret AC on the middle ectosylvian gyrus, we drew an equilateral triangle along the anterior and posterior suprasylvian sulcus and across the tip of the pseudosylvian sulcus (pss) (\* indicates the tip of pss). An internally tangent circle was drawn. Two lines were drawn along the anterior and posterior arms of the suprasylvian sulcus to form angle A. The third line was drawn just above the tip of the pseudosylvian sulcus and perpendicular to the dividing line of angle A, creating angle B. The intersection of the third line and the bisecting line of angle A is defined as point 0. The arrowheads point to several neurons in lateral AC that responded with a long latency (>100 ms) to sound stimuli, reflecting their location outside of the primary auditory areas. Such neurons were excluded from analysis. R represents rostral, C represents caudal, M represents medial, L represents lateral.

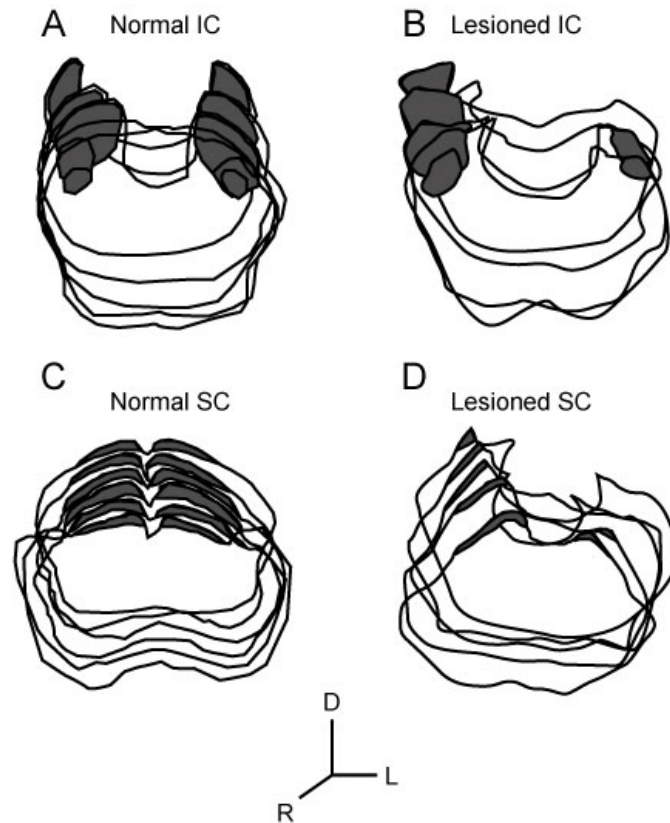


**Figure 3.2.** Assessment of midbrain damage. Dark areas represent the central nucleus of the inferior colliculus (ICc) (A, B) and the superficial layers of the superior colliculus (sSC) (C, D). A. An example of a series of sections through the normal IC. B. An example of a series of sections through the lesioned IC. C. An example of a series of sections through the superficial layers of normal SC. D. An example of a series of sections through the superficial layers of lesioned SC. The directional at bottom indicates dorsal (D), rostral (R) and left (L). The left side was oriented on the right in this figure in order to show rostral sections of ICc in the front after sectioning from caudal to rostral. In all panels several sections at 400 μm intervals are overlain.

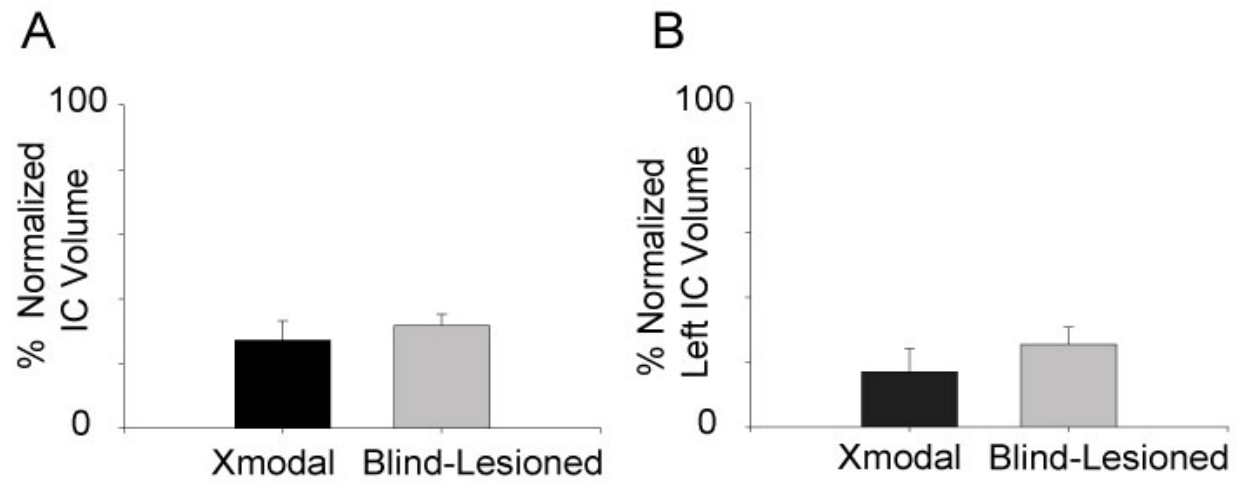
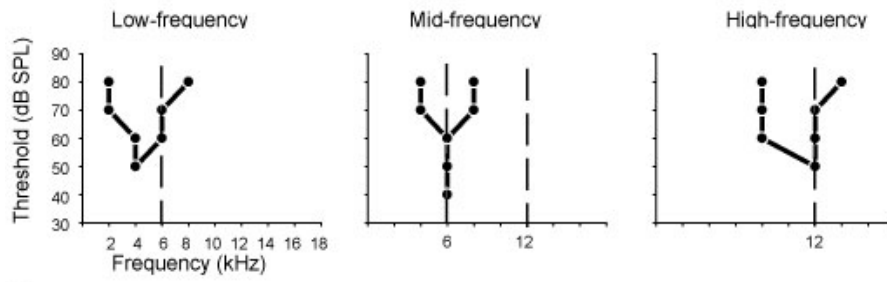


**Figure 3.3.** Statistical comparison of residual volume of inferior colliculi in Xmodal and blind-lesioned animals. Data represent Mean  $\pm$  S. E. M.

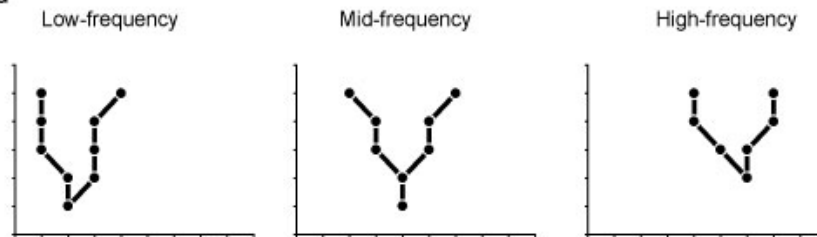
A

Normal



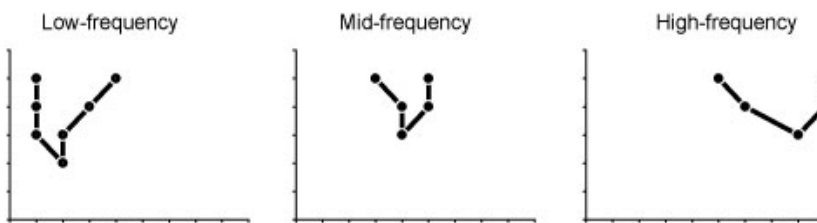
B

Blind



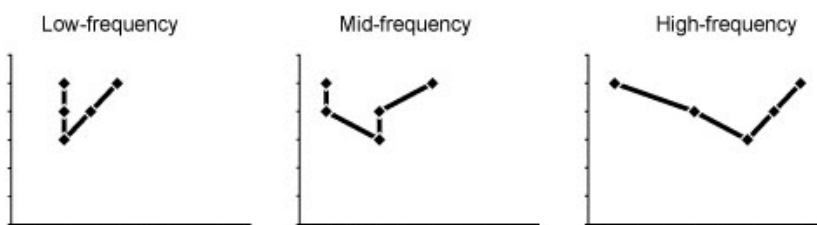
C

Blind-lesioned



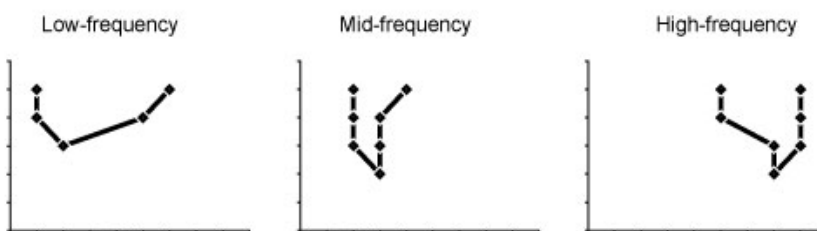
D

Auditory-XM



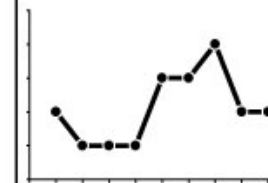
E

Multisensory-XM



F

No BF auditory neuron



G

Dual-peak auditory neuron



**Figure 3.4.** Examples of tuning curves of auditory and multisensory neurons. A. Tuning curves of auditory neurons in normal AC. The dashed lines represent frequencies at which neurons were divided into low-, mid-, and high-frequency bins. B. Tuning curves of auditory neurons in the AC of blind animals. C. Tuning curves of auditory neurons in the AC of blind-lesioned animals. D. Tuning curves of auditory neurons in the XMAC. E. Tuning curves of multisensory neurons in the XMAC. F. An example of a tuning curve from a No-BF auditory neuron. No BF auditory neurons respond to multiple pure tones but do not show any preference. G. An example of a tuning curve from a dual-peak auditory neuron. Dual-peak auditory neurons have two best frequencies.



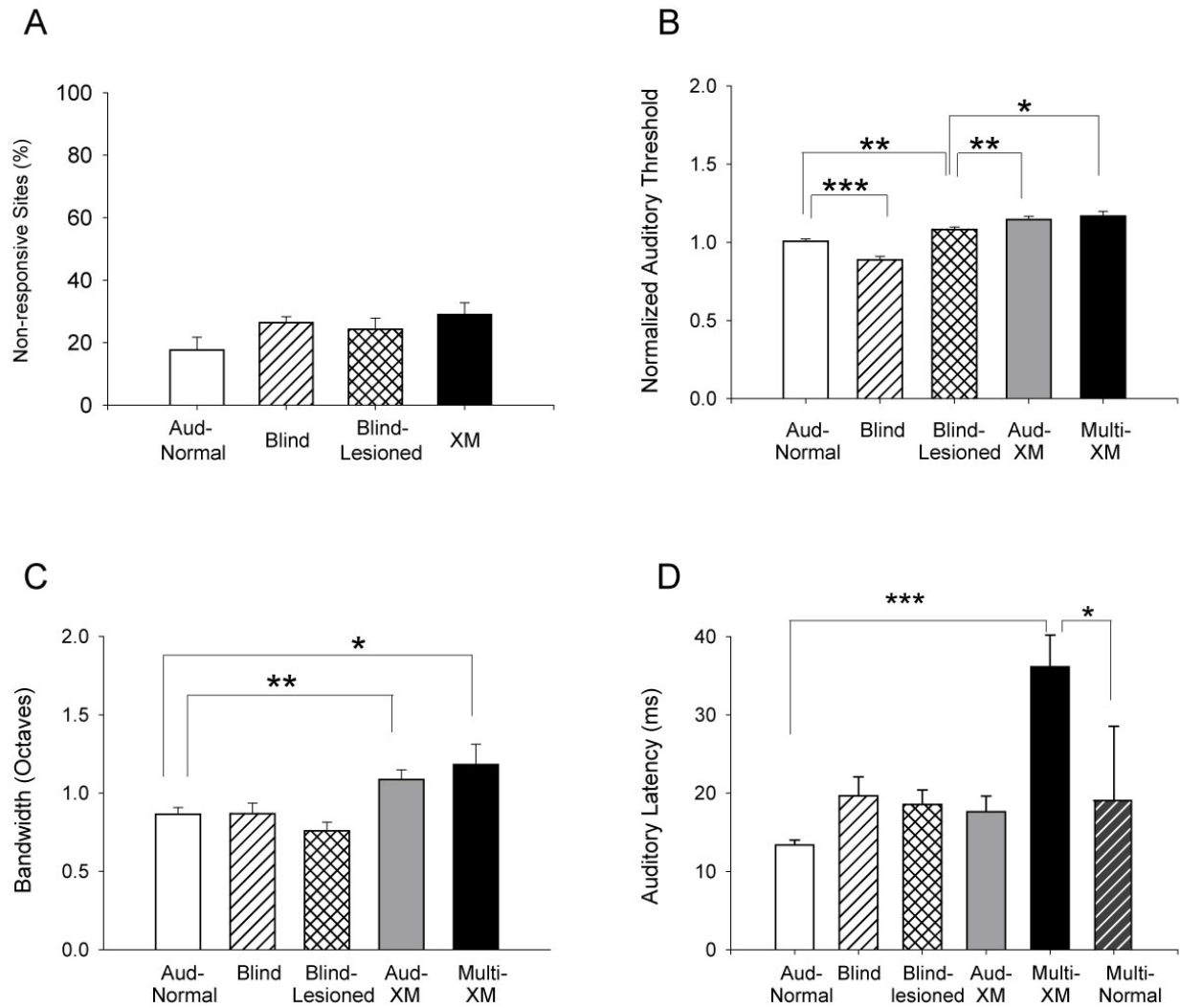


**Figure 3.5.** The response characteristics of neurons in Xmodal and control animals. A. The proportion of non-responsive recording sites across groups. No significant difference was found despite comparable sampling densities and locations. B. Normalized thresholds of auditory responses across groups. C. Bandwidth of auditory responses across groups. D. Latencies of auditory responses across groups. Error bars show  $\pm$  S.E.M.. \*\*\* indicates  $p < 0.001$ , \*\* indicates  $p < 0.01$  \* indicates  $p < 0.05$ .

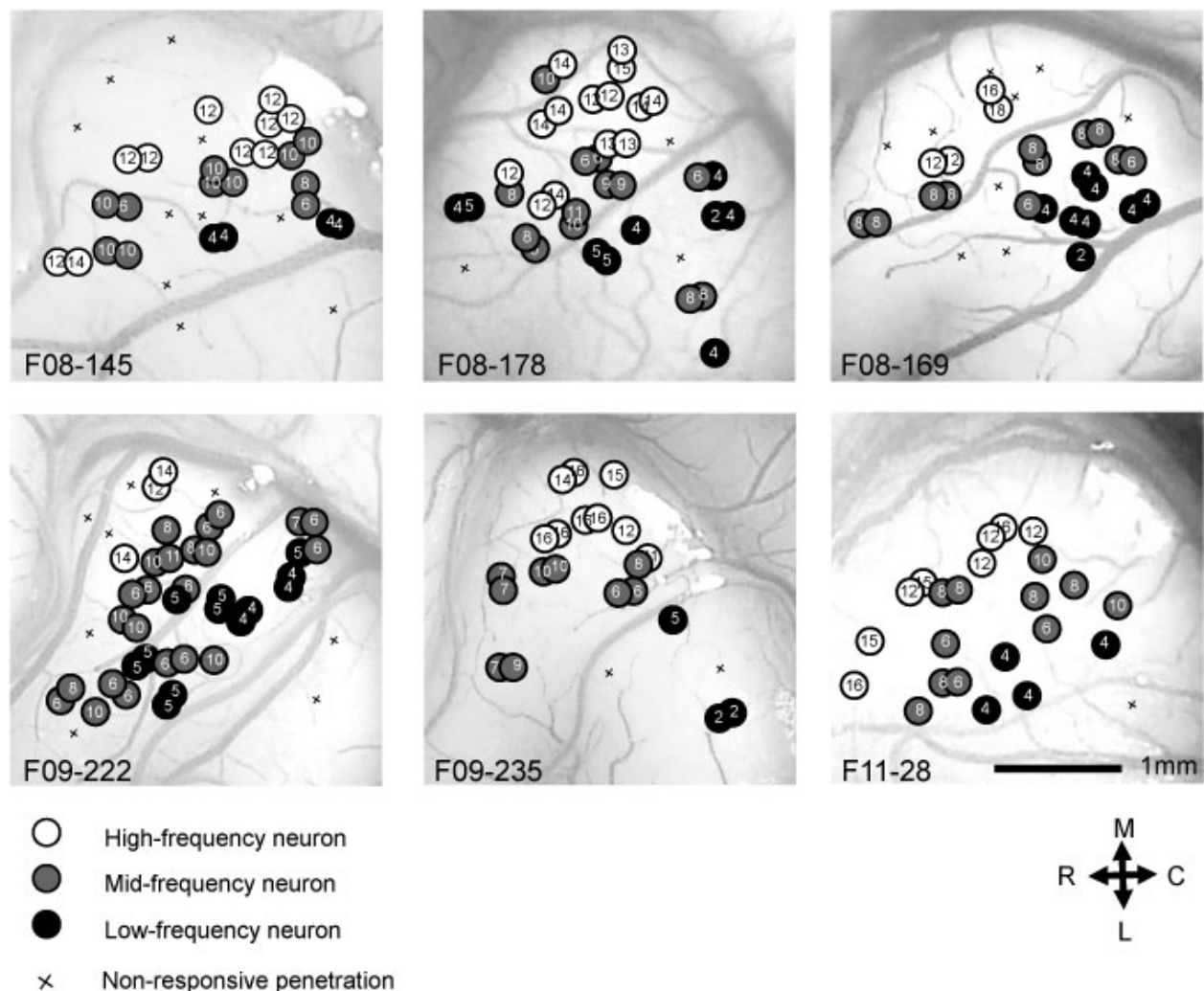


**Figure 3.6.** Reconstruction of locations of frequency-tuned neurons in normal AC. Each panel exhibits data from 1 animal (6 of 8 examples are shown). Each circle represents one auditory unit, and the numbers in the center indicate BFs, expressed in kHz. White circles represent high-frequency neurons (responding to sound  $\geq 12$  kHz). Gray circles represent mid-frequency neurons (responding to sound  $\geq 6$  kHz and  $< 12$  kHz). Dark circles represent low-frequency neurons (responding to sound  $< 6$  kHz). X indicates a non-responsive site. Scale bar: 1 mm.

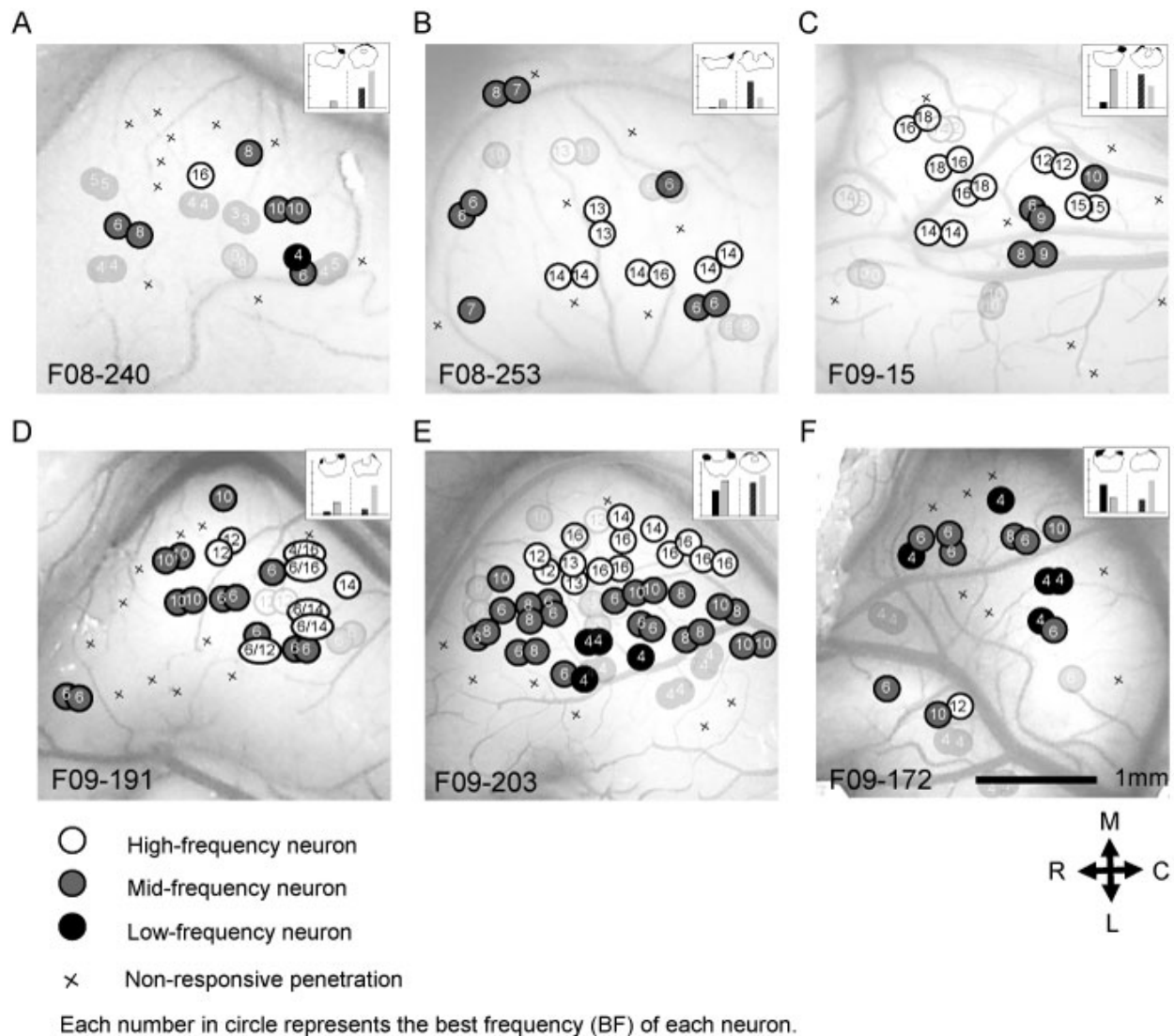


**Figure 3.7.** Reconstruction of locations of frequency-tuned auditory neurons in AC of Xmodal animals. Semitransparent circles represent multisensory neurons that were recorded at the same time. Each panel shows data from one animal (6 of 9 examples are shown). A-F. The panels are ordered from small residual left IC to large residual left IC. The insets show the volumes of residual midbrain from each animal. The Y axis represents the proportion of spared midbrain as a percent of the average volume of normal midbrains. The maximum is therefore 100%. Above the insets to the left is a section of IC and on the right is a section of SC from the same animal. The

dark areas in these insets represent the central nuclei of IC and the superficial layers of SC.

Corresponding to these two figures, the four histogram bars on the X axis represent the residual volumes of left IC, right IC, left SC and right SC, from left to right.

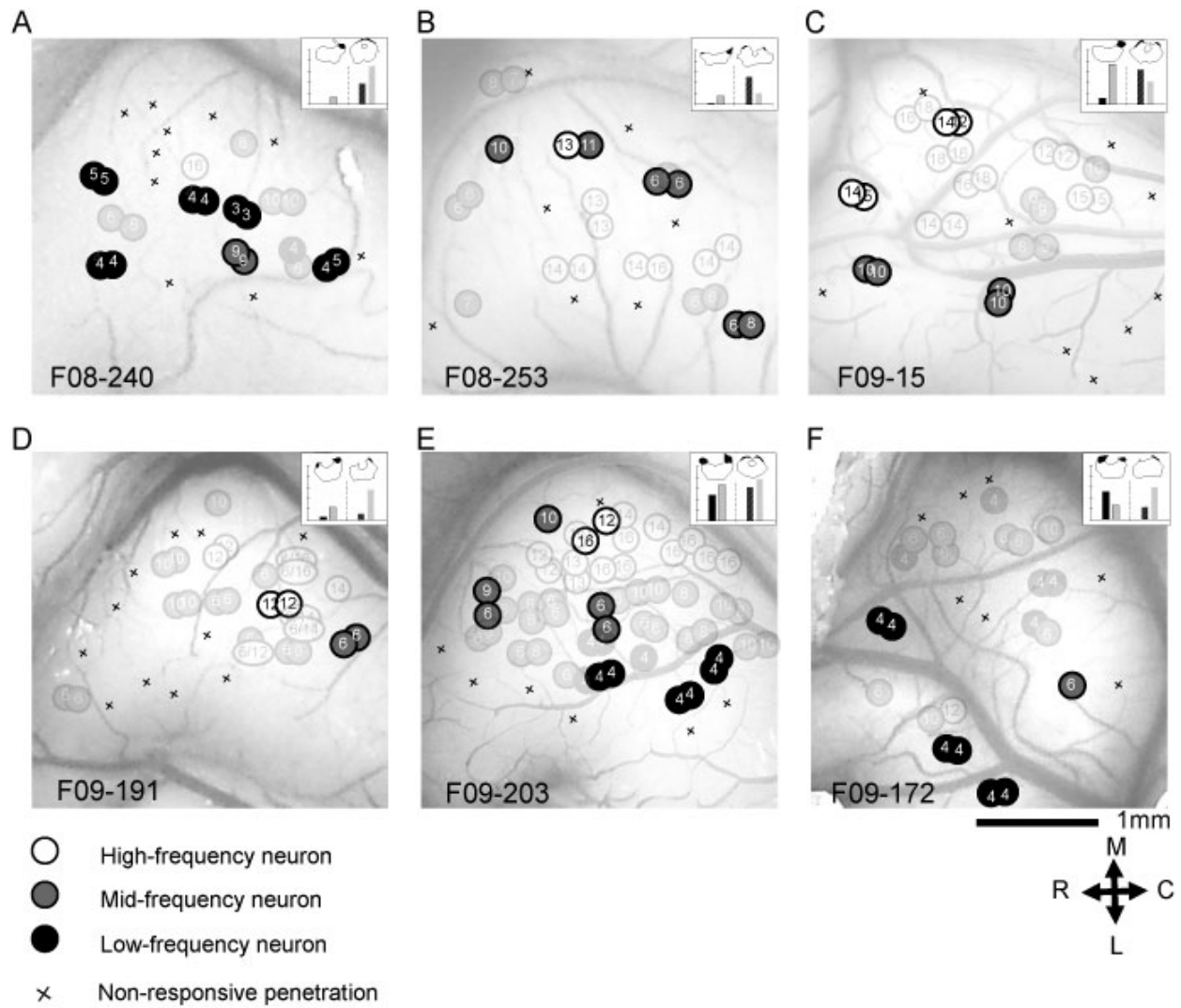


**Figure 3.8.** Reconstruction of locations of frequency-tuned multisensory neurons in AC of Xmodal animals. Semitransparent circles represent auditory neurons that were recorded in the same session. Each panel exhibits data from 1 animal (6 of 8 examples are shown). A-F. The panels are ordered from small residual left IC to large residual left IC. The insets show the volumes of residual midbrain from each animal (conventions as in Fig. 3.7.).

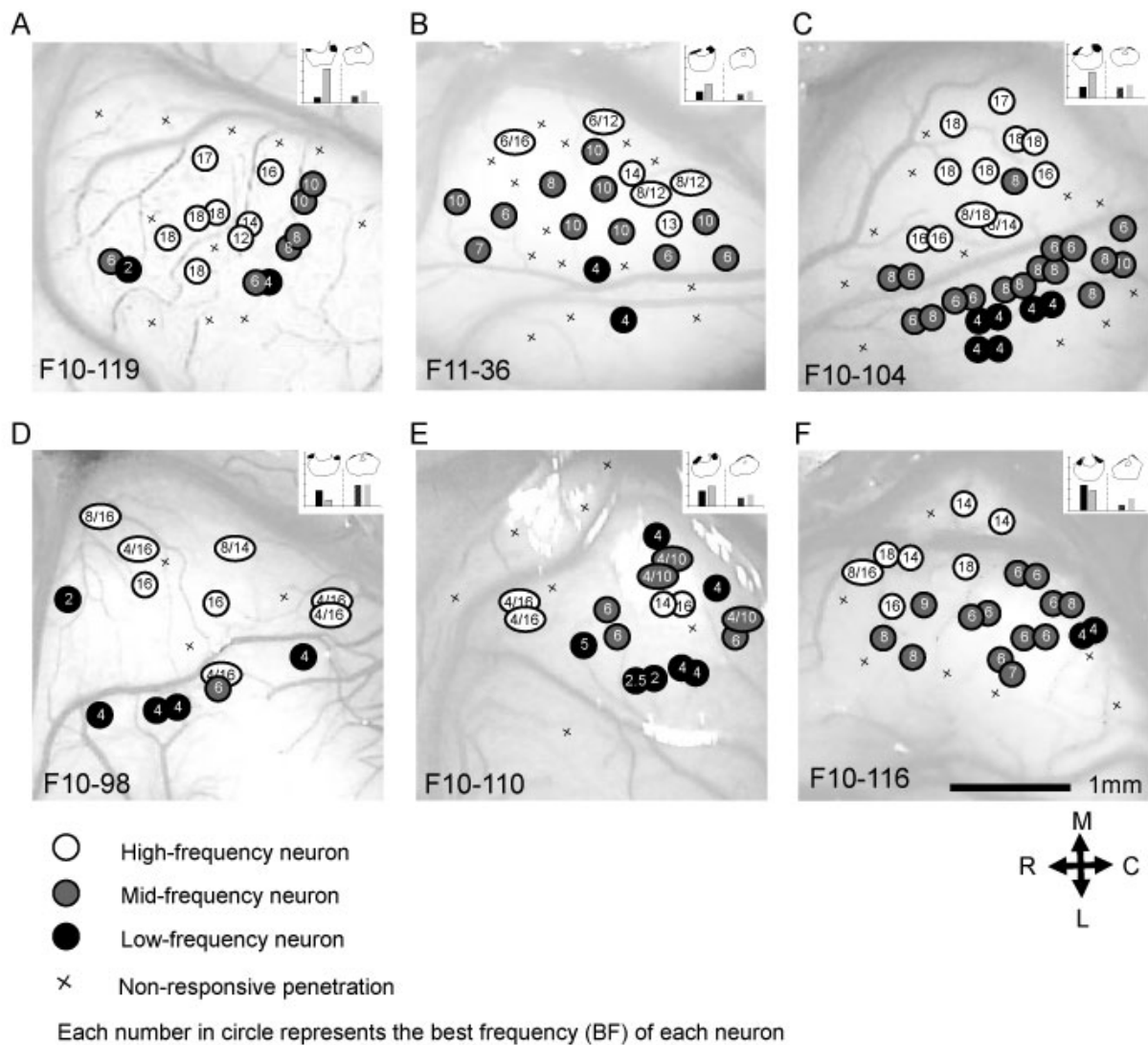


**Figure 3.9.** Reconstruction of locations of frequency-tuned neurons in AC of blind-lesioned animals. Each panel shows data from 1 animal (6 of 6 examples are shown). (A-F) Animals are listed in order from small residual left IC to large residual left IC. Conventions as in Fig. 3.7.

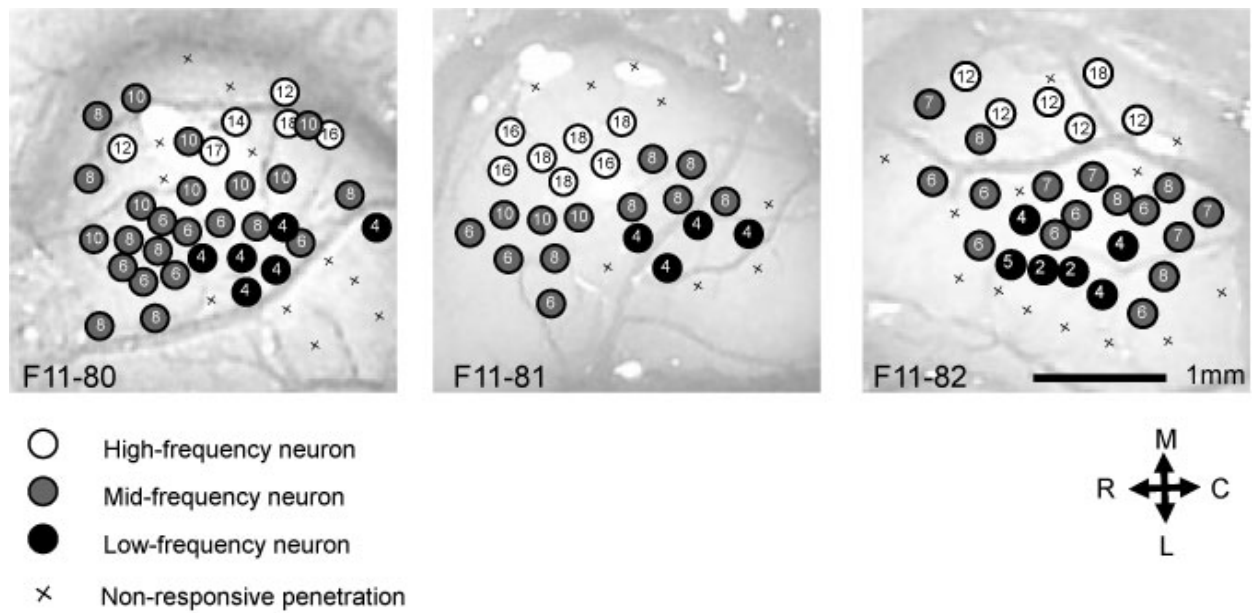
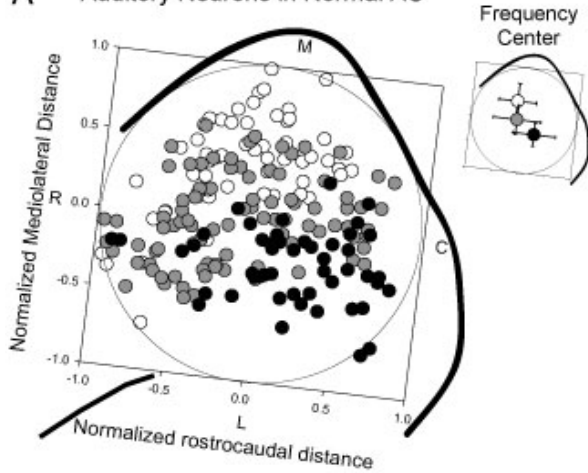
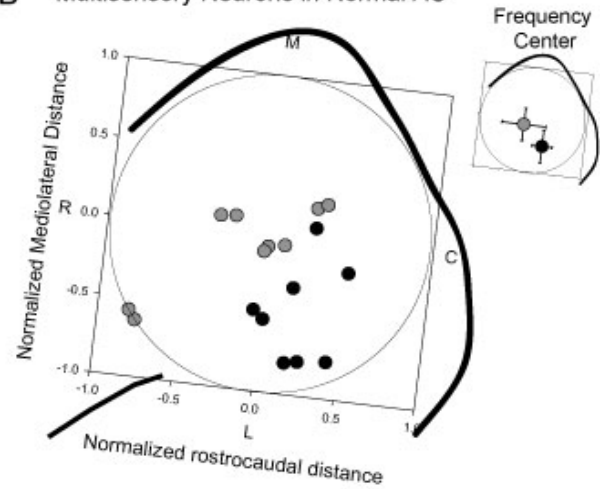


**Figure 3.10.** Reconstruction of locations of frequency-tuned neurons in AC of three blind animals. Scale bar: 1 mm.

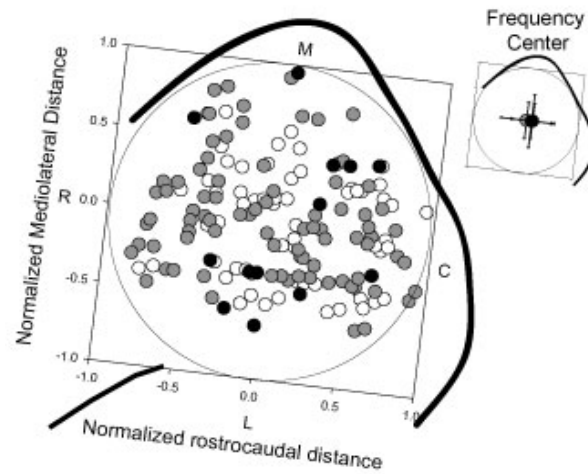
**A** Auditory Neurons in Normal AC



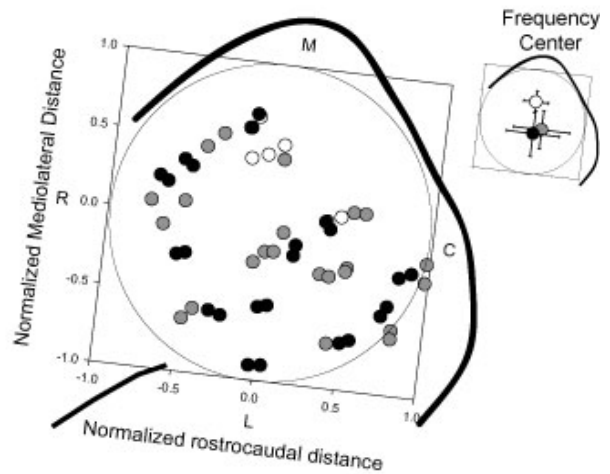
**B** Multisensory Neurons in Normal AC



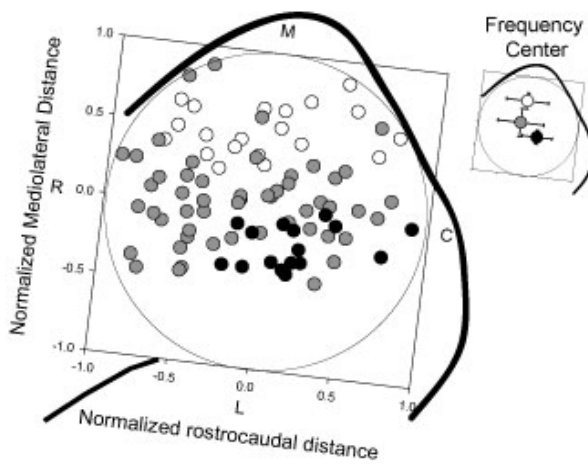
**C** Auditory Neurons in AC of X-modal Animals



**D** Multisensory Neurons in AC of X-modal Animals



**E** Auditory Neurons in AC of Blind Animals



**F** Auditory Neurons in AC of Blind-lesion Animals

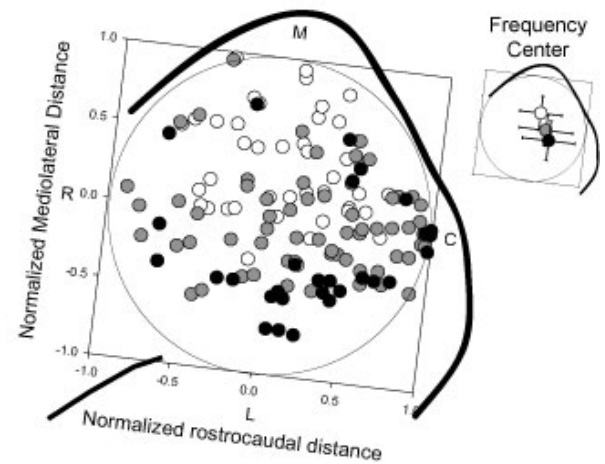




**Figure 3.11.** Distribution of frequency-tuned neurons in AC of ferrets using pooled data from each group. As in the micrographs, rostral is to the left and caudal to the right in these lateral views of the left AC. Open circles represent the class of high-frequency neurons. Gray circles represent mid-frequency neurons. Dark circles represent low-frequency neurons. The insets show the geographic centers  $\pm$  SE of the distribution of each frequency class. A. Distribution of auditory neurons pooled from 8 normal animals. Note that high frequencies are represented medially, mid frequencies centrally, and low frequencies laterally. B. Distribution of multisensory neurons pooled from 8 normal animals. These neurons are tuned appropriately for their location within the tonotopic map of auditory-only neurons. C. Distribution of auditory neurons pooled from 9 Xmodal animals. Note the lack of clear tonotopic order and the overlap in distribution centers in the inset. D. Distribution of multisensory neurons pooled from 9 Xmodal animals. E. Distribution of auditory neurons pooled from 3 blind animals. Tonotopy is normal. F. Distribution of auditory neurons pooled from 6 blind-lesioned animals. Tonotopy is clear and the orientation of the map is normal.

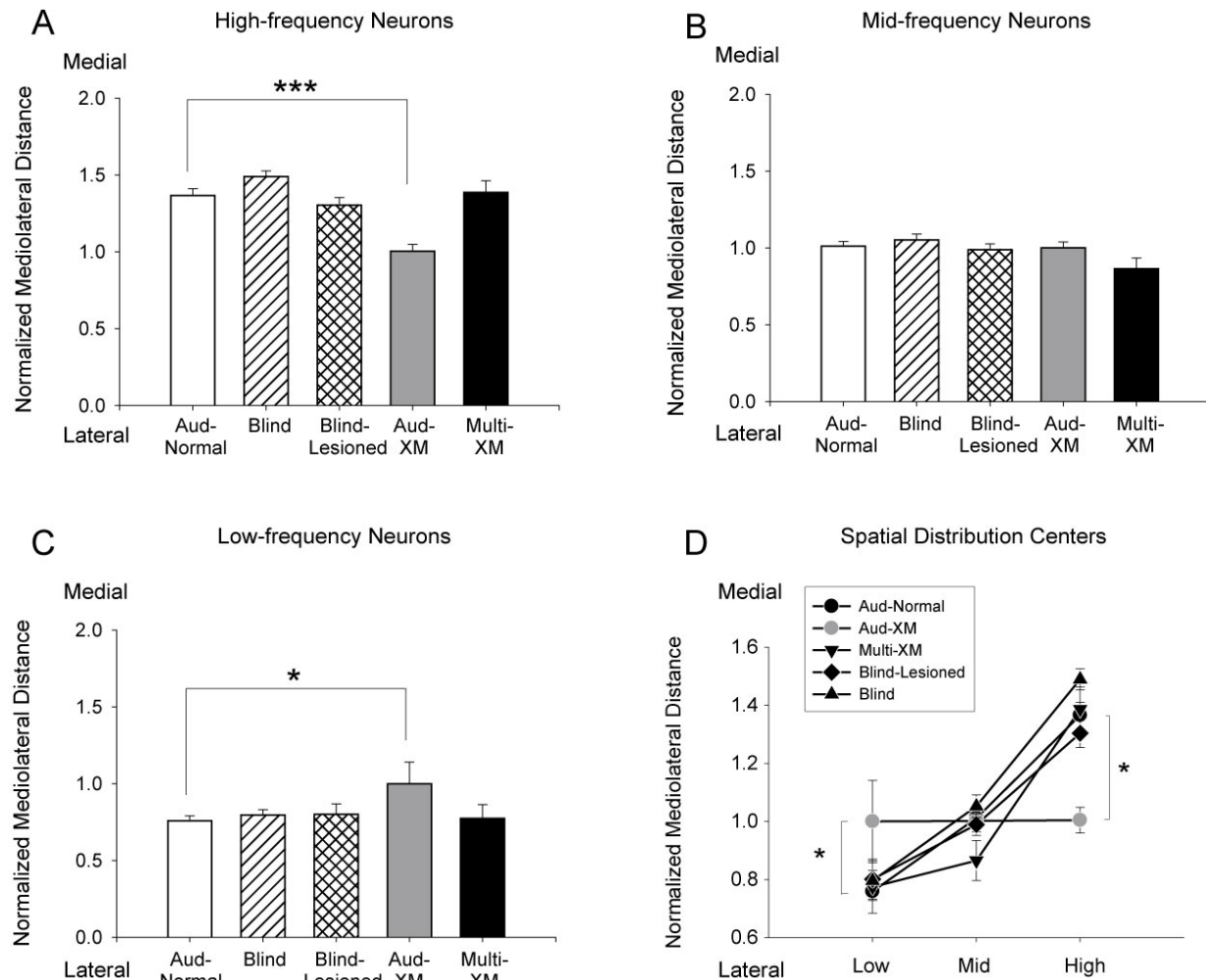
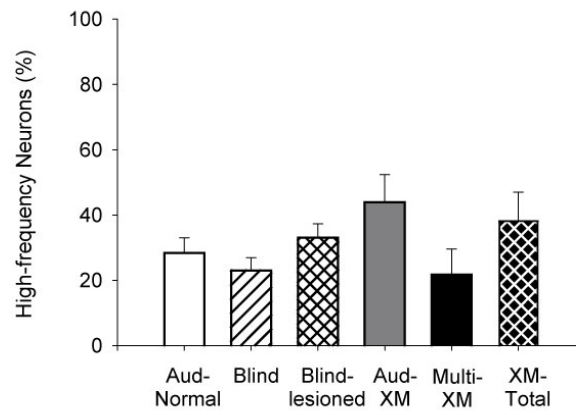


**Figure 3.12.** The location of frequency-tuned neurons in the 5 groups. A. High-frequency neurons in Xmodal AC were located significantly more laterally than those in normal AC. B. The locations of mid-frequency neurons in the five groups were not significantly different from each other. C. Low-frequency neurons in Xmodal AC were located significantly more medially than those in normal AC. D. Low-, mid- and high-frequency auditory neurons in the XM group were located at similar mediolateral locations (gray circle), showing a marked reduction in tonotopy compared to that in the normal group. Error bars show  $\pm$  S.E.M.. ( \*  $p < 0.05$ ; \*\*\*  $p < 0.001$ )

## Proportion

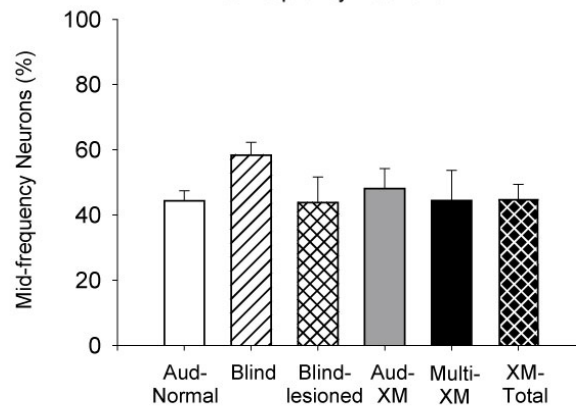
A

### High-frequency Neurons



B

### Mid-frequency Neurons



C

### Low-frequency Neurons

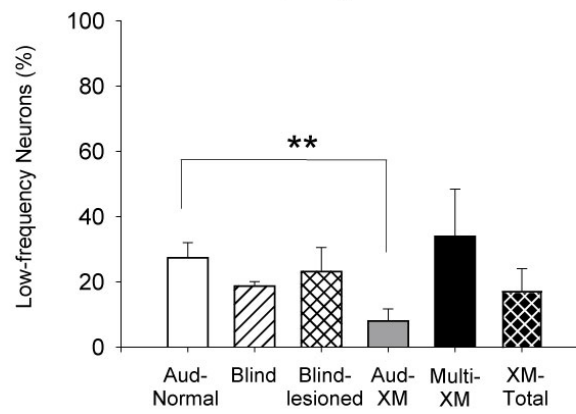


**Figure 3.13.** The proportion of frequency-tuned neurons in the 5 groups. A. The Y-axis represents the percentage of neurons tuned to high-frequency sounds. There was no significant difference in the proportion of high-frequency neurons between groups. B. There was no significant difference in the proportions of mid-frequency neurons between groups. C. The proportion of low-frequency neurons in the Aud-XM group was significantly lower than that in the normal group, but the proportion of low-frequency auditory and low-frequency multisensory neurons in the XM group considered together was not significantly different from that in the normal group. ( \*\*  $p < 0.01$ ). Error bars show  $\pm$  S.E.M..

## **CHAPTER 4 CROSS-MODAL PLASTICITY RESULTS IN INCREASED INHIBITION IN PRIMARY AUDITORY CORTICAL AREAS**

**by**

**Yu-Ting Mao and Sarah L Pallas**

## **1. Abstract**

Sensory cortices can be reorganized after deafferentation resulting from peripheral organ damage, sensory deprivation, or brain damage. In deaf or blind patients, cross-modal inputs from other sensory modalities invade and activate deafferented cortical areas. This cross-modal plasticity can be maladaptive, impairing recovery of the original function during rehabilitation, but the mechanism by which the original function is impaired remains unknown. Previous studies on recovery within one sensory modality suggest that inhibition is decreased in sensory-deprived or deafferented animals. We hypothesized that loss of inhibition may also be responsible for impaired recovery after cross-modal plasticity. Alternatively, inhibition may be increased to facilitate separate processing of the two modalities of information within one cortical area. We tested these hypotheses using ferrets in which retinal afferents had been induced at birth to innervate auditory thalamus, resulting in an auditory cortex in which visual and auditory inputs converge throughout postnatal development. The contribution of inhibition to sensory responses was measured using iontophoretic application of the GABA<sub>A</sub> receptor antagonist gabazine during *in vivo* electrophysiological recordings with visual and auditory stimulation. We found that levels of inhibition in auditory cortex (AC) of cross-modal animals were increased above normal. Blocking inhibition resulted in greater increases in responsiveness to auditory stimuli in the cross-modal group than in the normal group. In addition, tuning curves of auditory neurons in cross-modal AC broadened more than those in normal AC after removal of inhibition. These results suggest that decreased inhibition is not responsible for the compromised auditory function after cross-modal invasion of visual inputs to AC. We also found that blocking inhibition unmasked visual responses in some auditory neurons and auditory responses in some visual neurons of cross-modal AC, suggesting a role for inhibition in mutual suppression between

visual and auditory modalities. These results imply that increased inhibition may play a role in reorganizing sensory cortex after invasion by cross-modal inputs, causing it to represent visual and auditory stimuli in a way that impairs auditory function. Overall, our research provides further evidence that inhibitory plasticity is an important factor in designing clinical strategies aimed at recovery after brain injury or sensory deprivation.

## **2. Introduction**

Loss of sensory drive by sensory deprivation or sensory deafferentation can change responsiveness, sensory topography, and/or tuning characteristics in the affected sensory cortices. In animals deprived from birth, cortices and subcortical areas may fail to mature or maintain mature response properties, exhibiting unrefined receptive field and sensory tuning (Benevento et al. 1992; Blakemore and Price 1987; Carrasco and Pallas 2006; Carrasco et al. 2005; Imbert and Buisseret 1975). Loss of lateral inhibition is responsible for some aspects of deprivation-induced reorganization (Carrasco et al. 2011; Chen et al. 2001; Morales et al. 2002). In deafferented animals, loss of peripheral sensory inputs can lead to an increase in responses to neighboring inputs as a result of decreased inhibition (Calford and Tweedale 1988; Canu et al. 2006; Ralston et al. 1996). Although loss of inhibition is proposed as an underlying mechanism through which sensory deprivation and deafferentation have their effects, most studies have focused on a single sensory modality, overlooking the fact that loss of unisensory drive can result in changes in multiple modalities and in cross-modal plasticity. In deaf and blind patients who have lost sensory drive from early in life, it is common to observe enhanced abilities in the remaining senses. This enhancement results at least in part from recruitment of deafferented cortical areas by cross-modal inputs. This cross-modal plasticity provides novel inputs that can

induce both adaptive and maladaptive changes in the affected sensory areas. Our previous research has shown that primary auditory areas that are rewired with ectopic visual inputs (XMAC) retain tuning to sound frequency but the tonotopic map is disrupted and auditory tuning curves are broader than normal (Mao et al. 2011). Based on previous research on changes in inhibitory circuitry in sensory-deprived and -deafferented animals (Pallas 2010), we propose that inhibitory plasticity contributes to the degradation of auditory tuning and tonotopy in XMAC. Lateral inhibition may be decreased in order to compensate for the loss of sensory drive. Alternatively, inhibition may be increased, given that auditory cortex in the cross-modal animals manages both auditory and visual functions in the limited cortical area. To better process responses to different modalities, mutual inhibition may be required to suppress responses to the other modality. Here we tested these two hypotheses using electrophysiological and pharmacological methods. We found that the change in auditory responses after acute blockade of GABA<sub>A</sub> receptors was larger in the cross-modal group than in the normal group. Our results demonstrate that inhibition is increased in auditory cortex after deafferentation and subsequent invasion by ectopic visual inputs. We also found that blocking inhibition could unmask visual and auditory responses in auditory cortex, suggesting that subthreshold auditory and visual responses are suppressed by strong inhibition. Multisensory integration, however, could not be revealed by removal of inhibition. Our results provide important insight into maladaptive changes that can be associated with cross-modal plasticity and can guide further study on designing rehabilitative strategies in the context of compensatory plasticity during recovery from brain damage.



### **3. Materials and methods**

#### **a) Animals**

In total, 12 adult pigmented ferrets (*Mustela putorius furo*) were either purchased from Marshall Farms (North Rose, NY) or bred in house. Non-lactating adults were fed Marshall Farms ferret diet and kept on a 12/12 light/dark cycle. Seven ferrets were assigned to the normal group and the other 5 underwent neonatal surgery. All animal protocols were approved by the Institutional Animal Care and Use Committee (IACUC) at Georgia State University and met or exceeded standards of care established by the USDA and the Society for Neuroscience.

#### **b) Neonatal surgery**

Surgical procedures were similar to those described previously (Mao et al. 2011; Pallas et al. 1999). Under sterile conditions, ferret kits were deeply anesthetized by isoflurane (1-4% prn) within 24 hr of birth. After the brain was exposed, the left superficial layer of the superior colliculus (sSC) and the central nucleus of the inferior colliculi (ICc) on both sides were cauterized. The brachium of the left inferior colliculus was sectioned. The incision was closed by surgical adhesive (VetBond, 3M, St. Paul, MN). The kits recovered from anesthesia on a heating pad. Subcutaneous fluids and a respiratory stimulant (doxapram, 2 mg/kg, SQ) were given to help them recover. Analgesics (buprenorphine 0.01 mg/kg bid) were given if warranted to prevent postoperative pain.

#### **c) Preparation for adult electrophysiology**

Adult animals were prepared for terminal electrophysiology recording as described previously (Mao et al, 2011). The ear canal of each ferret was examined before surgery with an otoscope.

Animals were given atropine (0.4 mg/kg SQ) and doxapram (2 mg/kg, SQ) before anesthesia to counteract bradycardia and to reduce mucosal secretions. Anesthesia was induced by intramuscular injection of ketamine (40 mg/kg, IM) and diazepam (2 mg/kg, IM). Dexamethasone (1mg/kg, IM) was given every 24 hr to prevent cerebral edema. After the cephalic or femoral vein was cannulated, anesthesia was maintained by a continuous infusion (2-5 ml/hr, IV) of a mixture of dexmedetomidine (0.022 mg/kg/hr) and ketamine (5 mg/kg/hr) in lactated Ringer's with 5% dextrose (Bizley and King 2008; Bizley et al. 2005). Atropine (0.4 mg/kg, SQ) was given as necessary to counteract the bradycardia caused by dexmedetomidine. A tracheotomy was performed for artificial ventilation (SAR 830/P ventilator, CWE Inc, Ardmore, PA). Body temperature was maintained at 38° C with a heating pad. Vital signs including EKG, respiration rate, muscle tone, withdrawal reflexes, and end-tidal CO<sub>2</sub> were monitored during the entire process. Eyes were kept moist with commercial artificial tears solution. Animals were placed in a stereotaxic device to stabilize the head. After the skin on the top of head was incised by a scalpel, the temporal muscles were retracted bilaterally from the skull. Two burr holes (at coordinates A5.5 ±L1.5) were drilled for optic chiasm recording/stimulation electrodes. Saline was added around the drilling area frequently to prevent overheating. Two tungsten rods with Teflon insulation (0.008 inch bare, 0.011 inch coated, A-M systems, Inc., Carlsborg, WA) were lowered to a depth (8~10 mm) that yielded strong visual responses to a strobe light. The tungsten rods were connected to a preamplifier and then switched to connect to a stimulus isolation unit (BAK Electronics, Mount Airy, MD). A 0.8~1.0 cm diameter craniotomy was drilled over the left auditory cortex. The dura was removed and auditory cortex was covered with sterile saline. A metal bar was cemented on the contralateral (right) side of the skull to stabilize the head. The right ear bar was then released to allow access for auditory stimulation.

#### **d) Acoustic stimuli and visual stimuli**

Acoustic stimuli were generated by TDT system III hard- and software (Tucker-Davis Technologies, Alachua, FL). A calibrated earphone (ER-2 insert earphone, Etymotic Research, IL) was placed in the pinna at the entrance to the right ear canal. All auditory stimuli were given contralaterally. White noise bursts (5 ms ramp, 40-100 ms duration, 80 dB SPL) were used to search for sound-responsive units. After a responsive neuron was found, pure tones were given in a pseudorandom order ranging in 2 kHz steps from 2 kHz to 18 kHz or ranging in half octave steps from 500 Hz to 16 kHz with intensity of 30 to 80 dB SPL (50 ms duration, 5 ms ramp). Bipolar electrical stimulation of the optic chiasm was applied (single pulses at 0.5-1 mA, 60  $\mu$ s duration) to test whether the units were multisensory neurons. Light stimuli were presented on a computer screen ~40 cm from the eyes. Moving bars, gratings and flashes were used to elicit responses. After a visual neuron was found, the computer screen was moved to a location and height that aligned the center of the visual receptive field approximately at the center of the screen.

#### **e) Multibarrel electrodes for recording and iontophoresis.**

Three-barrel glass micropipettes (A-M systems Inc., Sequim, WA) were used to record evoked activity and for application of drugs. The multibarrel electrodes were pulled by a vertical puller (Kopf vertical pipette puller 720, David Kopf Instruments, Tujunga, CA). The tip diameter was observed under a microscope before recording. Any electrodes with a tip bigger than 15  $\mu$ m were discarded. The recording barrel was filled with 3 M NaCl. A silver wire was inserted into the recording barrel to connect it with the preamplifier. Another two barrels were used as iontophoresis barrels. Another barrel was filled with 3 mM gabazine (pH 3.0). The

iontophoresis barrels were connected to the headstage of a three-channel iontophoresis device (Cygnus Technology, Inc, Delaware Water Gap, PA) via silver wire. The headstage and the preamplifier were grounded together to the skin, which served as the ground for the entire recording apparatus. A retaining current (-10 nA) was applied in each barrel to prevent drug leakage. Ejecting currents were +5 ~ +10 nA. Application of drugs was maintained throughout the testing period. Typically it took 5 min for running a series of different sound frequencies for testing.

The electrode was advanced under the pial surface in 5  $\mu\text{m}$  steps up to 2000  $\mu\text{m}$  by a hydraulic microdrive (Kopf Instruments, Tujunga, CA). For each penetration, the first stable unit that was encountered was isolated and characterized. Only one recording was taken in each penetration so as to maximize sampling area. Penetrations were limited to primary auditory cortex (AI) and anterior auditory field (AAF) (Bizley et al. 2005; Mao et al. 2011). In order to avoid potential diffusion of iontophoretic drugs, penetration sites were at least ~400  $\mu\text{m}$  apart. Neural responses were amplified ( $\times 10000$ , BAK Electronics, Inc, Mount Airy, MD), bandpass filtered (500 Hz to 5 kHz), and monitored on a digital oscilloscope (Hameg Instruments, Mainhausen, Germany). Responses to 5-10 stimulus presentations were collected from each recording site and digitized at 25 kHz (Brainware software, Tucker-Davis Technologies Inc., Alachua, FL). The evoked responses were averaged and normalized to a sample of spontaneous activity recorded for 50 ms before each trial. The recording continued for 1-2 days, after which the animal was deeply anesthetized (65 mg/kg, IP) for perfusion and the brain was extracted for histological examination.

#### **f) Electrophysiological data analysis**

After recording, spike sorting was performed by Brainware software (Tucker-Davis Technologies Inc., Alachua, FL). Single units were isolated according to their waveform, amplitude, and width. For each isolated single unit, the response threshold was defined as the minimum sound intensity that could elicit responses at least 20% above the mean spontaneous firing rate (Bizley et al. 2005; Sutter and Schreiner 1991). The boundary of each frequency tuning curve was defined as the stimuli (intensity and frequency) that yielded excitatory responses at 20% above background (Moore et al. 1983; Sutter and Schreiner 1991). The best frequency (BF) of each unit was defined as the frequency at which responses are elicited at the lowest sound level. Bandwidth was determined as the width of the tuning curve at 10 dB above the minimum threshold. Multisensory units were defined either as neurons that responded both to visual and auditory stimuli or as neurons that only responded to one modality but could be significantly modulated by stimulation with the other modality (Stein and Meredith 1993). Statistical significance between groups was determined by comparing the number of spikes per trial in response to both stimulus modalities, using Student's t-test (significance at  $p < 0.05$ ).

#### **g) Statistical analysis**

Statistical comparisons were performed using Sigmastat software (Systat Software Inc, Chicago, IL) and PASW statistic 18 (SPSS Inc, Chicago, IL) and plotted with Sigmaplot software (Systat Software Inc, Chicago, IL). For within group comparison, paired-t tests were used for normally distributed data, whereas Wilcoxon rank-sum tests were used for non-normally distributed data. For between group comparisons, Student-t tests were used for normally distributed data and

Mann-Whitney U tests were used for non-normally distributed data. Means are given with standard errors of the mean ( $\pm$  SEM) throughout.

#### **4. Results**

Previous studies in our lab demonstrated that auditory function is impaired in XMAC, with broader tuning and less organized tonotopy than in normal animals. Here we investigated the mechanism underlying this auditory impairment. We hypothesized that weaker inhibition is the cause of the wider tuning in XMAC than in normal AC. Forty-one auditory neurons from 7 normal animals and 55 auditory neurons, 9 visual neurons, and 24 multisensory neurons from 5 Xmodal animals were recorded for the iontophoresis experiments.

##### **a) Gabazine increases responsiveness to auditory stimulation**

In order to test the hypothesis that inhibition contributes to the auditory impairment in XMAC, we examined the effect of gabazine, a GABA<sub>A</sub> receptor antagonist, on evoked responses to auditory stimulation. **Figure 4.1** shows the post stimulus time histogram (PSTH) of the responses of a single unit in AC from each group. Stimuli started 50 ms after data acquisition (Fig **4.1A, D**) so that a baseline firing level could be determined. As expected for a GABA<sub>A</sub> receptor antagonist, gabazine application led to an increase in spike numbers (Fig **4.1B, E**), which returned to normal after 30 minutes (Fig **4.1C, F**). In contrast, injection of a GABA<sub>A</sub> receptor agonist or an NMDA receptor antagonist decreased responsiveness to auditory stimuli (not shown).

##### **b) GABA<sub>A</sub> receptor blockade had a greater effect on auditory tuning in XMAC than in normal AC**

We hypothesized that loss of inhibition is responsible for the wider frequency tuning in XMAC than in normal AC that was reported in our previous study (Mao et al., 2011). To test the hypothesis, we compared the frequency tuning selectivity (bandwidth) and threshold of auditory responses in normal AC and XMAC. One example from each group is shown in **Fig 4.2**.

Although no change in best frequency was observed, we found that the average thresholds of auditory neurons in normal animals decreased significantly after blocking inhibition by gabazine application, from  $51 \pm 1.5$  dB to  $49 \pm 1.5$  dB ( $n=41$ ,  $p=0.03$ , Wilcoxon rank-sum test, **Fig 4.3A** ).

The thresholds of auditory neurons in XMAC were also significantly decreased by gabazine application, from  $58 \pm 1.5$  to  $53 \pm 1.7$  dB ( $n=55$ ,  $p<0.001$ , Wilcoxon rank-sum test, **Fig 4.3A**).

There was no significant difference in the average decrease in threshold between these two groups (normal AC  $-2.7 \pm 0.9$  dB, XMAC  $-5.3 \pm 1.0$ ;  $p=0.1$ , Mann-Whitney U test, **Fig 4. 3B**).

Blockade of inhibition by gabazine also significantly broadened the bandwidth of the tuning curves in both the normal group (from  $0.74 \pm 0.1$  to  $0.96 \pm 0.1$  octaves at 10 dB above threshold;  $n=41$ ,  $p<0.001$ , Wilcoxon rank-sum test, **Fig 4.3C**) and the XM group (from  $1.2 \pm 0.1$  to  $1.7 \pm 0.1$  octaves;  $n=55$ ,  $p<0.001$ , Wilcoxon rank-sum test, **Fig 4.3C**). This increase in bandwidth was significantly greater in the XM group than in the normal group (normal:  $0.2 \pm 0.06$  vs. XM:  $0.5 \pm 0.1$ ,  $p<0.05$ , Mann-Whitney U test, **Fig 4. 3D**). Thus, contrary to our hypothesis, this result suggests that auditory stimulation evoked stronger inhibition in XMAC than in normal AC.

### **c) GABA<sub>A</sub> receptor blockade had a greater effect on responsiveness to sound in XMAC than in normal AC**

We hypothesized that inhibition is changed in XMAC after invasion by visual inputs. In order to test this hypothesis, we compared the spontaneous activity levels in normal AC and XMAC.

Although blockade of GABA<sub>A</sub> receptors by gabazine increased spontaneous activity significantly both in normal AC and in XMAC (normal before gabazine:  $2.55 \pm 0.3$  spikes per trial vs. normal after gabazine:  $3.77 \pm 0.5$ ,  $p < 0.001$ ; XM before:  $1.73 \pm 0.2$  vs. XM after:  $2.7 \pm 0.3$ ,  $p < 0.001$ ; Wilcoxon rank-sum test, **Fig 4.4A**), the increase in spontaneous activity was not significantly different between these two groups (normal:  $63.83 \pm 11.5\%$  vs. Xmodal:  $90.62 \pm 16.0\%$ ,  $p > 0.05$ , Mann-Whitney U test, **Fig 4. 4B**). We also measured the strength of auditory responses before and after blocking inhibition. The evoked responses were normalized to the mean level of spontaneous activity during the 50 msec before each trial. We found that blockade of GABA<sub>A</sub> receptors by gabazine increased the mean number of spikes per trial significantly in both normal AC (from  $4.88 \pm 0.5$  to  $6.95 \pm 0.7$  spikes, normal before vs. normal after, Wilcoxon rank-sum test,  $p < 0.001$ ,  $n = 41$ , **Fig 4. 4C**) and XMAC (from  $5.53 \pm 0.7$  to  $8.28 \pm 0.6$  spikes, Xmodal before vs. after,  $p < 0.001$ ; Wilcoxon rank-sum test,  $n = 55$ , **Fig 4. 4C**). This represents a proportionally greater increase in spike number per stimulus in the XM group ( $88.28 \pm 14.1\%$ ,  $n=55$ , than that seen in the normal group ( $48.39 \pm 7.7\%$  ( $n = 41$ ),  $p < 0.05$ , Mann-Whitney U test, **Fig 4.4D**). Consistent with the significantly greater change in threshold and bandwidth in the XM compared to the normal group, these results further suggest that auditory neurons in XMAC receive stronger inhibition than neurons in normal AC.

#### **d) GABA<sub>A</sub> receptor blockade unmasks visual responses**

Our finding that inhibition is stronger in XMAC than in normal AC suggests that auditory and visual responses may inhibit each other in order to perform different functions within the same cortical area. To test this hypothesis, we assayed bisensory responsiveness before and after blockade of inhibition by gabazine. We found no auditory neurons in normal AC began to



respond to optic chiasm stimulation but 25.5% of the auditory neurons in XMAC (14 out of 55 neurons from 5 animals) began to respond to electrical stimulation of the optic chiasm after blocking inhibition (**Fig 4.5A, B**) The responses to optic chiasm stimulation were strong, although none of the neurons responded to light stimulation, perhaps due to insufficient drive from the retina to MGN even with unmasking. In normal multisensory cortex or subcortical areas, multisensory neurons show facilitation or depression to multisensory cues, however, no integration of bisensory stimuli was observed in these neurons (**Fig 4.5D**).

**e) GABA<sub>A</sub> receptor blockade does not unmask light responses or cross-modal facilitation in multisensory neurons.**

We reported previously that XMAC contains more multisensory neurons than normal AC (Mao et al. 2011), we observed that the majority of multisensory neurons in XMAC did not exhibit integration with bisensory stimuli. In this study, only 8.3% of the recorded multisensory neurons from 5 animals (2 out of 24) showed integration. We reasoned that the lack of integration in XMAC could be caused by GABAergic suppression of the opposing modality. If so, then blockade of inhibition should release facilitation or suppression. We were able to conduct a complete iontophoresis battery from 8 multisensory neurons from these 5 Xmodal animals. Contrary to our hypothesis, none of them showed integration either before or after blockade of inhibition. Before blockade of GABA<sub>A</sub> receptors, these neurons responded to both sound and optic chiasm stimulation (AOX; **Fig 4.6A**) but none of them showed either facilitation or depression when both stimuli were given ( $p > 0.05$ , t-test, **Fig 4.6C**). After blockade of inhibition, we still did not observe any significant facilitation or depression of responses by bisensory stimulation (**Fig 4.6B, D**) ( $p > 0.05$ , t-test). Furthermore, we did not find any multisensory neurons

originally responding to both auditory and optic chiasm stimulation that started to respond to light after removal of inhibition (Fig **4.6B**). These results suggest that inhibition may not contribute to multisensory integration in XMAC.

In contrast to the significant increase in auditory response levels that were seen after gabazine application, we found that optic chiasm response levels did not increase significantly after GABA<sub>A</sub> receptors blockade ( $p > 0.05$ , paired-t test, **Fig 4.7**). The mean spike numbers during optic chiasm stimulation before gabazine application ( $2.3 \pm 0.5$  per trial) were not significantly different from those seen after gabazine application ( $3.85 \pm 0.6$ ,  $n=8$ ,  $p > 0.05$ , paired t-test). These results suggest that inhibition of ectopic visual inputs to XMAC may have been decreased during recovery from neonatal brain lesion in order to create multisensory neurons that can respond to the other modality. If so, then application of gabazine would be expected to have little effect on visual responses. Although we cannot completely rule out the possibility that electrical activation of optic chiasm is such a strong stimulus that the OX responses are saturated, the mean spike numbers/trial for OX responses were generally less than the mean spike numbers /trial for auditory responses. Furthermore, we also tried to reduce optic chiasm stimulation current during multisensory recording but no integration was found (data are not shown).

#### **f) Neurons in which gabazine unmasked visual responses were spatially intermixed with auditory and multisensory neurons in XMAC**

We reported in previous research that auditory, visual, and multisensory neurons in XMAC are not segregated from each other (Mao et al. 2011). The finding of inhibition-masked visual responses in XMAC raised an interesting question concerning their distribution. To determine whether neurons that exhibited unmasking of bisensory capability were a spatially separate

population, we mapped the neuronal responses in XMAC. We found that auditory neurons that responded to optic chiasm stimuli after but not before blockade of inhibition were located randomly in XMAC (half white circles, Fig. 4.8), and not selectively in one area. They were found surrounded by or adjacent to either auditory or multisensory neurons (white and black circles, respectively, Fig 4.8). These results show that neurons exhibiting unmasking of bisensory responses were neither segregated nor clustered in their distribution.

## **5. Discussion**

We found that neurons in auditory cortex rewired at birth with ectopic visual inputs (XMAC) received stronger inhibition than normal auditory cortex. This result implies that the broadened auditory tuning found in XMAC does not result from decreased inhibition. The increased inhibition in XMAC may be involved in cortical reorganization. Blockade of inhibition unmasked responses to the other modality in some neurons. These findings argue that inhibition plays a role in suppressing responses to the opposing modality during unisensory stimulation. These results provide important information for rehabilitation from sensory dysfunction, particularly when cross-modal plasticity occurs.

### **a) Contribution of GABAergic inhibition to auditory impairment in XMAC**

After loss of inputs due to IC damage, we expected that inhibition in the affected brain regions would be decreased, as seen in other studies of deafferented sensory cortex. In somatosensory cortex, deafferentation induces an expansion of adjacent inputs into the affected area of the cortex (Kaas et al. 1983; Merzenich et al. 1983b; Wall et al. 1983). This reorganization results from removal of inhibition (Calford and Tweedale 1988; Canu et al. 2006; Ralston et al. 1996).

In the visual system, visual deprivation leads to broader visual tuning and larger receptive fields

in both cortical and subcortical areas (Carrasco et al. 2005; Imbert and Buisseret 1975). This change is caused at least in part by loss of inhibition (Benevento et al. 1992; Carrasco et al. 2011). In the auditory system, deaf animals exhibit a decrease in chloride conductance during IPSCs (Vale and Sanes 2002) and express reduced levels of GABA in inferior colliculus (Bledsoe et al. 1995). These studies suggest that inhibition is homeostatically decreased in deprived and deafferented animals to compensate for the loss of sensory drive (Turrigiano 2012).

Other investigators report that inhibition need not change at the neurotransmitter level or may change transiently. For example, in the olfactory system, deafferentation did not reduce GAD, the synthetic enzyme for GABA expression in the olfactory bulb (Parrish-Aungst et al. 2011). Similar results were found in visual cortex of dark-reared animals (Bear et al. 1985). In addition to GAD, the expression of GABA has also been reported to remain at normal levels in visual cortex of deafferented cats (Rosier et al. 1995). In other cases, the expression of GABA and the number of GABAergic neurons was reduced one week after sensory deafferentation but recovered to normal levels within a month, suggesting that the change in inhibition is transient (Wang et al. 2007). Our results showed that inhibition was increased in the auditory cortex of cross-modal animals. These findings suggest either that an initial loss of inhibition is transient or that there is no decrease in inhibition during recovery from sensory deafferentation in the cross-modal AC. Our recordings were all done in adults, thus we cannot currently distinguish between these possibilities. The impaired auditory function in the XMAC, therefore, does not result from a lasting loss of inhibition as we initially predicted. Alternatively or additionally, sprouting of residual auditory inputs to the cortex could contribute to the broader tuning seen in auditory neurons within XMAC, whereas a reduction in excitatory auditory inputs in XMAC is a possible explanation for the higher auditory thresholds.

In contrast to studies reporting deprivation-induced loss of inhibition as discussed above, other studies reported a compensatory increase in inhibition during recovery from sensory loss. In visual cortex, inputs from the two eyes compete for cortical territory, creating ocular dominance columns (Kratz and Spear 1976; Shatz and Stryker 1978; Stryker 1978). Monocular visual deprivation leads to a loss of visual responsiveness to the deprived eye (Rauschecker and Singer 1981). This decreased responsiveness may be caused in part by an increase in local inhibition (Maffei et al. 2006) as well as by LTD (Kirkwood et al. 1996). GABA receptor blockade can rescue the cortical responses to the deprived eye (Burchfiel and Duffy 1981; Ramoa et al. 1988), supporting the hypothesis that an increase in inhibition may be responsible for the competition for territory. In a previous study, we found that auditory and visual inputs compete for space in cross-modal AC (Mao et al. 2011). Here we provide information about the mechanism by which inputs from different modalities compete with each other. We not only found that inhibition was increased in cross-modal AC, but also that auditory responses could be unmasked after blockade of GABA<sub>A</sub> receptors, suggesting that inhibition is involved in the processing of both modalities within the same brain area.

#### **b) Multisensory processing in primary sensory areas.**

Multisensory neurons were first reported in the superior colliculus, and were defined as neurons that respond to multiple modalities and can be either facilitated or suppressed by bisensory or trisensory stimuli (Meredith and Stein 1983; 1986). Later research reported multisensory cortical neurons that only responded to one modality under normal conditions but could be modulated when more than one modality of stimulation was given (Allman et al. 2009b; Allman and Meredith 2007; Meredith and Allman 2009). Several recent studies have now

demonstrated multisensory responses in primary sensory areas (e.g. Bizley and King 2009; Bizley et al. 2007; Falchier et al. 2002), arguing that primary sensory cortex is not “primary” in the sense of receiving only unimodal thalamic input (Ghazanfar and Schroeder 2006).

Multisensory integration includes either facilitation or suppression of responses to multisensory stimuli, but some subthreshold multisensory responses are masked by inhibition and thus lack integration (Allman et al. 2008). Here we found subthreshold multisensory responses that could be unmasked by blockade of inhibition, but no integration was revealed, either as subthreshold or superthreshold multisensory responses. Multisensory integration is strongest when the single-modality stimuli are weakest for the recorded neuron (Stein and Meredith, 1993), but multisensory response magnitudes were generally consistent with linear summation of modality-specific influences (Stanford et al, 2005). Therefore, it is unlikely that the lack of integration between modalities in multisensory neurons from XMAC is caused by saturation of responses to single-modality. Our data also showed that inhibition could not contribute to multisensory integration in primary auditory areas, regardless of the existence of both super- and sub-threshold multisensory responses. These results emphasize the special role of primary auditory areas in sensory perception and behavior of both normal and cross-modal animals. When responses to multiple modalities are forced to co-exist in XMAC, multisensory integration would likely interfere with rather than improve sensory perception, especially for multisensory neurons that are tuned to pure tones. These findings reveal that convergence of inputs to one limited area could create neurons responding to different modalities but multisensory integration may be suppressed in order to optimize overall sensory processing.

### **c) Possible mechanism of impaired auditory tuning.**

Although the tonotopic organization from cochlea to cortex has been considered a basic trait of auditory systems for decades (Kelly et al. 1986; Phillips et al. 1988; Reale and Imig 1980; Winer et al. 2001), recent studies have challenged this classical view (Bandyopadhyay et al. 2010; Rothschild et al. 2010). Using two-photon imaging, tonotopic maps were seen on a large scale but not on a fine scale in mouse primary auditory cortex. It was argued that this fractured tonotopy might be caused by local intracortical inhibition, because of the subthreshold auditory responses exhibited in topographic clusters. We found orderly tonotopic mapping in auditory cortex of normal ferrets as others have reported (Kelly et al. 1986; Phillips et al. 1988), but not in auditory cortex of XM animals (Mao et al. 2011). Analogous to Bandyopadhyay and Rothschild's results, the fractured auditory map in XMAC might be caused by increased inhibition. I hypothesized that when auditory tuning is refined during development by inhibition, the best frequency of auditory neurons may be more sharply defined and auditory tonotopy would be better organized. Although blockade of GABA<sub>A</sub> receptors did not change the BF of auditory neurons nor rescue an ordered tonotopy, we did find an increased level of inhibition in XMAC that suppresses responses to the other modality. Bandyopadhyay and colleagues suggest that the fractured, suprathreshold map may result from parallel processing streams for different input features, as in cerebellar structures (Gonzalez et al. 1993; Shumway et al. 2005). We therefore propose that the disrupted tonotopy in the XMAC might be caused by invasion of visual inputs that were used for different tasks via strong inhibition.

The reason for our finding that loss of inhibition is not responsible for broader than normal tuning in XMAC may rely on the role of lateral inhibition in refinement of auditory

tuning curves. Local inhibition has been shown to shape sound frequency tuning in auditory cortex (Chen and Jen 2000; Jen and Zhang 2000; Sutter et al. 1999; Wang et al. 2000), but *in vivo* intracellular recordings of ipsp and epsps have shown that inhibitory inputs exhibit the same broad tuning as excitatory inputs (Tan et al. 2004; Wehr and Zador 2003; Zhang et al. 2003; but see Dorn et al), arguing that the tuning of the excitatory component is sufficient to build up a tuning curve for an auditory neuron. Although later studies found that inhibitory neurons in auditory cortex have broader tuning than excitatory neurons (Wu et al. 2008), excitatory inputs but not these broadly-tuned inhibitory inputs are refined during development (Sun et al. 2010). These studies further support the idea that refinement of auditory receptive fields relies more on the maturation of excitatory than inhibitory inputs. Here we found that inhibition was increased in XMAC after recovery from neonatal midbrain lesions, despite the fact that auditory tuning was broader in XMAC than in normal AC. Because refinement of auditory receptive fields could depend on narrowing of the axonal projections from excitatory thalamocortical inputs, the widened auditory tuning in XMAC may result from sprouting of auditory thalamocortical afferents after lesion of the inferior colliculi rather than from a decrease in lateral inhibition. Our data support the hypothesis that the sharpness of auditory tuning relies more on excitatory inputs than on lateral inhibition.

Overall, our results provide importance evidence that an increase in inhibition contributes to cross-modal reorganization of cortical areas after recovery from neonatal deafferentation. These findings can help further study on the design of rehabilitative strategies for patients who have brain damage, sensory/motor dysfunction or sensory deprivation.



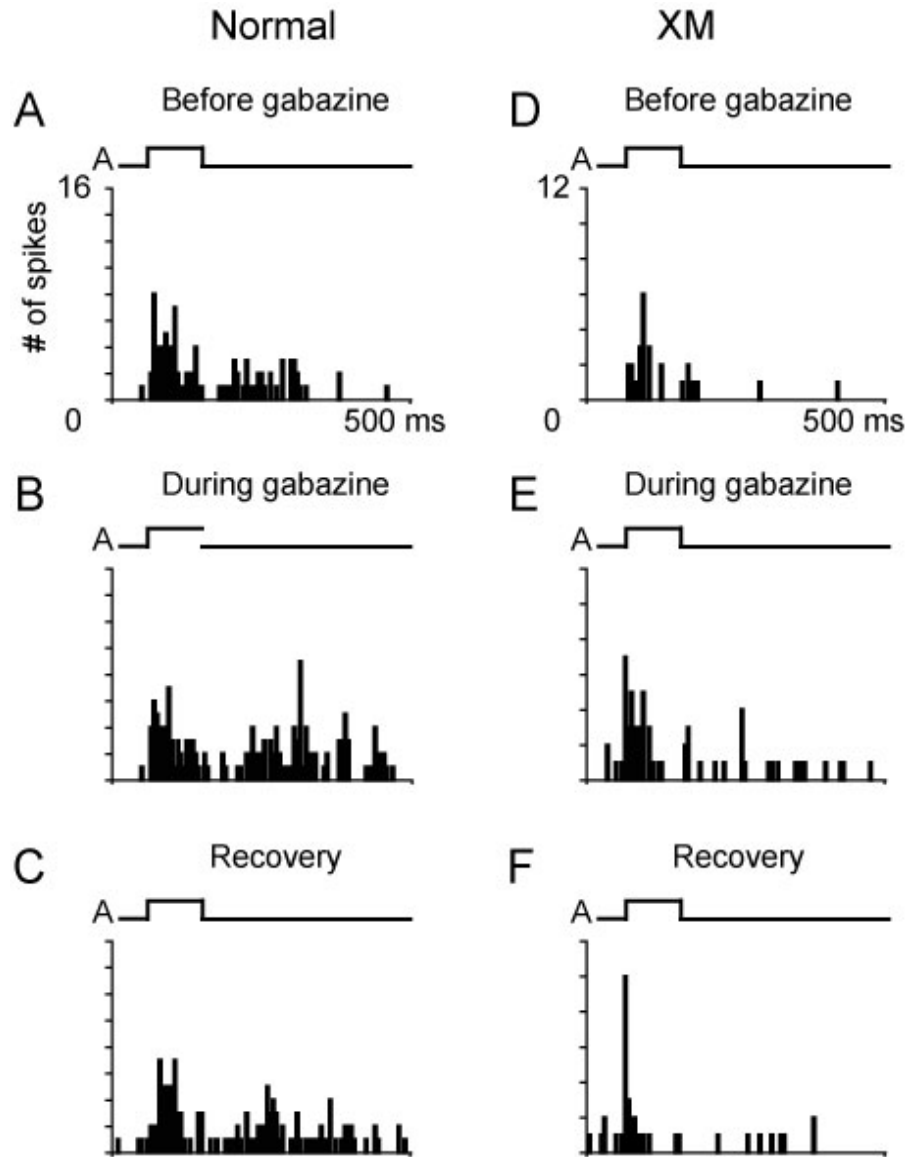


**Figure 4.1.** Effects of the GABA<sub>A</sub> receptor antagonist gabazine on evoked responses to sound. A-C. PSTH of the responses of a single unit to a pure tone at its BF in a normal animal, before, during, and after the gabazine application. D-F, PSTH of the responses of a single unit to a pure tone at its BF in a cross-modal animal. ‘A’ represents auditory stimulation. The duration of each auditory stimulus was 100 ms.

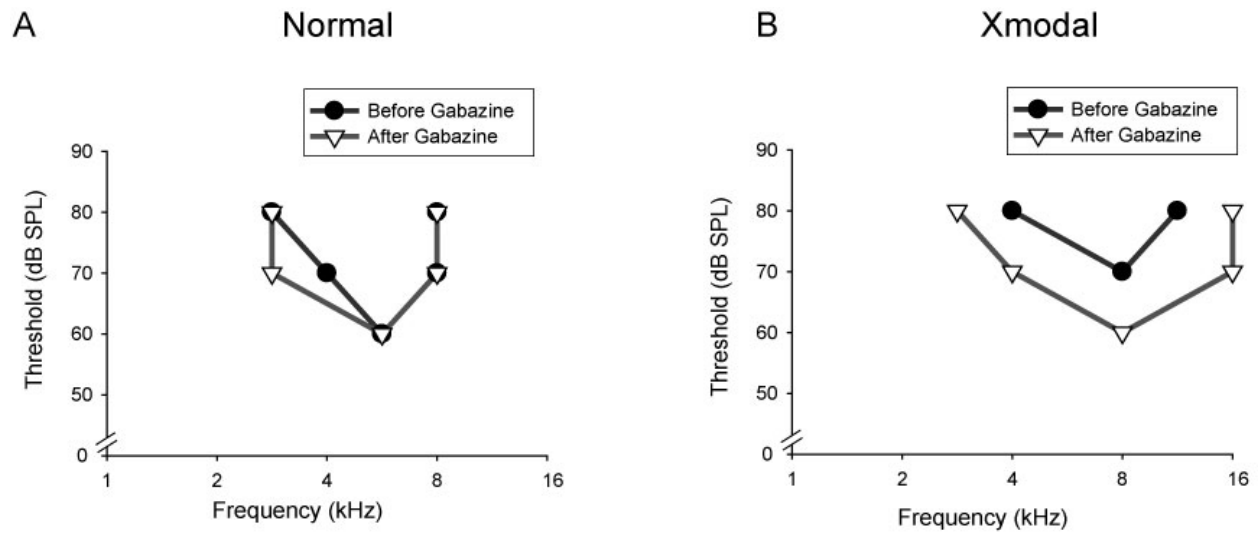


**Figure 4.2.** Two examples of the effect of gabazine on sound frequency tuning. A. Blockade of inhibition by gabazine decreased the sharpness of auditory tuning curves in normal AC. B. Blockade of inhibition by gabazine decreased the sharpness and the threshold of auditory tuning curves in XMAC.

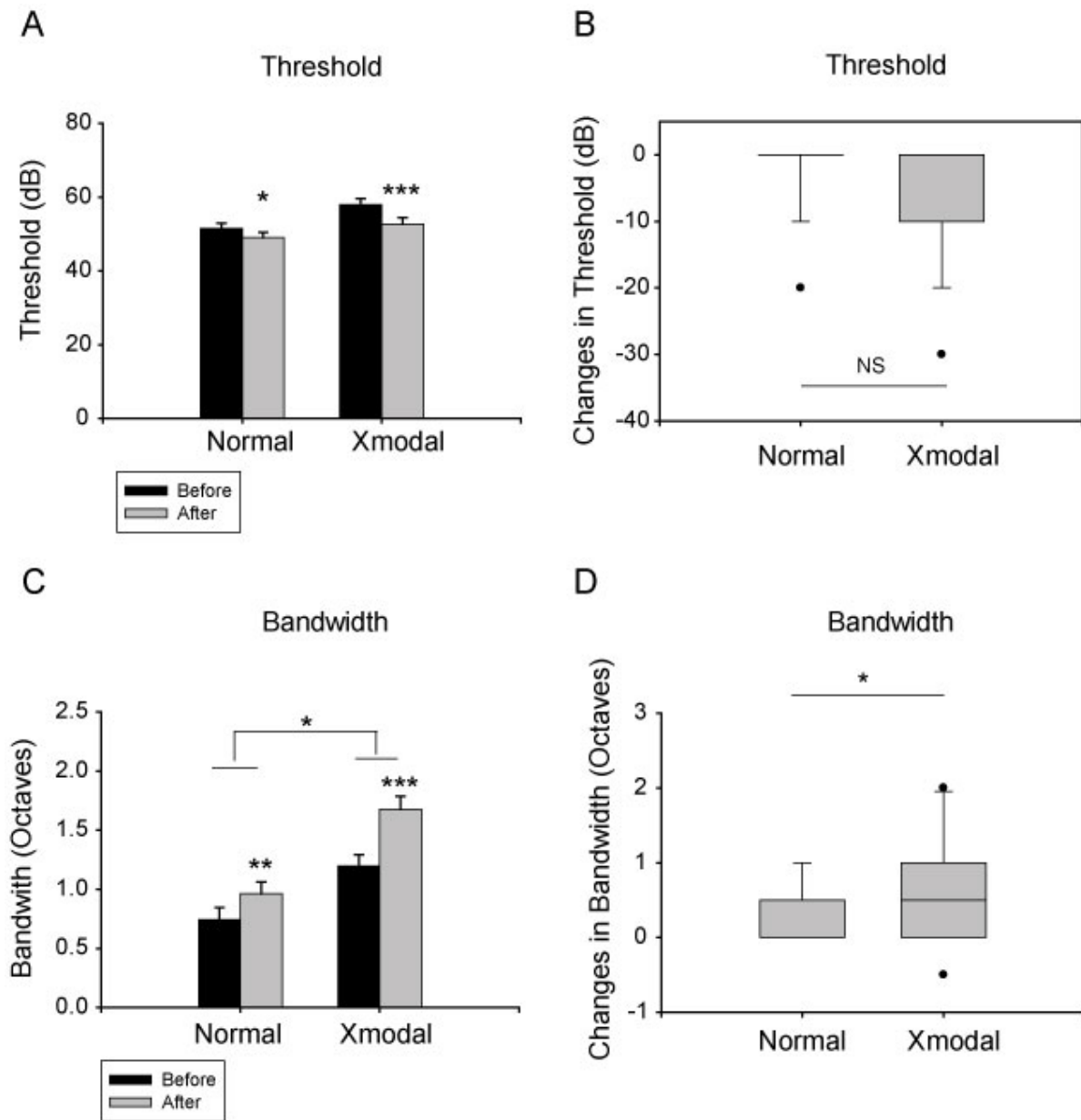


**Figure 4.3.** The effects of gabazine on thresholds and bandwidths of auditory tuning curves in the population of normal and XM neurons. A. Blockade of inhibition by gabazine decreased thresholds in both normal and Xmodal groups. B. The threshold changes in the Xmodal group were not significantly different from those in the normal group. C. Blockade of inhibition by gabazine increased bandwidths in both normal and Xmodal groups. D. The changes in bandwidth

in the Xmodal group were significantly larger than those of the normal group. \*  $p < 0.05$ ;

\*\* $p < 0.01$ ; \*\*\*  $p < 0.001$ ; NS: no significant difference. Data in A and C show Mean  $\pm$  S.E.M.

Data in B and D show Median  $\pm$  S.D.

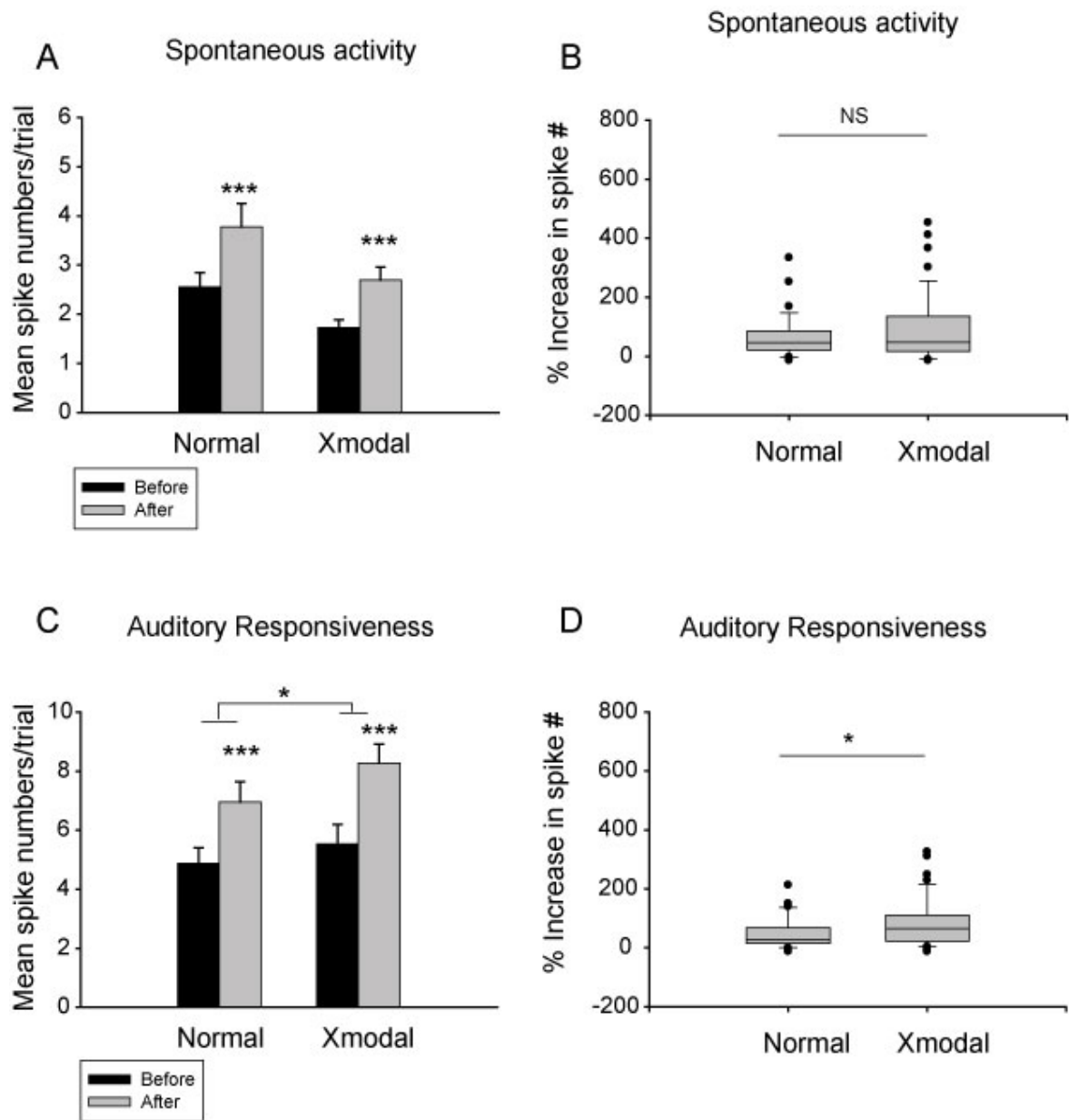


**Figure 4.4.** The effects of gabazine on spontaneous activity and auditory responsiveness. A. Blockade of inhibition by gabazine increased spontaneous activity in both normal and Xmodal groups. B. Spontaneous activity did not change significantly after gabazine administration in the Xmodal group compared to the normal group. C. Blockade of inhibition by gabazine increased mean spike numbers per trail in both normal and Xmodal groups. D. The changes in

responsiveness to sound stimuli after gabazine administration in the Xmodal group were significantly larger than those in the normal group.\*  $p < 0.05$ ; \*\*\*  $p < 0.001$ . NS: no significant difference. Data in A and C show Mean  $\pm$  S.E.M. Data in B and D. show Median  $\pm$  S.D.

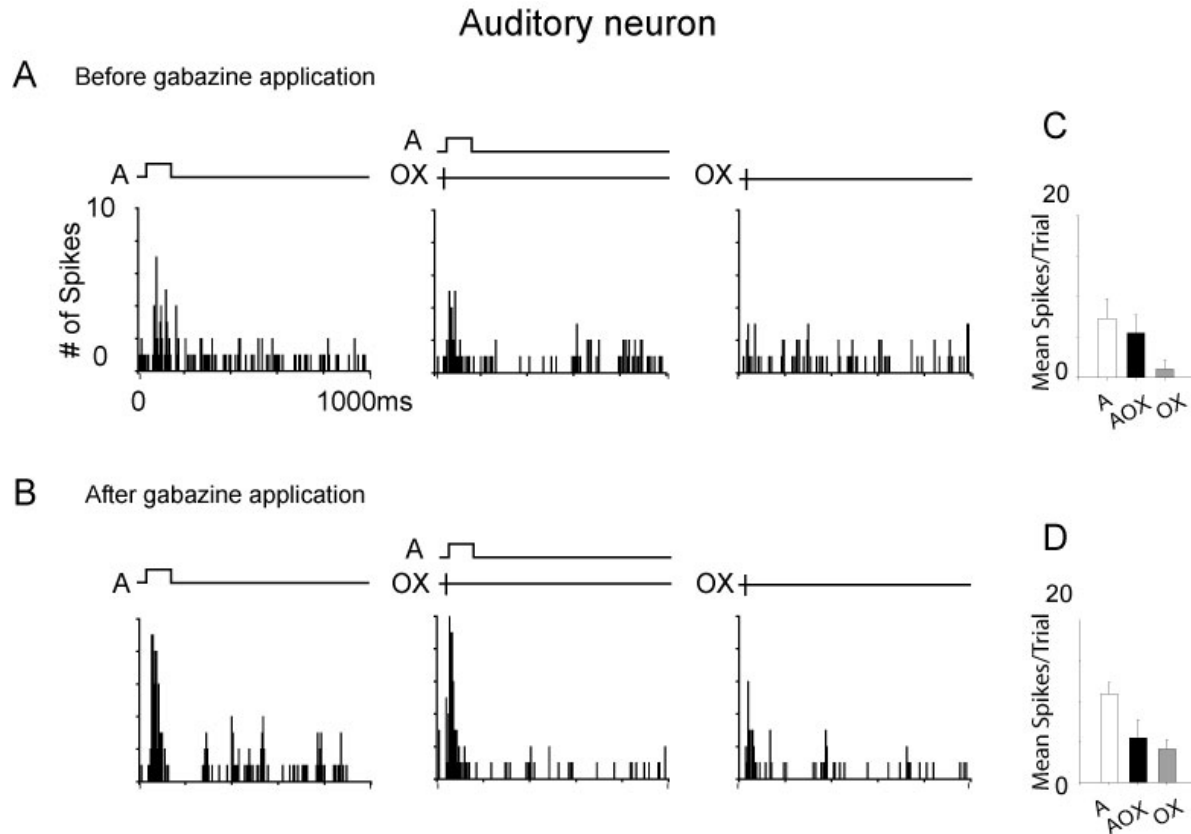


**Figure 4.5.** One example of auditory neuron responses to bisensory stimuli before and after blocking inhibition. A. Before gabazine application, this neuron responded to auditory but not to optic chiasm stimulation. B. After gabazine application, it responded to both auditory and optic chiasm stimulation. C. The mean spike numbers per trial before blockade of inhibition. D. The mean spike numbers per trial after blockade of inhibition. Neither facilitation nor depression was found when auditory and optic chiasm stimuli (AOX) were given simultaneously. Note that the neuron began to respond to OX stimulation only after blockade of inhibition.

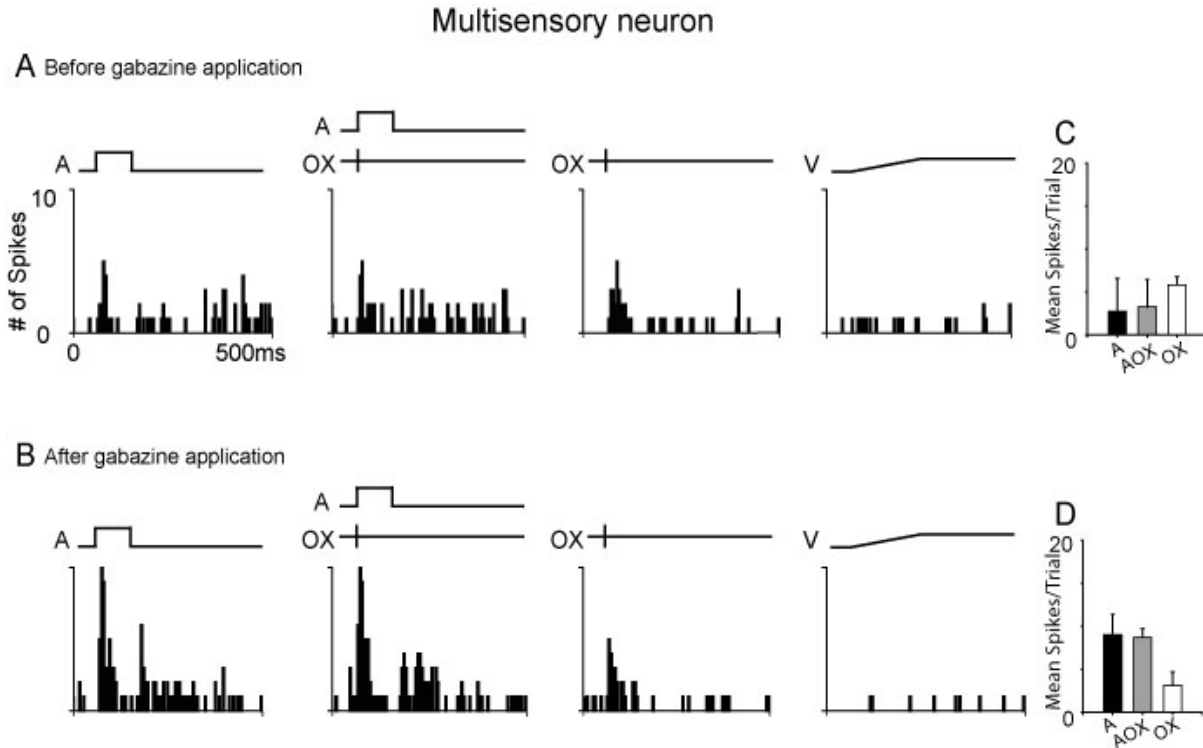


**Figure 4.6.** One example of the response of multisensory neurons to auditory and optic chiasm stimuli before and after blockade of inhibition by gabazine. A. Before gabazine application, this neuron responded to both auditory and optic chiasm stimuli but not to light stimuli. B. The response type was not changed by gabazine application. C. The mean spike numbers per trial before blockade of inhibition. Neither facilitation nor depression was found when auditory and optic chiasm stimuli (AOX) were given together. D. The mean spike numbers per trial after blockade of inhibition. Neither facilitation nor depression was found when bimodal stimuli were given. Note that responses to auditory stimuli but not to OX stimuli were increased after gabazine application. Other conventions as in Figure 4.5.



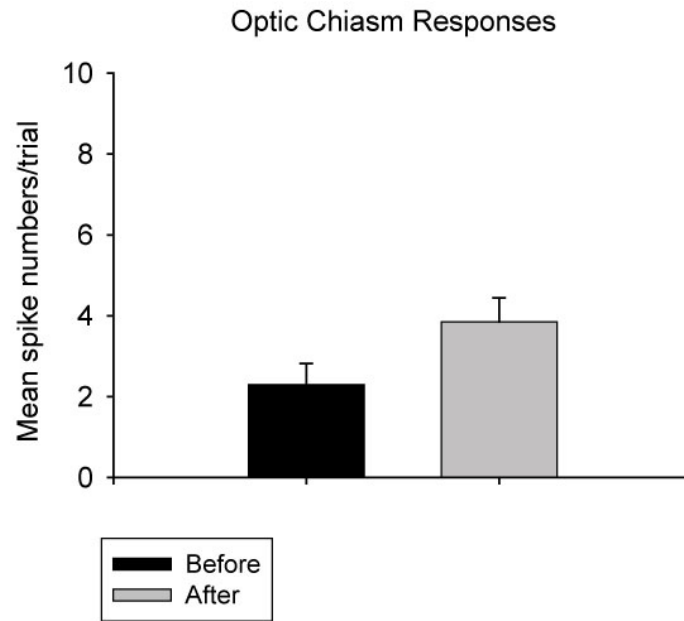


**Figure 4.7.** The comparison of mean spike numbers from responses to optic chiasm stimulation before and after gabazine application. No significant difference was found (Error bars show  $\pm$  S.E.M,  $p > 0.05$ , paired  $t$ -test).

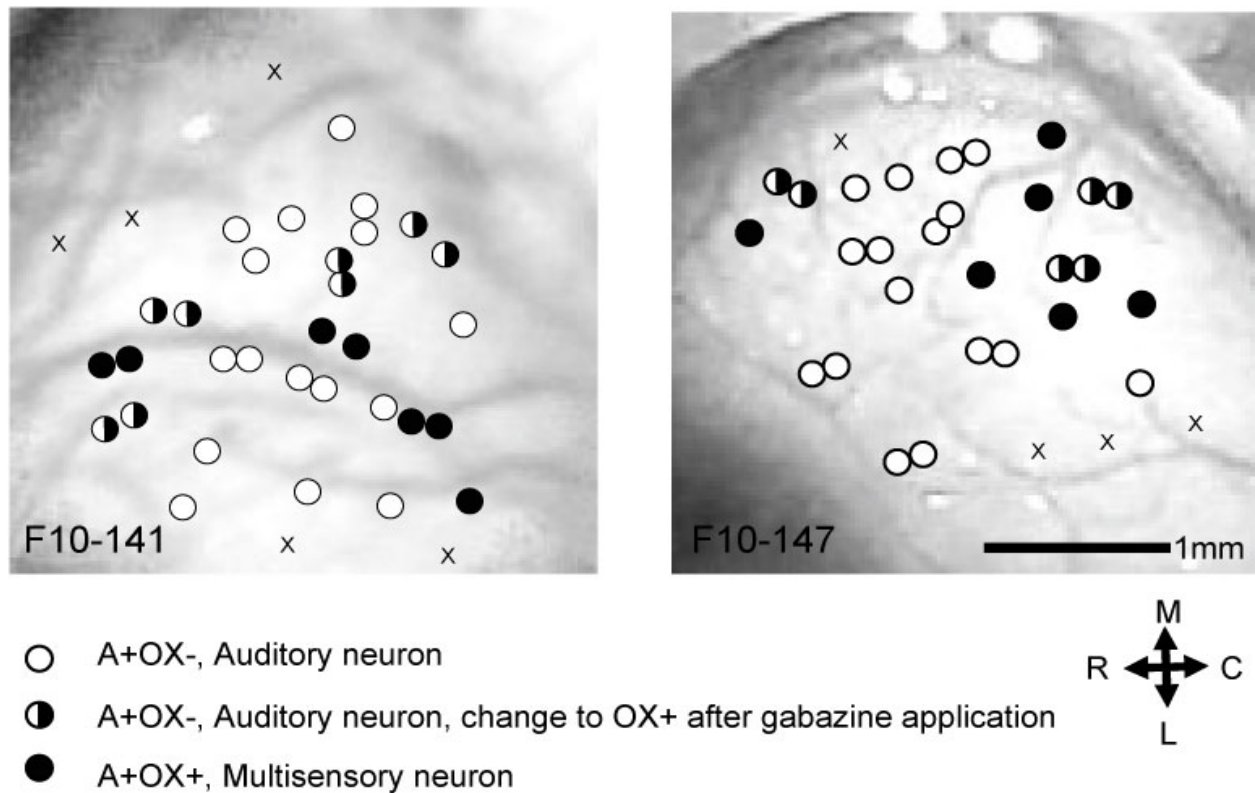


**Figure 4.8.** The distribution of neuronal response types before and after application of gabazine. Each figure represents data from one animal. Two examples are shown. A indicates auditory stimulation. OX indicates optic chiasm stimulation. The + symbols in the legend represent neurons that were responsive to that modality, whereas – symbols represent neurons that were not responsive to that modality. Unmasked visual responses were intermixed with auditory and multisensory neurons. X indicates a non-responsive recording site. Scale bar: 1 mm. Arrows at lower right show orientation. M, medial, L, lateral, R, rostral, C, caudal.

## CHAPTER 5 DISCUSSION

Our results demonstrate that the auditory cortex can be reorganized to manage multiple functions after recovery from damage to input pathways. Although invasion by ectopic visual inputs did not create segregation of auditory and visual neurons, cross-modal visual inputs compromised auditory function with respect to sensitivity, tuning, and topography. Inhibition in the auditory cortex was increased, and blockade of inhibition unmasked multisensory responses. Our findings provide important information regarding maladaptive plasticity during compensation for loss of brain functions. These results can provide guidance for designing rehabilitative strategies for brain damage and sensory/motor dysfunction.

### **1. Competition (fire together, wire together)**

Hebbian plasticity plays an important role in cortical development and cortical reorganization. 60 years ago, the psychologist Donald Hebb introduced the idea that any two cells increase the strength of their connectivity when they are repeatedly active together (Hebb 1949). This Hebbian rule has shaped thinking in the field of synaptic plasticity for many years. According to Hebbian rules, strong communication between cells can stabilize their contacts. During brain development, neuronal networks start with broad, exuberant connections and become more refined and narrow with time, largely as a result of their patterns of activity. This process occurs in learning and memory, maturation of sensory systems, and recovery from brain damage. In learning and memory, long-term potentiation enhances synaptic strength by high frequency stimulation of presynaptic axons or neurons (Bliss and Lømo 1973). During maturation of the visual cortex, competition between the two eyes results in segregation of their cortical territory into ocular dominance columns, whereas monocular deprivation causes loss of territory by the deprived eye (Guillery and Kaas 1974; Kratz and Spear 1976; Shatz and Stryker 1978; Stryker

1978). The refinement of sensory receptive fields is also activity-dependent (Kratz and Spear 1976). During recovery from early brain damage, activity can stabilize neuronal connections that might have been eliminated during normal development, in order to compensate for the loss of inputs (Kerr et al. 2011; Lund and Lund 1976). Because compensation may involve multiple brain areas and/or multiple modalities, inputs that respond to different modalities would compete for limited brain territory. In blind and deaf patients who have partially lost inputs from one sense or have rebuild the damage pathway by prosthesis, cross-modal projections take over the spared cortex that originally responded to the lost modality. These cross-modal inputs compete with residual sensory innervation when auditory or visual prostheses are implanted and the damaged sensory pathway is partially recovered (Gordon et al. 2011). Using cross-modal ferrets as an animal model to study rewiring and cross-modal plasticity, I report here that auditory cortex is reorganized after rewiring with visual inputs. I also found that the proportions of auditory neurons and visual neurons correlated with the residual volumes of subcortical auditory and visual midbrain, suggesting that the number of inputs determines the extent to which either modality can occupy the auditory cortex (Mao et al. 2011). These results imply that stronger inputs obtain more brain territory, consistent with a Hebbian mechanism (Hebb, 1949). Although both auditory and visual inputs to auditory cortex in the rewired animals arrive via the medial geniculate nucleus (MGN) (Pallas et al. 1990; Sur et al. 1988), I found that multisensory neurons in XMAC had longer latencies to auditory stimulation than auditory neurons in normal AC. These data suggest that auditory and visual thalamocortical inputs may compete for synaptic connections at the cellular level. Therefore, auditory neurons that receive direct thalamocortical auditory projections may be less likely to be reinnervated by thalamocortical visual inputs. Our

results further support the idea that interneuronal competition can operate between inputs carrying information from different modalities.

## **2. Reorganization of brain areas after sensory deafferentation, deprivation, or brain damage**

Topographic maps in cortical areas are maintained dynamically, which means they can adapt to changes in the environment. Loss of inputs by sensory deafferentation, deprivation, or brain damage results in reorganization of brain areas. In the visual system, eye enucleation causes an expansion of the ipsilateral retinotectal projection (Lund et al. 1976; Rhoades and Chalupa 1980). In the somatosensory system, Areas 3b and 1 in somatosensory cortical regions that originally represent some skin fields are taken over by inputs responding to adjacent skin surfaces after nerve transection (Merzenich et al. 1983). In addition to reorganization in primary somatosensory cortex, secondary somatosensory cortex can be occupied by an expansion of the foot representation after partial lesion of the hand representation in primary somatosensory cortex (Pons et al. 1988). In the auditory system, cochlear lesion results in an expanded representation of adjacent frequencies in auditory cortex (Robertson and Irvine 1989), and an expansion of regions neighboring a retinal lesion also occurs in the visual system (Kaas et al. 1990). Although studies demonstrate that reorganization of brain areas involves projections from neighboring peripheral sensory inputs, lesion of brain areas may cause different results. Removal of half of the superior colliculus does not eliminate half of the visual field but induces map compression (Finlay et al. 1979). Map compression in tectum was originally demonstrated in goldfish and hamster (Dunn-Meynell and Sharma 1984; Hodos and Yolen 1976; Schmidt 1983; Sharma and Romeskiel. 1977; Udin 1978). In our research, I found that recovery from neonatal auditory midbrain lesions resulted in nearly intact tonotopy, arguing that auditory topographic

maps may be compressed in IC as occurs in visual midbrain. Before the onset of hearing at about P30 in ferrets (Moore 1990), the auditory afferents reach the inferior colliculus but do not segregate into frequency bands (Brunso-Bechtold and Henkel 2005; Henkel et al. 2007). On postnatal day 4, a few synapses can be observed but are very immature (Brunso-Bechtold et al. 2006). This evidence suggests that the inferior colliculus in ferrets contains the potential to rearrange its connections with its afferents when it is damaged.

### **3. Cross-modal plasticity**

Cross-modal plasticity can occur after sensory deprivation, deafferentation or brain damage. In deafness and blindness, the spare cortices can be taken over by another modality (Cohen et al. 1997; Finney et al. 2001). The advantage of cross modal plasticity is the compensation for reduced sensory inputs. Research on cross modal plasticity has shown alterations of cortical areas from the molecular to the behavioral levels and from humans to other animals (Merabet and Pascual-Leone. 2010; Frasnelli J et al, 2011). The cross-modal paradigm used in our experiments employs neonatal midbrain lesions. After recovery from this damage, retinal projections are redirected to auditory thalamus, which carries their visual activity to auditory cortex, creating a rewired auditory cortical region that responds to visual stimuli. This retinal misrouting was first noted by Schneider and Frost after midbrain lesions in hamsters (Frost and Schneider 1979; Schneider 1973), and then the model was adopted in ferrets (Sur et al. 1988), in frogs (Scalia 1987; Scalia et al. 1995) and in mice (Lyckman et al. 2001). In frogs, retinal afferents were directed into olfactory cortex (Scalia 1992; Scalia et al. 1995). In hamsters, lesion of visual midbrain and visual cortex induced retinal projections to auditory or somatosensory thalamus (Frost 1981; 1982; 1999). In ferrets, retinal axons were rewired to auditory thalamus (MGN) (Sur 1988; Sur et al. 1988). This rewiring did not alter the thalamocortical projection

( Pallas et al 1990), allowing visual information to be transmitted from MGN to auditory cortex. The visual responses in XMAC have similarities to and differences from responses in primary visual cortex. The visual information in AC originates from W-type retinal ganglion cells (Pallas et al. 1994; Pallas and Sur 1994; Roe et al. 1993). Compared to X- and Y-driven visual neurons, visual neurons in cross-modal AC exhibited larger receptive fields, low responsiveness, and longer latencies. On the other hand, the visual neurons in XMAC have orientation and direction selectivity, and simple and complex receptive field organization like those in normal visual cortex (Roe et al. 1992). In addition to visual responses, here I show that auditory and multisensory responses coexist in XMAC. I further found that auditory responses in XMAC had wider tuning, higher thresholds than normal auditory neurons, and the tonotopic maps were disrupted by invasion of ectopic visual inputs. Previous cross-modal research found that XMAC contains a retinotopic map (Roe et al. 1990; Roe et al. 1992) and interconnections between neurons with similar orientation tuning (Sharma et al. 2000). Visual pathways in normal animals map visual information in two spatial dimensions, whereas auditory pathways map sound frequency information in one dimension. In order to acquire a retinotopic map and orientation tuning, thalamocortical excitatory inputs may adopt the two-dimensional pattern seen in normal animals. However, anatomical data argue against this hypothesis and show that the thalamocortical projection in cross-modal animals remains one-dimensional (Pallas et al. 1990). Therefore, visual neurons may modify intracortical connections in order to construct visual maps. I found stronger inhibition in XMAC, suggesting that intracortical inhibition may contribute to the sculpting of visual response properties. Possible interactions between auditory and visual circuits in XMAC were not addressed fully in this study and require further investigation.

#### **4. Maladaptive plasticity**

The term neuroplasticity is often used to refer to beneficial changes during recovery from brain damage or sensory dysfunction; however, plasticity is sometimes maladaptive. After amputation, the spared regions in somatosensory cortex can be occupied by inputs from other body surfaces. In contrast to beneficial reorganization, amputation may also cause phantom limb pain. It has been suggested that this negative aspect of recovery is caused by expansion of adjacent somatosensory cortex (Karl et al. 2001). Focal hand dystonia is another disorder resulting from maladaptive plasticity, which is often referred to as “writer’s cramp” or “musician’s cramp” (Pantev et al. 2001; Quartarone et al. 2006). After repetitious professional training and extensive hand movements, the motor cortex of musicians and writers actually develops abnormally, and merging of representative regions for individual digits can occur (Byl et al. 1996). Reductions in inhibition in sensorimotor cortex have been revealed in focal hand dystonia patients (Levy and Hallett 2002). Tinnitus is another phantom sensation that may also result from cross modal plasticity. Tinnitus patients claim that they can hear sounds in the absence of auditory stimuli. Some research has shown spontaneous activity in the auditory system during tinnitus, whereas other studies have found cross-modal facilitation or suppressive interaction in tinnitus patients (Langguth et al. 2005; Roberts et al. 2010). In my study, I found multisensory neurons that are specifically tuned to pure tones. Given that these neurons are visually responsive, they may contribute to the auditory phantom sensation of tinnitus. For example, visual stimuli can activate multisensory neurons in XMAC. Those multisensory neurons may communicate with the auditory pathway. Phantom sound then occurs without auditory stimuli. Therefore, neural plasticity may boost unwanted connections that can interfere with the original functions of the affected brain areas. I also found that after reorganization, auditory cortex in XM animals can



respond to both sound and light. The invasion of visual inputs impaired auditory function (Chapter 3). These data imply that cross-modal plasticity can interfere with the recovery of the original function, as has been found in deaf patients after cochlear implants (Lee et al. 2001). Our research provides further evidence that maladaptive plasticity can result from brain damage and then prevent a full recovery of the patient's hearing ability.

## **5. Inhibitory plasticity after sensory deprivation/deafferentation and brain damage**

### **a) The role of lateral inhibition**

Before concluding that lateral inhibition is responsible for the expansion of receptive fields in sensory cortices of deprived and deafferented animals, the role of lateral inhibition in shaping receptive fields of sensory neurons must first be discussed. Blockade of inhibition in visual cortex enlarges visual receptive fields (Sillito 1975), and decreases orientation selectivity (Sillito 1979; Sillito et al. 1980; Tsumoto et al. 1979; Worgotter and Eysel 1991). The original model of lateral inhibition suggests that lateral inhibition from neighboring neurons sharpens excitatory responses to sensory stimuli. If so then inhibitory neurons should either have broader tuning curves than excitatory neurons or be untuned. Recent research has challenged this classical model. Ozeki and colleagues found that iontophoretic application of GABA<sub>A</sub> receptor antagonist did not alter visual stimulus-size tuning (Ozeki et al. 2004). The disadvantage of the *in vivo* extracellular recording methods used in previous studies is that they can only record action potentials that result from summation of both excitatory and inhibitory inputs to a single neuron. In contrast to extracellular recording, intracellular whole cell patch-clamp recording can distinguish between excitatory (EPSP) and inhibitory postsynaptic potentials (IPSP). Using this method it has been reported that both IPSPs and EPSPs show well-tuned orientation selectivity

(Ferster 1986). The preferred orientations of EPSPs and IPSPs in one visual neuron are identical. These results argue that orientation of visual neurons is not created or sharpened by inhibition (Ferster 1986). Further research found that excitatory and inhibitory components of the recorded visual neuron are tuned to the same orientation but are temporally out of phase with one another (Priebe and Ferster 2005). Similar results have been found in the auditory system (Tan et al. 2004; Wehr and Zador 2003; Zhang et al. 2003). These intracellular recording results suggest that lateral inhibition may not be responsible for sharpening sensory tuning, in which case the broader tuning curves found in sensory-deprived and –deafferented animals may not result from loss of lateral inhibition. The intracellular studies mentioned above distinguish inhibitory and excitatory components of excitatory neurons, but few studies have recorded from inhibitory neurons *in vivo*. Recently, an impressive study using whole-cell recordings of inhibitory neurons has been done in rat primary auditory cortex (Wu et al. 2008). Their results show that inhibitory neurons have broader tuning curves than excitatory neurons, while another study has found that auditory tuning of excitatory but not inhibitory neurons gets sharper during development (Sun et al. 2010), suggesting that the refinement of auditory receptive field relies more on maturation of excitatory inputs than on inhibitory inputs. In the current project, I found that broader tuning of auditory neurons in XMAC is not correlated with loss of lateral inhibition. I suggest that excitatory input may play a more important role than inhibitory inputs in constructing auditory properties during recovery from midbrain damage.

#### **b) Changes in inhibition may be layer specific and not be reflected at the molecular level**

Although inhibition is decreased in sensory-deprived and deafferented animals (Garrahy et al. 1991; Vale and Sanes 2002), it is still debated whether and to what extent inhibition is altered in

this process. Physiological recordings suggest that GABAergic inhibition decreases in dark-reared animals. Some research reported that the number of GABAergic neurons decreased in sensory-deprived animals (Garrahy et al. 1991; Hendry and Jones, 1986), whereas some immunohistochemical studies show that expression of GAD does not change in visual cortex of dark-reared animals (Bear et al. 1985; Mower and Guo 2001). -In some cases, an expansion of adjacent representations is found in deafferented animals, but changes in GABA<sub>A</sub> receptors mRNA level and immunohistochemically stained neurons are not observed (Jones et al. 2002). Therefore, it is possible that physiological abnormalities are not reflected at the molecular level. Recent research proposes that deafferentation unmasks both excitatory and inhibitory inputs (Rajan 2001), therefore either there is no change in afferent strength or the changes are specific to layers or synaptic connections. For example, studies in barrel cortex show that the decreases in expression of GABAergic neurons, GABA receptors, or GAD are layer specific (Micheva and Beaulieu 1995b). The decrease in GABA<sub>A</sub> receptor expression in visual cortex of deprived animals is concentrated closer to the dendrites than to the axons (Katagiri et al. 2007). After central, binocular lesions of retina, the expression of GAD-positive puncta decreases, whereas GAD-positive somata increases, in visual cortex of cats (Rosier et al. 1995). Expression of GABA-positive somata and puncta does not change, nor does the expression of GABA<sub>A</sub> and GABA<sub>B</sub> receptors (Rosier et al. 1995). The inconsistent results across the literature suggest that loss of inhibition in sensory-deprived or deafferented animals may only be reflected at the physiological level.

**c) Reductions in inhibition may be transient, with the recovery stage requiring strong inhibition.**

The decrease of inhibition within one modality after loss of inputs may be transient. It has been found that GABA expression in sensorimotor cortex is reduced quickly after forearm nerve block (Levy et al. 2002), but can recover to normal levels in adult sensory-deprived or -deafferented animals. For example, the expression of GABA in IC is decreased after unilateral cochlear lesions, but returns to normal levels one month later (Wang et al. 2007). I did not find the bandwidths of tuning curves in AC of the blind-lesioned animals to be significantly different from those in normal animals (Chapter 3), suggesting that thalamocortically-activated lateral inhibition may recover to normal levels after IC lesions.

After transient changes following damage to sensory pathways, re-establishment of receptive fields and excitability levels is the long-term goal of cortical reorganization. Increasing inhibition may play an important role during this process. Removal of the olfactory bulb in rats shows that GAD-positive terminals are denser in the lateral olfactory tract than normal one. (Westenbroek et al. 1988). Deafferentation of rat spinal cord results in an increase in GAD-67 mRNA that coincides with the sprouting of unaffected afferents (Feldblum et al. 1998). After vibrissal deafferentation, GABA-immunostained boutons are increased in the ventrobasal thalamic complex, indicating a compensatory increase in inhibition (Hamori et al. 1986). The increase in inhibition has also been found in brain regions across modalities. In mice that have olfactory deficits, whisking responses in the barrel cortex are upregulated. With this upregulation, the number of GABAergic neurons is increased (Ni et al. 2010). In my research, midbrain lesions were associated with increased inhibition in the auditory cortex, consistent with Ni et al.'s results.. Based on the results mentioned above in chapter 3, I suggest that the increased inhibition is caused by the invasion of visual inputs but not by the loss of auditory inputs. After recovery from visual invasion, XMAC is reorganized to manage responses to both auditory and visual

stimuli. Because auditory and visual neurons are not segregated from each other (Chapter 2), responses to a single modality may be disturbed by responses to the other modality. In order to cope with this dilemma, mutual inhibition may be increased in XMAC in order to suppress neighboring firing that may represent a different modality.

#### **d) Inhibition is increased when inputs compete for territory**

Visual deprivation in early life can induce permanent loss of visual responsiveness (reduced visual acuity, loss of tuning, etc.) to the deprived eye. These changes may be caused by depression of excitatory intracortical inputs (Kirkwood et al. 1996). Alternatively, they could also be caused by an increase in cortical inhibition (Maffei et al. 2006). Research has demonstrated that the weaker responses to the deprived eye in ocular dominance columns result at least in part from stronger inhibition (Duffy et al. 1976; Sillito et al. 1981). Ionophoretic application of bicuculline, a GABA<sub>A</sub> receptor antagonist, can restore neuronal activity to the deprived eye at 5 months of age in cats (Burchfiel and Duffy 1981) and induce significantly more changes in ocular dominance in monocularly-deprived than in normal animals (Mower and Christen 1989). Our current study found competition between the auditory and visual inputs that are both activating auditory cortex in XM animals. Therefore, residual auditory responses may have been suppressed by ectopic visual activity, which is similar to-- the activity from non-deprived eye in monocular-deprived animals. I suggest that increased inhibition plays a significant role during cross-modal plasticity to manipulate bimodal modalities.

### **6. Clinical applications**

Cross modal plasticity occurs in deaf or blind patients and patients recovering from brain damage. Maladaptive compensation is not optimal, but is the situation that rehabilitation strategies must

cope with. After stroke, cortical representations are rearranged and excitability thresholds are increased (Traversa et al. 1997). Behavioral training is applied to encourage specific movements. These movements can enlarge their own cortical representations after training (Nudo et al. 1996a; Nudo et al. 1996b). This use-dependent plasticity provides important cues for designing rehabilitation therapy. The disadvantages of maladaptive plasticity include possible unwanted projections or cortical reorganization. Preventing activation of mis-wired connections or boosting activity from residual connections may help to eliminate disadvantageous cortical reorganization. Another important rehabilitative strategy is pharmacotherapy. Neurotransmitters and their receptors can target certain circuits that are involved in brain reorganization. Recently, a study found that inhibition is increased in the peri-infarct zone in mice after stroke. The researchers applied the GABA<sub>A</sub> benzodiazepine agonist L655,708-- and found that motor function was recovered, suggesting that pharmacological treatment is a possible way to counteract abnormal function after maladaptive plasticity (Clarkson et al. 2010). In my study, I also found an increase in inhibition in XMAC. Auditory function was compromised by invasion of visual inputs. In order to rebuild auditory function, possible strategies include exposure to enriched auditory environments and blockade of inhibition. Further research is required to address these questions.

## **7. Evolutionary implications**

The brain differentiates into functional areas during development, and this is especially obvious in neocortex. It has been proposed that although all mammals have basic sensory areas in common, some new areas were added in more recently evolved animals (Kaas 1989). The emergence of new functional areas may be caused by duplication, differentiation, or invasion by axons from other structures (Kaas 1989; 1993); however, the process of brain evolution remains

elusive. Sensory cortex and motor cortex in mammals are topographically arranged (Kaas 1997). Although each sensory cortex has its own unique topographic map that corresponds to its modality, most of these maps still follow the order of the receptor sheet, suggesting common and possibly interchangeable characteristics between them (Kaas 1997). Comparative studies have shown that the size and divisions of sensory cortices in different species relate to their life styles (Catania 2000). Because they are living underground almost their entire life, blind mole rats have evolved a reduced visual cortex and an expanded somatosensory cortex (Mann et al. 1997). The sizes of sensory cortices may rely on neural activity and sensory experience; the existence of primary sensory cortex, however, cannot be altered by environmental change or even by gene knockout (Hunt et al. 2006; Karlen and Krubitzer 2009; Merzenich et al. 1983). The occurrence of new cortical areas may also relate to gene mutation. For example, knockout of the axon guidance molecules called ephrins can induce retinal inputs to project to the auditory pathway (Lyckman et al. 2001). A large body of work has been done to show that the rerouted retinal afferents can bring visual information to auditory cortex and change auditory cortex to be visually responsive (Roe et al. 1992; Sharma et al. 2000; Sur et al. 1988). These studies suggest that the sensory cortex can be altered to perform a significantly different function by changes in gene expression or activity, implying an evolutionary possibility for emergence of new cortical areas. Here I show that rewired auditory cortex actually responded to both auditory and visual cues. Although auditory and visual neurons were not segregated from each other, multisensory neurons were created by convergence of auditory and visual inputs. In rodents, multisensory neurons exist at the border of unisensory cortex (Wallace et al. 2004). In blind animals with cross-modal projections, multisensory neurons occur in areas between primary sensory cortices (Hunt et al. 2006; Kahn and Krubitzer 2002). Our data further support the idea that the evolution

of new multisensory areas could be a developmental mistake of axon rerouting and provide crucial information for brain evolution in general.

Overall, our results on cross-modal plasticity shed light on the implications of maladaptive outcomes after recovery and on compensatory changes in inhibitory circuits. These results provide important knowledge for future study of recovery from sensory/motor dysfunction and brain damage and also add more understanding of plasticity in general to the literature.



## REFERENCES

- Aitkin L, Irvine DRF, and Webster WR.** Central neural mechanisms of hearing. In: *Handbook of Physiology: The Nervous System III*. Bethesda: Amer. Physiol. Soc., 1984, p. 675-737.
- Allison JD, Kabara JF, Snider RK, Casagrande VA, and Bonds AB.** GABA<sub>B</sub>-receptor-mediated inhibition reduces the orientation selectivity of the sustained response of striate cortical neurons in cats. *Vis Neurosci* 13: 559-566, 1996.
- Allman BL, Bittencourt-Navarrete RE, Keniston LP, Medina AE, Wang MY, and Meredith MA.** Do cross-modal projections always result in multisensory integration? *Cereb Cortex* 18: 2066-2076, 2008.
- Allman BL, Keniston LP, and Meredith MA.** Adult deafness induces somatosensory conversion of ferret auditory cortex. *Proc Natl Acad Sci U S A* 106: 5925-5930, 2009a.
- Allman BL, Keniston LP, and Meredith MA.** Not just for bimodal neurons anymore: the contribution of unimodal neurons to cortical multisensory processing. *Brain Topogr* 21: 157-167, 2009b.
- Allman BL, and Meredith MA.** Multisensory processing in "unimodal" neurons: cross-modal subthreshold auditory effects in cat extrastriate visual cortex. *J Neurophysiol* 98: 545-549, 2007.
- Angelucci A, Clasca F, Bricolo E, Cramer KS, and Sur M.** Experimentally induced retinal projections to the ferret auditory thalamus: development of clustered eye-specific patterns in a novel target. *J Neurosci* 17: 2040-2055, 1997.
- Angelucci A, Clasca F, and Sur M.** Brainstem inputs to the ferret medial geniculate nucleus and the effect of early deafferentation on novel retinal projections to the auditory thalamus. *J Comp Neurol* 400: 417-439, 1998.

- Arckens L, Eysel UT, Vanderhaeghen JJ, Orban GA, and Vandesande F.** Effect of sensory deafferentation on the GABAergic circuitry of the adult cat visual system. *Neuroscience* 83: 381-391, 1998.
- Bandyopadhyay S, Shamma SA, and Kanold PO.** Dichotomy of functional organization in the mouse auditory cortex. *Nat Neurosci* 13: 361-368, 2010.
- Bavelier D, Dye MW, and Hauser PC.** Do deaf individuals see better? *Trends Cogn Sci* 10: 512-518, 2006.
- Bavelier D, and Neville HJ.** Cross-modal plasticity: where and how? *Nat Rev Neurosci* 3: 443-452, 2002.
- Bear MF, and Colman H.** Binocular competition in the control of geniculate cell size depends upon visual cortical N-methyl-D-aspartate receptor activation. *Proc Natl Acad Sci U S A* 87: 9246-9249, 1990.
- Bear MF, Kleinschmidt A, Gu QA, and Singer W.** Disruption of experience-dependent synaptic modifications in striate cortex by infusion of an NMDA receptor antagonist. *J Neurosci* 10: 909-925, 1990.
- Bear MF, Schmechel DE, and Ebner FF.** Glutamic acid decarboxylase in the striate cortex of normal and monocularly deprived kittens. *J Neurosci* 5: 1262-1275, 1985.
- Beauchamp MS, and Ro T.** Neural substrates of sound-touch synesthesia after a thalamic lesion. *J Neurosci* 28: 13696-13702, 2008.
- Benevento LA, Bakkum BW, Port JD, and Cohen RS.** The effects of dark-rearing on the electrophysiology of the rat visual cortex. *Brain Res* 572: 198-207, 1992.

**Benson TE, Ryugo DK, and Hinds JW.** Effects of sensory deprivation on the developing mouse olfactory system: a light and electron microscopic, morphometric analysis. *J Neurosci* 4: 638-653, 1984.

**Bizley JK, and King AJ.** Visual-auditory spatial processing in auditory cortical neurons. *Brain Res* 1242: 24-36, 2008.

**Bizley JK, and King AJ.** Visual influences on ferret auditory cortex. *Hear Res* 258: 55-63, 2009.

**Bizley JK, Nodal FR, Bajo VM, Nelken I, and King AJ.** Physiological and anatomical evidence for multisensory interactions in auditory cortex. *Cereb Cortex* 17: 2172-2189, 2007.

**Bizley JK, Nodal FR, Nelken I, and King AJ.** Functional organization of ferret auditory cortex. *Cereb Cortex* 15: 1637-1653, 2005.

**Blakemore C, and Price DJ.** Effects of dark-rearing on the development of area 18 of the cat's visual cortex. *J Physiol* 384: 293-309, 1987.

**Bledsoe SC, Jr., Nagase S, Miller JM, and Altschuler RA.** Deafness-induced plasticity in the mature central auditory system. *NeuroReport* 7: 225-229, 1995.

**Bliss TV, and Lomo T.** Long-lasting potentiation of synaptic transmission in the dentate area of the anaesthetized rabbit following stimulation of the perforant path. *J Physiol* 232: 331-356, 1973.

**Bognar L, Fischer C, Turjman F, Michel F, Villanyi E, Mottollese C, Guyotat J, and Lapras C.** Tectal plate gliomas. Part III: Apparent lack of auditory consequences of unilateral inferior collicular lesion due to localized glioma surgery. *Acta Neurochir (Wien)* 127: 161-165, 1994.

**Briner A, De Roo M, Dayer A, Muller D, Kiss JZ, and Vutskits L.** Bilateral whisker trimming during early postnatal life impairs dendritic spine development in the mouse somatosensory barrel cortex. *J Comp Neurol* 518: 1711-1723, 2010.

**Bronchti G, Heil P, Sadka R, Hess A, Scheich H, and Wollberg Z.** Auditory activation of "visual" cortical areas in the blind mole rat (*Spalax ehrenbergi*). *Eur J Neurosci* 16: 311-329, 2002.

**Bronchti G, Schönenberger N, Welker E, and Van der Loos H.** Barreldfield expansion after neonatal eye removal in mice. *NeuroReport* 3: 489-492, 1992.

**Brunso-Bechtold JK, Evans SD, and Henkel CK.** Synaptogenesis in the inferior colliculus of the pre-hearing postnatal ferret. *Hear Res* 218: 1-4, 2006.

**Brunso-Bechtold JK, and Henkel CK.** Development of auditory afferents to the central nucleus of the inferior colliculus. In: *The Inferior Colliculus*, edited by Winer JA, and Schreiner CESpringer New York, 2005, p. 537-558.

**Buckley KA, and Tobey EA.** Cross-modal plasticity and speech perception in pre- and postlingually deaf cochlear implant users. *Ear Hear* 32: 2-15, 2011.

**Buonomano DV, and Merzenich MM.** Cortical plasticity: from synapses to maps. *Annu Rev Neurosci* 21: 149-186, 1998.

**Burchfiel JL, and Duffy FH.** Role of intracortical inhibition in deprivation amblyopia: reversal by microiontophoretic bicuculline. *Brain Res* 206: 479-484, 1981.

**Byl NN, Merzenich MM, and Jenkins WM.** A primate genesis model of focal dystonia and repetitive strain injury: I. Learning-induced dedifferentiation of the representation of the hand in the primary somatosensory cortex in adult monkeys. *Neurology* 47: 508-520, 1996.

**Cacace AT.** Expanding the biological basis of tinnitus: crossmodal origins and the role of neuroplasticity. *Hear Res* 175: 112-132, 2003.

**Calford MB, and Tweedale R.** Immediate and chronic changes in responses of somatosensory cortex in adult flying-fox after digit amputation. *Nature* 332: 446-448, 1988.

**Campi KL, Bales KL, Grunewald R, and Krubitzer L.** Connections of auditory and visual cortex in the prairie vole (*Microtus ochrogaster*): evidence for multisensory processing in primary sensory areas. *Cereb Cortex* 20: 89-108, 2010.

**Canu MH, Treffort N, Picquet F, Dubreucq G, Guerardel Y, and Falempin M.**

Concentration of amino acid neurotransmitters in the somatosensory cortex of the rat after surgical or functional deafferentation. *Exp Brain Res* 173: 623-628, 2006.

**Cappe C, and Barone P.** Heteromodal connections supporting multisensory integration at low levels of cortical processing in the monkey. *Eur J Neurosci* 22: 2886-2902, 2005.

**Carrasco MM, Mao YT, Balmer TS, and Pallas SL.** Inhibitory plasticity underlies visual deprivation-induced loss of receptive field refinement in the adult superior colliculus. *Eur J Neurosci* 33: 58-68, 2011.

**Carrasco MM, and Pallas SL.** Early visual experience prevents but cannot reverse deprivation-induced loss of refinement in adult superior colliculus. *Vis Neurosci* 23: 845-852, 2006.

**Carrasco MM, Razak KA, and Pallas SL.** Visual experience is necessary for maintenance but not development of receptive fields in superior colliculus. *J Neurophysiol* 94: 1962-1970, 2005.

**Catania KC.** Cortical organization in insectivora: the parallel evolution of the sensory periphery and the brain. *Brain Behav Evol* 55: 311-321, 2000.

**Chabot N, Charbonneau V, Laramee ME, Tremblay R, Boire D, and Bronchti G.**

Subcortical auditory input to the primary visual cortex in anophthalmic mice. *Neurosci Lett* 433: 129-134, 2008.

**Chabot N, Robert S, Tremblay R, Miceli D, Boire D, and Bronchti G.** Audition differently activates the visual system in neonatally enucleated mice compared with anophthalmic mutants. *Eur J Neurosci* 26: 2334-2348, 2007.

- Champoux F, Lepore F, Gagne JP, and Theoret H.** Visual stimuli can impair auditory processing in cochlear implant users. *Neuropsychologia* 47: 17-22, 2009.
- Chen L, Yang C, and Mower GD.** Developmental changes in the expression of GABA<sub>A</sub> receptor subunits ( $\alpha_1$ ,  $\alpha_2$ ,  $\alpha_3$ ) in the cat visual cortex and the effects of dark rearing. *Brain Res Mol Brain Res* 88: 135-143, 2001.
- Chen QC, and Jen PH.** Bicuculline application affects discharge patterns, rate-intensity functions, and frequency tuning characteristics of bat auditory cortical neurons. *Hear Res* 150: 161-174, 2000.
- Chino YM, Kaas JH, Smith EL, 3rd, Langston AL, and Cheng H.** Rapid reorganization of cortical maps in adult cats following restricted deafferentation in retina. *Vision Res* 32: 789-796, 1992.
- Chklovskii DB, and Koulakov AA.** Maps in the brain: what can we learn from them? *Annu Rev Neurosci* 27: 369-392, 2004.
- Chklovskii DB, Schikorski T, and Stevens CF.** Wiring optimization in cortical circuits. *Neuron* 34: 341-347, 2002.
- Clancy B, Darlington RB, and Finlay BL.** Translating developmental time across mammalian species. *Neuroscience* 105: 7-17, 2001.
- Clarkson AN, Huang BS, MacIsaac SE, Mody I, and Carmichael ST.** Reducing excessive GABA-mediated tonic inhibition promotes functional recovery after stroke. *Nature* 468: 305-309, 2010.
- Cohen LG, Celnik P, Pascual-Leone A, Corwell B, Falz L, Dambrosia J, Honda M, Sadato N, Gerloff C, Catala MD, and Hallett M.** Functional relevance of cross-modal plasticity in blind humans. *Nature* 389: 180-183, 1997.

**Cohen LG, Weeks RA, Sadato N, Celnik P, Ishii K, and Hallett M.** Period of susceptibility for cross-modal plasticity in the blind. *Ann Neurol* 45: 451-460, 1999.

**Collignon O, and De Volder AG.** Further evidence that congenitally blind participants react faster to auditory and tactile spatial targets. *Can J Exp Psychol* 63: 287-293, 2009.

**Crair MC, Ruthazer ES, Gillespie DC, and Stryker MP.** Relationship between the ocular dominance and orientation maps in visual cortex of monocularly deprived cats. *Neuron* 19: 307-318, 1997.

**D'Ausilio A, Altenmüller E, Olivetti Belardinelli M, and Lotze M.** Cross-modal plasticity of the motor cortex while listening to a rehearsed musical piece. *Eur J Neurosci* 24: 955-958, 2006.

**Dahl CD, Logothetis NK, and Kayser C.** Spatial organization of multisensory responses in temporal association cortex. *J Neurosci* 29: 11924-11932, 2009.

**Darian-Smith C, and Gilbert CD.** Axonal sprouting accompanies functional reorganization in adult cat striate cortex. *Nature* 368: 737-740, 1994.

**de la Mothe LA, Blumell S, Kajikawa Y, and Hackett TA.** Thalamic connections of the auditory cortex in marmoset monkeys: core and medial belt regions. *J Comp Neurol* 496: 72-96, 2006.

**Dehay C, Giroud P, Berland M, Killackey H, and Kennedy H.** Contribution of thalamic input to the specification of cytoarchitectonic cortical fields in the primate: effects of bilateral enucleation in the fetal monkey on the boundaries, dimensions, and gyrification of striate and extrastriate cortex. *J Comp Neurol* 367: 70-89, 1996.

**Doron N, and Wollberg Z.** Cross-modal neuroplasticity in the blind mole rat *Spalax ehrenbergi*: a WGA-HRP tracing study. *NeuroReport* 5: 2697-2701, 1994.

**Dorrn A, Yuan K, Barker AJ, Schreiner CE, and Froemke RC.** Developmental sensory experience balance cortical excitation and inhibition. *Nature* 465: 932-936, 2010

**Doucet ME, Bergeron F, Lassonde M, Ferron P, and Lepore F.** Cross-modal reorganization and speech perception in cochlear implant users. *Brain* 129: 3376-3383, 2006.

**Duffy FH, Burchfiel JL, and Conway JL.** Bicuculline reversal of deprivation amblyopia in the cat. *Nature* 260: 256-257, 1976.

**Dunn-Meynell AA, and Sharma SC.** Changes in the topographically organized connections between the nucleus isthmi and the optic tectum after partial tectal ablation in adult goldfish. *J Comp Neurol* 227: 497-510, 1984.

**Dye MW, Baril DE, and Bavelier D.** Which aspects of visual attention are changed by deafness? The case of the Attentional Network Test. *Neuropsychologia* 45: 1801-1811, 2007.

**Elbert T, Sterr A, Rockstroh B, Pantev C, Muller MM, and Taub E.** Expansion of the tonotopic area in the auditory cortex of the blind. *J Neurosci* 22: 9941-9944, 2002.

**Fagiolini M, Katagiri H, Miyamoto H, Mori H, Grant SG, Mishina M, and Hensch TK.** Separable features of visual cortical plasticity revealed by *N*-methyl-D-aspartate receptor 2A signaling. *Proc Natl Acad Sci U S A* 100: 2854-2859, 2003.

**Falchier A, Clavagnier S, Barone P, and Kennedy H.** Anatomical evidence of multimodal integration in primate striate cortex. *J Neurosci* 22: 5749-5759, 2002.

**Fallon JB, Shepherd RK, Brown M, and Irvine DR.** Effects of neonatal partial deafness and chronic intracochlear electrical stimulation on auditory and electrical response characteristics in primary auditory cortex. *Hear Res* 257: 93-105, 2009.



**Feldblum S, Anoal M, Lapsher S, Dumoulin A, and Privat A.** Partial deafferentation of the developing rat spinal cord delays the spontaneous repression of GAD67 mRNAs in spinal cells.

*Perspect Dev Neurobiol* 5: 131-143, 1998.

**Ferster D.** Orientation selectivity of synaptic potentials in neurons of cat primary visual cortex. *J Neurosci* 6: 1284-1301, 1986.

**Fine I, Finney EM, Boynton GM, and Dobkins KR.** Comparing the effects of auditory deprivation and sign language within the auditory and visual cortex. *J Cogn Neurosci* 17: 1621-1637, 2005.

**Finlay BL, Schneps SE, and Schneider GE.** Orderly compression of the retinotectal projection following partial tectal ablation in the newborn hamster. *Nature* 280: 153-155, 1979.

**Finnerty GT, Roberts LS, and Connors BW.** Sensory experience modifies the short-term dynamics of neocortical synapses. *Nature* 400: 367-371, 1999.

**Finney EM, Fine I, and Dobkins KR.** Visual stimuli activate auditory cortex in the deaf. *Nat Neurosci* 4: 1171-1173, 2001.

**Florence SL, and Kaas JH.** Large-scale reorganization at multiple levels of the somatosensory pathway follows therapeutic amputation of the hand in monkeys. *J Neurosci* 15: 8083-8095, 1995.

**Florence SL, Taub HB, and Kaas JH.** Large-scale sprouting of cortical connections after peripheral injury in adult macaque monkeys. *Science* 282: 1117-1121, 1998.

**Fox JG, and Bell JA.** Growth, Reproduction, and Breeding. In: *Biology and Diseases of the Ferret, 2nd edition*, edited by Fox JG. Baltimore, MD Williams and Wilkins, 1998.

**Fox K.** Anatomical pathways and molecular mechanisms for plasticity in the barrel cortex. *Neuroscience* 111: 799-814, 2002.

**Frasnelli J, Collignon O, Voss P, and Lepore F.** Crossmodal plasticity in sensory loss. *Prog Brain Res* 191: 233-249, 2011.

**Frassinetti F, Bolognini N, Bottari D, Bonora A, and Ladavas E.** Audiovisual integration in patients with visual deficit. *J Cogn Neurosci* 17: 1442-1452, 2005.

**Froster DO.** Orderly anomalous retinal projections to the medial geniculate, ventrobasal, and lateral posterior nuclei of the hamster. *J Comp Neurol* 203: 227-256, 1981.

**Froster DO.** Anomalous visual connections to somatosensory and auditory system following brain lesions in early life. *Brain Res* 255: 627-635, 1982.

**Frost DO.** Functional organization of surgically created visual circuits. *Restor Neurol Neurosci* 15: 107-113, 1999.

**Frost DO, and Schneider GE.** Plasticity of retinofugal projections after partial lesions of the retina in newborn Syrian hamsters. *J Comp Neurol* 185: 517-567, 1979.

**Fuchs JL, and Salazar E.** Effects of whisker trimming on GABA<sub>A</sub> receptor binding in the barrel cortex of developing and adult rats. *J Comp Neurol* 395: 209-216, 1998.

**Gao WJ, and Pallas SL.** Cross-modal reorganization of horizontal connectivity in auditory cortex without altering thalamocortical projections. *J Neurosci* 19: 7940-7950, 1999.

**Garraghty PE, LaChica EA, and Kaas JH.** Injury-induced reorganization of somatosensory cortex is accompanied by reductions in GABA staining. *Somatosens Mot Res* 8: 347-354, 1991.

**Ghazanfar AA, and Schroeder CE.** Is neocortex essentially multisensory? *Trends Cogn Sci* 10: 278-285, 2006.

**Gilbert CD, and Wiesel TN.** Receptive field dynamics in adult primary visual cortex. *Nature* 356: 150-152, 1992.

**Gonzalez L, Shumway C, Morissette J, and Bower JM.** Developmental plasticity in cerebellar tactile maps: fractured maps retain a fractured organization. *J Comp Neurol* 332: 487-498, 1993.

**Gordon KA, Wong DD, Valero J, Jewell SF, Yoo P, and Papsin BC.** Use it or lose it? lessons learned from the developing brains of children who are deaf and use cochlear implants to hear. *Brain Topogr* 2011.

**Guillery RW, and Kaas JH.** The effects of monocular lid suture upon the development of the visual cortex in squirrels (*Sciureus carolinensis*). *J Comp Neurol* 154: 443-452, 1974.

**Hamori J, Savy C, Madarasz M, Somogyi J, Takacs J, Verley R, and Farkas-Bargeton E.** Morphological alterations in subcortical vibrissal relays following vibrissal follicle destruction at birth in the mouse. *J Comp Neurol* 254: 166-183, 1986.

**Hardingham NR, Gould T, and Fox K.** Anatomical and sensory experiential determinants of synaptic plasticity in layer 2/3 pyramidal neurons of mouse barrel cortex. *J Comp Neurol* 519: 2090-2124, 2011.

**Harrison RV, Ibrahim D, and Mount RJ.** Plasticity of tonotopic maps in auditory midbrain following partial cochlear damage in the developing chinchilla. *Exp Brain Res* 123: 449-460, 1998.

**Harrison RV, Stanton SG, Ibrahim D, Nagasawa A, and Mount RJ.** Neonatal cochlear hearing loss results in developmental abnormalities of the central auditory pathways. *Acta Otolaryngol* 113: 296-302, 1993.

**Hebb DO.** *The organization of behavior; a neuropsychological theory*. New York,: Wiley, 1949, p. xix, 335 p.

**Heil P.** Invasion of visual cortex by the auditory system in the naturally blind mole rat. *NeuroReport* 7: 41-51, 1991.

**Hendry SH, and Jones EG.** Reduction in number of immunostained GABAergic neurones in deprived-eye dominance columns of monkey area 17. *Nature* 320: 750-753, 1986.

**Hendry SH, and Miller KL.** Selective expression and rapid regulation of GABA<sub>A</sub> receptor subunits in geniculocortical neurons of macaque dorsal lateral geniculate nucleus. *Vis Neurosci* 13: 223-235, 1996.

**Henkel CK, Keiger CJ, Franklin SR, and Brunso-Bechtold JK.** Development of banded afferent compartments in the inferior colliculus before onset of hearing in ferrets. *Neuroscience* 146: 225-235, 2007.

**Herraiz C, Hernandez-Calvin FJ, Plaza G, Toledano A, and De los Santos G.** [Multi-sensory interaction in tinnitus: visual evoked potentials and somatosensory stimulation]. *Acta Otorrinolaringol Esp* 54: 329-336, 2003.

**Herrmann K, Antonini A, and Shatz CJ.** Ultrastructural evidence for synaptic interactions between thalamocortical axons and subplate neurons. *Eur J Neurosci* 6: 1729-1742, 1994.

**Hodos W, and Yolen NM.** Behavioral correlates of 'tectal compression' in goldfish. II. Visual acuity. *Brain Behav Evol* 13: 468-474, 1976.

**Hoistad DL, and Hain TC.** Central hearing loss with a bilateral inferior colliculus lesion. *Audiol Neurotol* 8: 111-113, 2003.

**Hubel DH, and Wiesel TN.** Receptive fields, binocular interaction and functional architecture in the cat's visual cortex. *J Physiol* 160: 106-154, 1962.

**Hubel DH, and Wiesel TN.** Shape and arrangement of columns in cat's striate cortex. *J Physiol* 165: 559-568, 1963.

**Hunt DL, King B, Kahn DM, Yamoah EN, Shull GE, and Krubitzer L.** Aberrant retinal projections in congenitally deaf mice: how are phenotypic characteristics specified in development and evolution? *Anat Rec A Discov Mol Cell Evol Biol* 287: 1051-1066, 2005.

**Hunt DL, Yamoah EN, and Krubitzer L.** Multisensory plasticity in congenitally deaf mice: how are cortical areas functionally specified? *Neuroscience* 139: 1507-1524, 2006.

**Imbert M, and Buisseret P.** Receptive field characteristics and plastic properties of visual cortical cells in kittens reared with or without visual experience. *Exp Brain Res* 22: 25-36, 1975.

**Insanally MN, Kover H, Kim H, and Bao S.** Feature-dependent sensitive periods in the development of complex sound representation. *J Neurosci* 29: 5456-5462, 2009.

**Irvine DR.** Injury- and use-related plasticity in the adult auditory system. *J Commun Disord* 33: 293-311; quiz 311-292, 2000.

**Irvine DR, Rajan R, and Brown M.** Injury- and use-related plasticity in adult auditory cortex. *Audiol Neurotol* 6: 192-195, 2001.

**Irvine DR, Rajan R, and Smith S.** Effects of restricted cochlear lesions in adult cats on the frequency organization of the inferior colliculus. *J Comp Neurol* 467: 354-374, 2003.

**Izraeli R, Koay G, Lamish M, Hecklen-Klein AJ, Heffner HE, Heffner RS, and Wollberg Z.** Cross-modal neuroplasticity in neonatally enucleated hamsters: structure, electrophysiology and behaviour. *Eur J Neurosci* 15: 693-712, 2002.

**Jastreboff PJ.** Phantom auditory perception (tinnitus): mechanisms of generation and perception. *Neurosci Res* 8: 221-254, 1990.

**Jen PH, and Zhang J.** The role of GABAergic inhibition on direction-dependent sharpening of frequency tuning in bat inferior collicular neurons. *Brain Res* 862: 127-137, 2000.

- Jones EG.** Cortical and subcortical contributions to activity-dependent plasticity in primate somatosensory cortex. *Annu Rev Neurosci* 23: 1-37, 2000.
- Jones EG, Woods TM, and Manger PR.** Adaptive responses of monkey somatosensory cortex to peripheral and central deafferentation. *Neuroscience* 111: 775-797, 2002.
- Jung SC, and Shin HC.** Suppression of temporary deafferentation-induced plasticity in the primary somatosensory cortex of rats by GABA antagonist. *Neurosci Lett* 334: 87-90, 2002.
- Kaas JH.** The evolution of complex sensory systems in mammals. *J Exp Biol* 146: 165-176, 1989.
- Kaas JH.** Evolution of multiple areas and modules within neocortex. *Perspect Dev Neurobiol* 1: 101-107, 1993.
- Kaas JH.** Evolution of the neocortex. *Curr Biol* 16: R910-914, 2006.
- Kaas JH.** Plasticity of sensory and motor maps in adult mammals. *Annu Rev Neurosci* 14: 137-167, 1991.
- Kaas JH.** Topographic maps are fundamental to sensory processing. *Brain Res Bull* 44: 107-112, 1997.
- Kaas JH, Krubitzer LA, Chino YM, Langston AL, Polley EH, and Blair N.** Reorganization of retinotopic cortical maps in adult mammals after lesions of the retina. *Science* 248: 229-231, 1990.
- Kahn DM, and Krubitzer L.** Massive cross-modal cortical plasticity and the emergence of a new cortical area in developmentally blind mammals. *Proc Natl Acad Sci U S A* 99: 11429-11434, 2002.

- Kakigi A, Hirakawa H, Harel N, Mount RJ, and Harrison RV.** Tonotopic mapping in auditory cortex of the adult chinchilla with amikacin-induced cochlear lesions. *Audiology* 39: 153-160, 2000.
- Kalaska J, and Pomeranz B.** Chronic peripheral nerve injuries alter the somatotopic organization of the cuneate nucleus in kittens. *Brain Res* 236: 35-47, 1982.
- Kamke MR, Brown M, and Irvine DR.** Plasticity in the tonotopic organization of the medial geniculate body in adult cats following restricted unilateral cochlear lesions. *J Comp Neurol* 459: 355-367, 2003.
- Karl A, Birbaumer N, Lutzenberger W, Cohen LG, and Flor H.** Reorganization of motor and somatosensory cortex in upper extremity amputees with phantom limb pain. *J Neurosci* 21: 3609-3618, 2001.
- Karlen SJ, Kahn DM, and Krubitzer L.** Early blindness results in abnormal corticocortical and thalamocortical connections. *Neuroscience* 142: 843-858, 2006.
- Karlen SJ, and Krubitzer L.** Effects of bilateral enucleation on the size of visual and nonvisual areas of the brain. *Cereb Cortex* 19: 1360-1371, 2009.
- Katagiri H, Fagiolini M, and Hensch TK.** Optimization of somatic inhibition at critical period onset in mouse visual cortex. *Neuron* 53: 805-812, 2007.
- Katz LC, and Shatz CJ.** Synaptic activity and the construction of cortical circuits. *Science* 274: 1133-1138, 1996.
- Kelly JB, Judge PW, and Phillips DP.** Representation of the cochlea in primary auditory cortex of the ferret (*Mustela putorius*). *Hear Res* 24: 111-115, 1986.
- Kerr AL, Cheng SY, and Jones TA.** Experience-dependent neural plasticity in the adult damaged brain. *J Commun Disord* 44: 538-548, 2011.

**Kimiskidis VK, Lalaki P, Papagiannopoulos S, Tsitouridis I, Tolika T, Serasli E, Kazis D, Tsara V, Tsalighopoulos MG, and Kazis A.** Sensorineural hearing loss and word deafness caused by a mesencephalic lesion: clinicoelectrophysiologic correlations. *Otol Neurotol* 25: 178-182, 2004.

**King AJ, and Parsons CH.** Improved auditory spatial acuity in visually deprived ferrets. *Eur J Neurosci* 11: 3945-3956, 1999.

**Kingsbury MA, Fraf ER, and Finlay BL.** Altered development of visual subcortical projections following neonatal thalamic ablation in the hamster. *J Comp Neurol* 424: 165-178, 2000.

**Kingsbury MA, Lettman NA, and Finlay BL.** Reduction of early thalamic input alters adult corticocortical connectivity. *Brain Res Dev Brain Res* 138: 35-43, 2002.

**Kirkwood A, Rioult MC, and Bear MF.** Experience-dependent modification of synaptic plasticity in visual cortex. *Nature* 381: 526-528, 1996.

**Klinke R, Hartmann R, Heid S, Tillein J, and Kral A.** Plastic changes in the auditory cortex of congenitally deaf cats following cochlear implantation. *Audiol Neurotol* 6: 203-206, 2001.

**Korte M, and Rauschecker JP.** Auditory spatial tuning of cortical neurons is sharpened in cats with early blindness. *J Neurophysiol* 70: 1717-1721, 1993.

**Kral A.** Unimodal and cross-modal plasticity in the 'deaf' auditory cortex. *Int J Audiol* 46: 479-493, 2007.

**Kral A, and Sharma A.** Developmental neuroplasticity after cochlear implantation. *Trends in Neurosciences* 35: 111-122, 2012.

**Kratz KE, and Spear PD.** Effects of visual deprivation and alterations in binocular competition on responses of striate cortex neurons in the cat. *J Comp Neurol* 170: 141-151, 1976.



**Kujala T, Alho K, Huotilainen M, Ilmoniemi RJ, Lehtokoski A, Leinonen A, Rinne T, Salonen O, Sinkkonen J, Standertskjold-Nordenstam CG, and Naatanen R.**

Electrophysiological evidence for cross-modal plasticity in humans with early- and late-onset blindness. *Psychophysiology* 34: 213-216, 1997.

**Kujala T, Alho K, and Naatanen R.** Cross-modal reorganization of human cortical functions. *Trends Neurosci* 23: 115-120, 2000.

**Kujala T, Huotilainen M, Sinkkonen J, Ahonen AI, Alho K, Hamalainen MS, Ilmoniemi RJ, Kajola M, Knuutila JE, Lavikainen J, and et al.** Visual cortex activation in blind humans during sound discrimination. *Neurosci Lett* 183: 143-146, 1995.

**Kupers R, Fumal A, de Noordhout AM, Gjedde A, Schoenen J, and Ptito M.** Transcranial magnetic stimulation of the visual cortex induces somatotopically organized qualia in blind subjects. *Proc Natl Acad Sci U S A* 103: 13256-13260, 2006.

**Laemle LK, Strominger NL, and Carpenter DO.** Cross-modal innervation of primary visual cortex by auditory fibers in congenitally anophthalmic mice. *Neurosci Lett* 396: 108-112, 2006.

**Lakatos P, Chen CM, O'Connell MN, Mills A, and Schroeder CE.** Neuronal oscillations and multisensory interaction in primary auditory cortex. *Neuron* 53: 279-292, 2007.

**Lambertz N, Gizewski ER, de Greiff A, and Forsting M.** Cross-modal plasticity in deaf subjects dependent on the extent of hearing loss. *Brain Res Cogn Brain Res* 25: 884-890, 2005.

**Langguth B, Eichhammer P, Zowe M, Kleinjung T, Jacob P, Binder H, Sand P, and Hajak G.** Altered motor cortex excitability in tinnitus patients: a hint at crossmodal plasticity. *Neurosci Lett* 380: 326-329, 2005.

**Law MI, Zahs KR, and Stryker MP.** Organization of primary visual cortex (area 17) in the ferret. *J Comp Neurol* 278: 157-180, 1988.

**Lee DS, Lee JS, Oh SH, Kim SK, Kim JW, Chung JK, Lee MC, and Kim CS.** Cross-modal plasticity and cochlear implants. *Nature* 409: 149-150, 2001.

**Lee SS, Cha SH, Lee SY, and Song CJ.** Reversible inferior colliculus lesion in metronidazole-induced encephalopathy: magnetic resonance findings on diffusion-weighted and fluid attenuated inversion recovery imaging. *J Comput Assist Tomogr* 33: 305-308, 2009.

**Levy LM, and Hallett M.** Impaired brain GABA in focal dystonia. *Ann Neurol* 51: 93-101, 2002.

**Levy LM, Ziemann U, Chen R, and Cohen LG.** Rapid modulation of GABA in sensorimotor cortex induced by acute deafferentation. *Ann Neurol* 52: 755-761, 2002.

**Linden DC, Guillery RW, and Cucchiaro J.** The dorsal lateral geniculate nucleus of the normal ferret and its postnatal development. *J Comp Neurol* 203: 189-211, 1981.

**Liu BH, Wu GK, Arbuckle R, Tao HW, and Zhang LI.** Defining cortical frequency tuning with recurrent excitatory circuitry. *Nat Neurosci* 10: 1594-1600, 2007.

**Lomber SG, Meredith MA, and Kral A.** Adaptive crossmodal plasticity in deaf auditory cortex: areal and laminar contributions to supranormal vision in the deaf. *Prog Brain Res* 191: 251-270, 2011.

**Lomber SG, Meredith MA, and Kral A.** Cross-modal plasticity in specific auditory cortices underlies visual compensations in the deaf. *Nat Neurosci* 13: 1421-1427, 2010.

**Lund JS, Remington FL, and Lund RD.** Differential central distribution of optic nerve components in the rat. *Brain Res* 116: 83-100, 1976

**Lund RD, and Lund JS.** Plasticity in the developing visual system: the effects of retinal lesions made in young rats. *J Comp Neurol* 169: 133-154, 1976.

**Lyckman AW, Jhaveri S, Feldheim DA, Vanderhaeghen P, Flanagan JG, and Sur M.**

Enhanced plasticity of retinothalamic projections in an ephrin-A2/A5 double mutant. *J Neurosci* 21: 7684-7690, 2001.

**Maffei A, Nataraj K, Nelson SB, and Turrigiano GG.** Potentiation of cortical inhibition by visual deprivation. *Nature* 443: 81-84, 2006.

**Maguire EA, Gadian DG, Johnsrude IS, Good CD, Ashburner J, Frackowiak RS, and Frith CD.** Navigation-related structural change in the hippocampi of taxi drivers. *Proc Natl Acad Sci U S A* 97: 4398-4403, 2000.

**Mann MD, Rehkamper G, Reinke H, Frahm HD, Necker R, and Nevo E.** Size of somatosensory cortex and of somatosensory thalamic nuclei of the naturally blind mole rat, *Spalax ehrenbergi*. *J Hirnforsch* 38: 47-59, 1997.

**Mao YT, Hua TM, and Pallas SL.** Competition and convergence between auditory and cross-modal visual inputs to primary auditory cortical areas. *J Neurophysiol* 105: 1558-1573, 2011.

**Mao YT, Hua TM, and Pallas SL.** Cross-modal ferret auditory cortex contains both auditory and visual representations. *Soc Neurosci Abstr* 36: 2, 2007.

**Mao YT, and Pallas SL.** Inhibition is increased in auditory cortex after invasion by ectopic visual inputs. *Soc Neurosci Abstr* 912: 01, 2011.

**Mao YT, and Pallas SL.** Invasion of ectopic visual inputs compromises auditory function in primary auditory cortex. *Front Neurosci Conference Abstract:2010 South East Nerve Net (SENN) and Georgia/South Carolina Neuroscience Consortium (GASCNC) conferences.:* 2010.

**Masuda S, Takeuchi K, Tsuruoka H, Ukai K, and Sakakura Y.** Word deafness after resection of a pineal body tumor in the presence of normal wave latencies of the auditory brain stem response. *Ann Otol Rhinol Laryngol* 109: 1107-1112, 2000.

**Merabet LB, Battelli L, Obretenova S, Maguire S, Meijer P, and Pascual-Leone A.**

Functional recruitment of visual cortex for sound encoded object identification in the blind.

*NeuroReport* 20: 132-138, 2009.

**Merabet LB, and Pascual-Leone A.** Neural reorganization following sensory loss: the

opportunity of change. *Nat Rev Neuroscit* 11: 44-52, 2010.

**Meredith MA, and Allman BL.** Subthreshold multisensory processing in cat auditory cortex.

*NeuroReport* 20: 126-131, 2009.

**Meredith MA, Kryklywy J, McMillan AJ, Malhotra S, Lum-Tai R, and Lomber SG.**

Crossmodal reorganization in the early deaf switches sensory, but not behavioral roles of auditory cortex. *Proc Natl Acad Sci U S A* 108: 8856-8861, 2011.

**Meredith MA, and Lomber SG.** Somatosensory and visual crossmodal plasticity in the anterior

auditory field of early-deaf cats. *Hear Res* 2011.

**Meredith MA, and Stein BE.** Interactions among converging sensory inputs in the superior

colliculus. *Science* 221: 389-391, 1983.

**Meredith MA, and Stein BE.** Visual, auditory, and somatosensory convergence on cells in

superior colliculus results in multisensory integration. *J Neurophysiol* 56: 640-662, 1986.

**Merzenich MM, Kaas JH, Wall J, Nelson RJ, Sur M, and Felleman D.** Topographic

reorganization of somatosensory cortical areas 3b and 1 in adult monkeys following restricted deafferentation. *Neuroscience* 8: 33-55, 1983.

**Merzenich MM, and Reid MD.** Representation of the cochlea within the inferior colliculus of

the cat. *Brain Res* 77: 397-415, 1974.

**Meyer B, Kral T, and Zentner J.** Pure word deafness after resection of a tectal plate glioma with preservation of wave V of brain stem auditory evoked potentials. *J Neurol Neurosurg Psychiatry* 61: 423-424, 1996.

**Micheva KD, and Beaulieu C.** An anatomical substrate for experience-dependent plasticity of the rat barrel field cortex. *Proc Natl Acad Sci U S A* 92: 11834-11838, 1995a.

**Micheva KD, and Beaulieu C.** Neonatal sensory deprivation induces selective changes in the quantitative distribution of GABA-immunoreactive neurons in the rat barrel field cortex. *J Comp Neurol* 361: 574-584, 1995b.

**Middlebrooks JC, Bierer JA, and Snyder RL.** Cochlear implants: the view from the brain. *Curr Opin Neurobiol* 15: 488-493, 2005.

**Miller KD, Keller JB, and Stryker MP.** Ocular dominance column development: analysis and simulation. *Science* 245: 605-615, 1989.

**Montey KL, and Quinlan EM.** Recovery from chronic monocular deprivation following reactivation of thalamocortical plasticity by dark exposure. *Nat Commun* 2: 317, 2011.

**Moore DR.** Auditory brainstem of the ferret: early cessation of developmental sensitivity of neurons in the cochlear nucleus to removal of the cochlea. *J Comp Neurol* 302: 810-823, 1990.

**Moore DR, and Hine JE.** Rapid development of the auditory brainstem response threshold in individual ferrets. *Dev Brain Res* 66: 229-235, 1992.

**Moore DR, Kotak VC, and Sanes DH.** Commissural and lemniscal synaptic input to the gerbil inferior colliculus. *J Neurophysiol* 80: 2229-2236, 1998.

**Moore DR, and Kowalchuk NE.** Auditory brainstem of the ferret: effects of unilateral cochlear lesions on cochlear nucleus volume and projections to the inferior colliculus. *J Comp Neurol* 272: 503-515, 1988.

- Moore DR, Semple MN, and Addison PD.** Some acoustic properties of neurones in the ferret inferior colliculus. *Brain Res* 269: 69-82, 1983.
- Morales B, Choi SY, and Kirkwood A.** Dark rearing alters the development of GABAergic transmission in visual cortex. *J Neurosci* 22: 8084-8090, 2002.
- Mountcastle VB.** The columnar organization of the neocortex. *Brain* 120 ( Pt 4): 701-722, 1997.
- Mower GD, and Christen WG.** Evidence for an enhanced role of GABA inhibition in visual cortical ocular dominance of cats reared with abnormal monocular experience. *Brain Res Dev Brain Res* 45: 211-218, 1989.
- Mower GD, and Guo Y.** Comparison of the expression of two forms of glutamic acid decarboxylase (GAD67 and GAD65) in the visual cortex of normal and dark-reared cats. *Brain Res Dev Brain Res* 126: 65-74, 2001.
- Murphy EH.** Effects of pattern deprivation on visual cortical cells in the rabbit: a reevaluation. *J Neurophysiol* 53: 1535-1550, 1985.
- Musiek FE, Charette L, Morse D, and Baran JA.** Central deafness associated with a midbrain lesion. *J Am Acad Audiol* 15: 133-151; quiz 172-133, 2004.
- Necker R, Rehkamper G, and Nevo E.** Electrophysiological mapping of body representation in the cortex of the blind mole rat. *NeuroReport* 3: 505-508, 1992.
- Neville HJ.** Intermodal competition and compensation in development. Evidence from studies of the visual system in congenitally deaf adults. *Ann N Y Acad Sci* 608: 71-87; discussion 87-91, 1990.
- Neville HJ, Schmidt A, and Kutas M.** Altered visual-evoked potentials in congenitally deaf adults. *Brain Res* 266: 127-132, 1983.

**Newton JR, Sikes RW, and Skavenski AA.** Cross-modal plasticity after monocular enucleation of the adult rabbit. *Exp Brain Res* 144: 423-429, 2002.

**Ni H, Huang L, Chen N, Zhang F, Liu D, Ge M, Guan S, Zhu Y, and Wang JH.**

Upregulation of barrel GABAergic neurons is associated with cross-modal plasticity in olfactory deficit. *PLoS One* 5: e13736, 2010.

**Nishimura H, Doi K, Iwaki T, Hashikawa K, Oku N, Teratani T, Hasegawa T, Watanabe A,**

**Nishimura T, and Kubo T.** Neural plasticity detected in short- and long-term cochlear implant users using PET. *NeuroReport* 11: 811-815, 2000.

**Nudo RJ, Milliken GW, Jenkins WM, and Merzenich MM.** Use-dependent alterations of movement representations in primary motor cortex of adult squirrel monkeys. *J Neurosci* 16: 785-807, 1996a.

**Nudo RJ, Wise BM, SiFuentes F, and Milliken GW.** Neural substrates for the effects of rehabilitative training on motor recovery after ischemic infarct. *Science* 272: 1791-1794, 1996b.

**Obata S, Obata J, Das A, and Gilbert CD.** Molecular correlates of topographic reorganization in primary visual cortex following retinal lesions. *Cereb Cortex* 9: 238-248, 1999.

**Ozeki H, Sadakane O, Akasaki T, Naito T, Shimegi S, and Sato H.** Relationship between excitation and inhibition underlying size tuning and contextual response modulation in the cat primary visual cortex. *J Neurosci* 24: 1428-1438, 2004.

**Pallas SL.** *Developmental plasticity of inhibitory circuitry*. New York: Springer, 2010, p. xi, 190 p.

**Pallas SL, and Finlay BL.** Conservation of receptive-field properties of superior colliculus cells after developmental rearrangements of retinal input. *Vis Neurosci* 2: 121-135, 1989.

**Pallas SL, Hahm J, and Sur M.** Morphology of retinal axons induced to arborize in a novel target, the medial geniculate nucleus. I. Comparison with arbors in normal targets. *J Comp Neurol* 349: 343-362, 1994.

**Pallas SL, Littman T, and Moore DR.** Cross-modal reorganization of callosal connectivity without altering thalamocortical projections. *Proc Natl Acad Sci U S A* 96: 8751-8756, 1999.

**Pallas SL, Roe AW, and Sur M.** Visual projections induced into the auditory pathway of ferrets. I. Novel inputs to primary auditory cortex (AI) from the LP/pulvinar complex and the topography of the MGN-AI projection. *J Comp Neurol* 298: 50-68, 1990.

**Pallas SL, and Sur M.** Morphology of retinal axon arbors induced to arborize in a novel target, the medial geniculate nucleus. II. Comparison with axons from the inferior colliculus. *J Comp Neurol* 349: 363-376, 1994.

**Pallas SL, and Sur M.** Visual projections induced into the auditory pathway of ferrets: II. Corticocortical connections of primary auditory cortex. *J Comp Neurol* 337: 317-333, 1993.

**Pantev C, Engelien A, Candia V, and Elbert T.** Representational cortex in musicians. Plastic alterations in response to musical practice. *Ann N Y Acad Sci* 930: 300-314, 2001.

**Pantev C, Ross B, Fujioka T, Trainor LJ, Schulte M, and Schulz M.** Music and learning-induced cortical plasticity. *Ann N Y Acad Sci* 999: 438-450, 2003.

**Park MH, Lee HJ, Kim JS, Lee JS, Lee DS, and Oh SH.** Cross-modal and compensatory plasticity in adult deafened cats: a longitudinal PET study. *Brain Res* 1354: 85-90, 2010.

**Parrish-Aungst S, Kiyokage E, Szabo G, Yanagawa Y, Shipley MT, and Puche AC.** Sensory experience selectively regulates transmitter synthesis enzymes in interglomerular circuits. *Brain Res* 1382: 70-76, 2011.



**Phillips DP, Judge PW, and Kelly JB.** Primary auditory cortex in the ferret (*Mustela putorius*): neural response properties and topographic organization. *Brain Res* 443: 281-294, 1988.

**Philpot BD, Espinosa JS, and Bear MF.** Evidence for altered NMDA receptor function as a basis for metaplasticity in visual cortex. *J Neurosci* 23: 5583-5588, 2003.

**Philpot BD, Sekhar AK, Shouval HZ, and Bear MF.** Visual experience and deprivation bidirectionally modify the composition and function of NMDA receptors in visual cortex. *Neuron* 29: 157-169, 2001.

**Piché M, Chabot N, Bronchti G, Miceli D, Lepore F, and Guillemot JP.** Auditory responses in the visual cortex of neonatally enucleated rats. *Neuroscience* 145: 1144-1156, 2007.

**Piche M, Robert S, Miceli D, and Bronchti G.** Environmental enrichment enhances auditory takeover of the occipital cortex in anophthalmic mice. *Eur J Neurosci* 20: 3463-3472, 2004.

**Pons TP, Garraghty PE, and Mishkin M.** Lesion-induced plasticity in the second somatosensory cortex of adult macaques. *Proc Natl Acad Sci U S A* 85: 5279-5281, 1988.

**Popescu MV, and Polley DB.** Monaural deprivation disrupts development of binaural selectivity in auditory midbrain and cortex. *Neuron* 65: 718-731, 2010.

**Priebe NJ, and Ferster D.** Direction selectivity of excitation and inhibition in simple cells of the cat primary visual cortex. *Neuron* 45: 133-145, 2005.

**Quartarone A, Siebner HR, and Rothwell JC.** Task-specific hand dystonia: can too much plasticity be bad for you? *Trends Neurosci* 29: 192-199, 2006.

**Quinlan EM, Philpot BD, Hugarir RL, and Bear MF.** Rapid, experience-dependent expression of synaptic NMDA receptors in visual cortex *in vivo*. *Nat Neurosci* 2: 352-357, 1999.

**Rajan R.** Plasticity of excitation and inhibition in the receptive field of primary auditory cortical neurons after limited receptor organ damage. *Cereb Cortex* 11: 171-182, 2001.

**Rajan R.** Receptor organ damage causes loss of cortical surround inhibition without topographic map plasticity. *Nat Neurosci* 1: 138-143, 1998.

**Rajan R, Irvine DR, Wise LZ, and Heil P.** Effect of unilateral partial cochlear lesions in adult cats on the representation of lesioned and unlesioned cochleas in primary auditory cortex. *J Comp Neurol* 338: 17-49, 1993.

**Ralston HJ, 3rd, Ohara PT, Meng XW, Wells J, and Ralston DD.** Transneuronal changes of the inhibitory circuitry in the macaque somatosensory thalamus following lesions of the dorsal column nuclei. *J Comp Neurol* 371: 325-335, 1996.

**Ramoa AS, Paradiso MA, and Freeman RD.** Blockade of intracortical inhibition in kitten striate cortex: effects on receptive field properties and associated loss of ocular dominance plasticity. *Exp Brain Res* 73: 285-296, 1988.

**Rauschecker JP.** Compensatory plasticity and sensory substitution in the cerebral cortex. *Trends Neurosci* 18: 36-43, 1995a.

**Rauschecker JP.** Developmental plasticity and memory. *Behav Brain Res* 66: 7-12, 1995b.

**Rauschecker JP.** Neuronal mechanisms of developmental plasticity in the cat's visual system. *Hum Neurobiol* 3: 109-114, 1984.

**Rauschecker JP.** Substitution of visual by auditory inputs in the cat's anterior ectosylvian cortex. *Prog Brain Res* 112: 313-323, 1996.

**Rauschecker JP, and Kniepert U.** Auditory localization behaviour in visually deprived cats. *Eur J Neurosci* 6: 149-160, 1994.

**Rauschecker JP, and Korte M.** Auditory compensation for early blindness in cat cerebral cortex. *J Neurosci* 10: 4538-4548, 1993.

**Rauschecker JP, and Singer W.** The effects of early visual experience on the cat's visual cortex and their possible explanation by Hebb synapses. *J Physiol* 310: 215-239, 1981.

**Rauschecker JP, Tian B, Korte M, and Egert U.** Crossmodal changes in the somatosensory vibrissa/barrel system of visually deprived animals. *Proc Natl Acad Sci U S A* 89: 5063-5067, 1992.

**Reale RA, and Imig TJ.** Tonotopic organization in auditory cortex of the cat. *J Comp Neurol* 192: 265-291, 1980.

**Reh TA, and Constantine-Paton M.** Eye-specific segregation requires neural activity in three-eyed *Rana pipiens*. *J Neurosci* 5: 1132-1143, 1985.

**Restrepo CE, Manger PR, and Innocenti GM.** Retinofugal projections following early lesions of the visual cortex in the ferret. *Eur J Neurosci* 16: 1713-1719, 2002.

**Rhoades RW, and Chalupa LM.** Effects of neonatal enucleation on receptive-field properties of visual neurons in superior colliculus of the golden hamster. *J Neurophysiol* 43: 595-611, 1980.

**Ribak CE, and Robertson RT.** Effects of neonatal monocular enucleation on the number of GAD-positive puncta in rat visual cortex. *Exp Brain Res* 62: 203-206, 1986.

**Ringo JL.** Neuronal interconnection as a function of brain size. *Brain Behav Evol* 38: 1-6, 1991.

**Ro T, Farne A, Johnson RM, Wedeen V, Chu Z, Wang ZJ, Hunter JV, and Beauchamp MS.** Feeling sounds after a thalamic lesion. *Ann Neurol* 62: 433-441, 2007.

**Roberts LE, Eggermont JJ, Caspary DM, Shore SE, Melcher JR, and Kaltenbach JA.** Ringing ears: the neuroscience of tinnitus. *J Neurosci* 30: 14972-14979, 2010.

**Robertson D, and Irvine DR.** Plasticity of frequency organization in auditory cortex of guinea pigs with partial unilateral deafness. *J Comp Neurol* 282: 456-471, 1989.

- Roder B, Teder-Salejarvi W, and Neville HJ.** Improved auditory spatial tuning in blind humans. *Nature* 400: 162-166, 1999.
- Roe AW, Garraghty PE, Esguerra M, and Sur M.** Experimentally induced visual projections to the auditory thalamus in ferrets: evidence for a W cell pathway. *J Comp Neurol* 334: 263-280, 1993.
- Roe AW, Pallas SL, Hahm JO, and Sur M.** A map of visual space induced in primary auditory cortex. *Science* 250: 818-820, 1990.
- Roe AW, Pallas SL, Kwon YH, and Sur M.** Visual projections routed to the auditory pathway in ferrets: receptive fields of visual neurons in primary auditory cortex. *J Neurosci* 12: 3651-3664, 1992.
- Rosier AM, Arckens L, Demeulemeester H, Orban GA, Eysel UT, Wu YJ, and Vandesande F.** Effect of sensory deafferentation on immunoreactivity of GABAergic cells and on GABA receptors in the adult cat visual cortex. *J Comp Neurol* 359: 476-489, 1995.
- Rothschild G, Nelken I, and Mizrahi A.** Functional organization and population dynamics in the mouse primary auditory cortex. *Nat Neurosci* 13: 353-360, 2010.
- Ryugo DK.** Increased spine density in auditory cortex following visual or somatic deafferentation. *Brain Res* 90: 143-146, 1975.
- Sadaka Y, Weinfeld E, Lev DL, and White EL.** Changes in mouse barrel synapses consequent to sensory deprivation from birth. *J Comp Neurol* 457: 75-86, 2003.
- Sadato N.** Activation of the primary visual cortex by Braille reading in blind subjects. *Nature* 380: 526-528, 1996.

**Saito DN, Okada T, Honda M, Yonekura Y, and Sadato N.** Practice makes perfect: the neural substrates of tactile discrimination by Mah-Jong experts include the primary visual cortex. *BMC Neurosci* 7: 79, 2006.

**Sarno S, Erasmus LP, Lipp B, and Schlaegel W.** Multisensory integration after traumatic brain injury: a reaction time study between pairings of vision, touch and audition. *Brain Inj* 17: 413-426, 2003.

**Sathian K, and Stilla R.** Cross-modal plasticity of tactile perception in blindness. *Restor Neurol Neurosci* 28: 271-281, 2010.

**Scalia F.** Further study of the aberrant optic nerve projection to olfactory cortex. *J Comp Neurol* 324: 415-426, 1992.

**Scalia F.** Synapse formation in the olfactory cortex by regenerating optic axons: ultrastructural evidence for polyspecific chemoaffinity. *J Comp Neurol* 263: 497-513, 1987.

**Scalia F, Grant AC, Reyes M, and Lettvin JY.** Functional properties of regenerated optic axons terminating in the primary olfactory cortex. *Brain Res* 685: 187-197, 1995.

**Schmidt JT.** Regeneration of the retinotectal projection following compression onto a half tectum in goldfish. *J Embryol Exp Morphol* 77: 39-51, 1983.

**Schneider GE.** Early lesions of superior colliculus: factors affecting the formation of abnormal retinal projections. *Brain Behav Evol* 8: 73-109, 1973.

**Schroeder CE, Smiley J, Fu KG, McGinnis T, Oconnell MN, and Hackett TA.** Anatomical mechanisms and functional implications of multisensory convergence in early cortical processing. *Int J Psychophysiol* 50: 5-17, 2003.

**Serviere J, Webster WR, and Calford MB.** Isofrequency labelling revealed by a combined [ $^{14}\text{C}$ ]-2-deoxyglucose, electrophysiological, and horseradish peroxidase study of the inferior colliculus of the cat. *J Comp Neurol* 228: 463-477, 1984.

**Sharma A, Gilley PM, Dorman MF, and Baldwin R.** Deprivation-induced cortical reorganization in children with cochlear implants. *Int J Audiol* 46: 494-499, 2007.

**Sharma A, Nash AA, and Dorman M.** Cortical development, plasticity and re-organization in children with cochlear implants. *J Commun Disord* 42: 272-279, 2009.

**Sharma J, Angelucci A, and Sur M.** Induction of visual orientation modules in auditory cortex. *Nature* 404: 841-847, 2000.

**Sharma SC, Romeskie M.** Immediate 'compression' of the goldfish retinal projection to a tectum devoid of degenerating debris. *Brain Res* 133: 367-370, 1977.

**Shatz CJ.** Impulse activity and the patterning of connections during CNS development. *Neuron* 5: 745-756, 1990.

**Shatz CJ, and Stryker MP.** Ocular dominance in layer IV of the cat's visual cortex and the effects of monocular deprivation. *J Physiol* 281: 267-283, 1978.

**Sheskin D.** *Handbook of parametric and nonparametric statistical procedures*. Boca Raton, Fla.: Chapman & Hall/CRC, 2004, p. xxxiii, 1193 p.

**Shumway C, Morissette J, and Bower JM.** Mechanisms underlying reorganization of fractured tactile cerebellar maps after deafferentation in developing and adult rats. *J Neurophysiol* 94: 2630-2643, 2005.

**Sillito AM.** The contribution of inhibitory mechanisms to the receptive field properties of neurones in the striate cortex of the cat. *J Physiol* 250: 305-329, 1975.

- Sillito AM.** Inhibitory mechanisms influencing complex cell orientation selectivity and their modification at high resting discharge levels. *J Physiol* 289: 33-53, 1979.
- Sillito AM, Kemp JA, and Blakemore C.** The role of GABAergic inhibition in the cortical effects of monocular deprivation. *Nature* 291: 318-320, 1981.
- Sillito AM, Kemp JA, Milson JA, and Berardi N.** A re-evaluation of the mechanisms underlying simple cell orientation selectivity. *Brain Res* 194: 517-520, 1980.
- Sillito AM, and Versiani V.** The contribution of excitatory and inhibitory inputs to the length preference of hypercomplex cells in layers II and III of the cat's striate cortex. *J Physiol* 273: 775-790, 1977.
- Smiley JF, Hackett TA, Ulbert I, Karmas G, Lakatos P, Javitt DC, and Schroeder CE.** Multisensory convergence in auditory cortex, I. Cortical connections of the caudal superior temporal plane in macaque monkeys. *J Comp Neurol* 502: 894-923, 2007.
- Somogyi J, Eysel U, and Hamori J.** A quantitative study of morphological reorganization following chronic optic deafferentation in the adult cat dorsal lateral geniculate nucleus. *J Comp Neurol* 255: 341-350, 1987.
- Stanford TR, Quessy S, and Stein BE.** Evaluating the operations underlying multisensory integration in the cat superior colliculus. *J Neurosci* 25: 6499-6508, 2005.
- Stein BE, and Meredith MA.** *The merging of the senses*. Cambridge, Mass.: MIT Press, 1993, p. xv, 211 p.
- Stein BE, Meredith MA, and Wallace MT.** The visually responsive neuron and beyond: multisensory integration in cat and monkey. *Prog Brain Res* 95: 79-90, 1993.
- Sterr A, Green L, and Elbert T.** Blind Braille readers mislocate tactile stimuli. *Biol Psychol* 63: 117-127, 2003.

**Stevens AA, and Weaver KE.** Functional characteristics of auditory cortex in the blind. *Behav Brain Res* 196: 134-138, 2009.

**Stryker MP.** Postnatal development of ocular dominance columns in layer IV of the cat's visual cortex and the effects of monocular deprivation. *Arch Ital Biol* 116: 420-426, 1978.

**Stryker MP.** Role of visual afferent activity in the development of ocular dominance columns. *Neurosci Res Program Bull* 20: 540-549, 1982.

**Stryker MP, and Zahs KR.** On and off sublaminae in the lateral geniculate nucleus of the ferret.

*J Neurosci* 3: 1943-1951, 1983**Stryker MP, and Harris WA.** Binocular impulse blockade prevents the formation of ocular dominance columns in cat visual cortex. *J Neurosci* 6: 2117-2133, 1986.

**Sun YJ, Wu GK, Liu BH, Li P, Zhou M, Xiao Z, Tao HW, and Zhang LI.** Fine-tuning of pre-balanced excitation and inhibition during auditory cortical development. *Nature* 465: 927-931, 2010.

**Sur M.** Visual projections induced into auditory thalamus and cortex: implications for thalamic and cortical information processing. *Prog Brain Res* 75: 129-136, 1988.

**Sur M, Garraghty PE, and Roe AW.** Experimentally induced visual projections into auditory thalamus and cortex. *Science* 242: 1437-1441, 1988.

**Sutter ML, and Schreiner CE.** Physiology and topography of neurons with multi-peaked tuning curves in cat primary auditory cortex. *J Neurophysiol* 65: 1207-1226, 1991.

**Sutter ML, Schreiner CE, McLean M, O'Connor K N, and Loftus WC.** Organization of inhibitory frequency receptive fields in cat primary auditory cortex. *J Neurophysiol* 82: 2358-2371, 1999.



**Tan AY, Zhang LI, Merzenich MM, and Schreiner CE.** Tone-evoked excitatory and inhibitory synaptic conductances of primary auditory cortex neurons. *J Neurophysiol* 92: 630-643, 2004.

**Toldi J, Feher O, and Wolff JR.** Neuronal plasticity induced by neonatal monocular (and binocular) enucleation. *Prog Neurobiol* 48: 191-218, 1996.

**Toldi J, Rojik I, and Fehér O.** Neonatal monocular enucleation-induced cross-modal effects observed in the cortex of adult rat. *Neuroscience* 62: 105-114, 1994.

**Traversa R, Cicinelli P, Bassi A, Rossini PM, and Bernardi G.** Mapping of motor cortical reorganization after stroke. A brain stimulation study with focal magnetic pulses. *Stroke* 28: 110-117, 1997.

**Trevelyan AJ, and Thompson ID.** Neonatal monocular enucleation and the geniculo-cortical system in the golden hamster: shrinkage in dorsal lateral geniculate nucleus and area 17 and the effects on relay cell size and number. *Vis Neurosci* 12: 971-983, 1995.

**Tsumoto T, Eckart W, and Creutzfeldt OD.** Modification of orientation sensitivity of cat visual cortex neurons by removal of GABA-mediated inhibition. *Exp Brain Res* 34: 351-363, 1979.

**Turlejski K, and Kossut M.** Decrease in the number of synapses formed by subcortical inputs to the striate cortex of binocularly deprived cats. *Brain Res* 331: 115-125, 1985.

**Turrigiano G.** Homeostatic synaptic plasticity: local and global mechanisms for stabilizing neuronal function. *Cold Spring Harb Perspect Biol* 4: a005736, 2012.

**Turrigiano G.** Too many cooks? Intrinsic and synaptic homeostatic mechanisms in cortical circuit refinement. *Annu Rev Neurosci* 34: 89-103, 2011.

**Turrigiano GG.** Homeostatic plasticity in neuronal networks: the more things change, the more they stay the same. *Trends Neurosci* 22: 221-227, 1999.

**Udin S.** Retinal compression in the hamster: a quantitative study with horseradish peroxidase [proceedings]. *J physiol* 280: 47-48, 1978

**Vale C, and Sanes DH.** The effect of bilateral deafness on excitatory and inhibitory synaptic strength in the inferior colliculus. *Eur J Neurosci* 16: 2394-2404, 2002.

**von Melchner L, Pallas SL, and Sur M.** Visual behaviour mediated by retinal projections directed to the auditory pathway. *Nature* 404: 871-876, 2000.

**Voss P, Lassonde M, Gougoux F, Fortin M, Guillemot JP, and Lepore F.** Early- and late-onset blind individuals show supra-normal auditory abilities in far-space. *Curr Biol* 14: 1734-1738, 2004.

**Wallace MT, Meredith MA, and Stein BE.** Integration of multiple sensory modalities in cat cortex. *Exp Brain Res* 91: 484-488, 1992.

**Wallace MT, Ramachandran R, and Stein BE.** A revised view of sensory cortical parcellation. *Proc Natl Acad Sci U S A* 101: 2167-2172, 2004.

**Wang J, Caspary D, and Salvi RJ.** GABA-A antagonist causes dramatic expansion of tuning in primary auditory cortex. *NeuroReport* 11: 1137-1140, 2000.

**Wang Q, Hua Q, Wang S, Xiao B, and Liao H.** [The changes of GABA and GABAergic neurons in inferior colliculus of unilateral cochlear damage rats]. *Lin Chung Er Bi Yan Hou Tou Jing Wai Ke Za Zhi* 21: 321-323, 2007.

**Wehr M, and Zador AM.** Balanced inhibition underlies tuning and sharpens spike timing in auditory cortex. *Nature* 426: 442-446, 2003.

- Westenbroek RE, Westrum LE, Hendrickson AE, and Wu JY.** Ultrastructure of synaptic remodeling in piriform cortex of adult rats after neonatal olfactory bulb removal: an immunocytochemical study. *J Comp Neurol* 274: 334-346, 1988.
- Wimmer VC, Broser PJ, Kuner T, and Bruno RM.** Experience-induced plasticity of thalamocortical axons in both juveniles and adults. *J Comp Neurol* 518: 4629-4648, 2010.
- Winer JA, Diehl JJ, and Larue DT.** Projections of auditory cortex to the medial geniculate body of the cat. *J Comp Neurol* 430: 27-55, 2001.
- Wittenberg GF, Werhahn KJ, Wassermann EM, Herscovitch P, and Cohen LG.** Functional connectivity between somatosensory and visual cortex in early blind humans. *Eur J Neurosci* 20: 1923-1927, 2004.
- Worgotter F, and Eysel UT.** Topographical aspects of intracortical excitation and inhibition contributing to orientation specificity in area 17 of the cat visual cortex. *Eur J Neurosci* 3: 1232-1244, 1991.
- Wu GK, Arbuckle R, Liu BH, Tao HW, and Zhang LI.** Lateral sharpening of cortical frequency tuning by approximately balanced inhibition. *Neuron* 58: 132-143, 2008.
- Yaka R, Yinon U, and Wollberg Z.** Pathological and experimentally induced blindness induces auditory activity in the cat primary visual cortex. *Exp Brain Res* 131: 144, 2000.
- Zahs KR, and Stryker MP.** Segregation of ON and OFF afferents to ferret visual cortex. *J Neurophysiol* 59: 1410-1429, 1988.
- Zhang LI, Bao S, and Merzenich MM.** Disruption of primary auditory cortex by synchronous auditory inputs during a critical period. *Proc Natl Acad Sci U S A* 99: 2309-2314, 2002.
- Zhang LI, Bao S, and Merzenich MM.** Persistent and specific influences of early acoustic environments on primary auditory cortex. *Nat Neurosci* 4: 1123-1130, 2001.

**Zhang LI, Tan AY, Schreiner CE, and Merzenich MM.** Topography and synaptic shaping of direction selectivity in primary auditory cortex. *Nature* 424: 201-205, 2003.